

THE ROLE OF PALS1 IN MAMMALIAN EPITHELIAL POLARITY

by

Qian Wang

A dissertation submitted in partial fulfillment
of the requirements for the degree of
Doctor of Philosophy
(Biological Chemistry)
in The University of Michigan
2007

Doctoral Committee:

Professor Benjamin L. Margolis, Chair
Professor Eric R. Fearon
Professor Robert S. Fuller
Professor Kunliang Guan
Associate professor Anne B. Vojtek

To

my parents, who have made me who I am;

and my husband Xiaowei, who has accompanied me to where I am.

ACKNOWLEDGMENTS

This work is the result of the dedicated efforts of many individuals who willingly provided both professional and personal assistance. All the past and current members of the Margolis lab, especially Toby Hurd, Shuling Fan, Kunyoo Shin, Jennifer Harder, Eileen Whiteman, Albert Liu, Michael Roh, Sam Straight, Jay Pieczinski, Dave Karnak, Vanessa Fogg, Sunyoung Moon and Stephanie Laurinec, were not only colleagues who provided great collaboration in research and everyday lab work but also friends who were always ready to help. I am especially grateful for the comments from Toby Hurd, Jennifer Harder and Eileen Whiteman during the writing of this thesis. This work would not have been even possible without the mentorship of my advisor Ben Margolis. With great insight for science and a big heart for life, he has always supported me, believed in me, and he guided me through the entire graduate study and prepared me as a passionate and enterprising professional for my future career. I would also like to thank the members of my thesis committee for their suggestions and instructions on my research.

I have been blessed with the care and encouragement from my parents and other family members, who are thousands of miles away on the other side of the earth. It is them who enabled me to see the world they have not been able to see, both geographically and intellectually.

My sincere thanks also go to all the local and remote friends who have shared the sweetness and bitterness with me along the way. Among them, I would like to specially

thank my best friend, my husband Xiaowei Chen. The encouragement, the communication and the companionship are all invaluable, let alone the collaboration in science. Because of him this journey has been more colorful and invigorating than I could ever imagine.

PREFACE

All the content in Chapter 1 has been submitted as an invited review to the journal *Kidney International*. All the content in Chapter 2 has been published in the *Journal of Biological Chemistry* 279(29):30715-21, 2004. All the content in Chapter 3 has been published in the journal *Molecular Biology of the Cell* 18(3):874-85, 2007. Figure 1.2 was provided by Kunyoo Shin and it was published in the journal *Annual Review of Cell and Developmental Biology* 22:207-35, 2006. Figure 2.2 and 2.3 were prepared by Toby Hurd and Figure 3.17 was prepared by Xiaowei Chen.

TABLE OF CONTENTS

DEDICATION	ii
ACKNOWLEDGMENTS	iii
PREFACE	iv
LIST OF FIGURES	x
CHAPTERS	
1. INTRODUCTION	1
1.1 Epithelial cell polarity and apical junctional complexes	1
1.2 Apical polarity complexes	3
1.2.1 Function of the PAR complex in epithelial cell polarity	3
1.2.1.1 Structure of the PAR complex components and protein-protein interactions	4
1.2.1.2 Molecular actions of the PAR complex in epithelial polarity	7
1.2.2 Function of the CRB complex in epithelial cell polarity	9
1.2.2.1 Crumbs	10
1.2.2.2 PATJ	11
1.2.2.3 PALS1/Stardust	13
1.2.3 Interplay between CRB complex and PAR complex	14

2. TIGHT JUNCTION PROTEIN PAR6 INTERACTS WITH AN	
EVOLUTIONARILY CONSERVED REGION IN THE AMINO	
TERMINUS OF PALS1/STARDUST	23
2.1 Introduction	23
2.2 Materials and methods	25
2.2.1 Antibodies	25
2.2.2 Cell culture	25
2.2.3 MDCK stable cell lines	26
2.2.4 DNA constructs	26
2.2.5 Immunoprecipitation and blotting	26
2.2.6 Immunofluorescence microscopy and imaging	27
2.3 Results	28
2.3.1 PALS1 interacts with PAR6 through an evolutionarily conserved region in its amino terminus	28
2.3.2 Point mutations in the PALS1 ECR1 reduce the interactions with PAR6	30
2.3.3 PAR6 binding site in Drosophila stardust	32
2.3.4 Interaction between the PALS1 ECR1 and PAR6 CRIB-PDZ domains	34
2.3.5 PALS1 V37G mutant is localized to the tight junction	37
2.3.6 PAR6 interferes with PATJ in binding PALS1	38
2.4 Discussion	39

3. PALS1 REGULATES E-CADHERIN TRAFFICKING IN MAMMALIAN

EPITHELIAL CELLS	46
3.1 Introduction	46
3.2 Materials and methods	48
3.2.1 DNA constructs	48
3.2.2 Cell culture and calcium switch experiment	49
3.2.3 Antibodies	49
3.2.4 Immunoblotting	50
3.2.5 Immunostaining and microscopy	50
3.2.6 Cell surface biotinylation	51
3.2.7 Metabolic labeling and pulse-chase	52
3.2.8 E-cadherin endocytosis assay	52
3.2.9 10-15-20-30% Opti-prep gradient	53
3.3 Results	53
3.3.1 Depletion of PALS1 disrupts both tight junctions and adherens junctions in MDCK cell	53
3.3.2 Wild type PALS1 and two PALS1 mutants rescued the defects in junction formation	57
3.3.3 There is less E-cadherin on the surface of the PALS1 KD cells	61
3.3.4 E-cadherin is retained in intracellular puncta in PALS1 KD cells	65
3.3.5 E-cadherin is not effectively exocytosed to the cell surface	67
3.3.6 Exocyst is mislocalized in the PALS1 knockdown cells	71
3.4 Discussion	76

4. PALS1 CARBOXYL-TERMINUS UNDERGOES INTRAMOLECULAR INTERACTION	86
4.1 Introduction	86
4.2 Materials and methods	88
4.2.1 Cell culture	88
4.2.2 DNA constructs	88
4.2.3 Immunoprecipitation and blotting	88
4.3 Results	88
4.4 Discussion	93
5. CONCLUSIONS AND PERSPECTIVES	96
5.1 PALS1 is an important regulator mammalian epithelial cell polarity	96
5.1.1 The PALS1-PAR6 interaction represents an unconventional mode of PDZ action	97
5.1.2 PALS1 and CRB3 differentially regulates PAR6	99
5.1.3 The Lin-7-PALS1-PATJ stabilization hierarchy	100
5.1.4 The adhesion-to-polarity model versus the polarity-to-adhesion hypothesis	102
5.1.5 PALS1 regulates adherens junction formation	104
5.2 Perspectives	107

LIST OF FIGURES

Figure

1.1	Domain structures of components of the PAR complex and the CRB complex	6
1.2	Mutual exclusion of polarity complexes in apico-basal polarity	9
2.1	Schematic illustration of the domain structure of PALS1 and PAR6	28
2.2	Alignment of the amino-terminal conserved regions in <i>Drosophila (Dm)</i> , zebrafish (<i>Dr</i>), mouse (<i>Mm</i>), and human (<i>Hs</i>) PALS1	29
2.3	Deletion of ECR1 prevents pulldown of HA-PAR6	29
2.4	Val37 and Asp38 are critical for the interaction between PALS1 and PAR6 ..	31
2.5	Confirmation of the binding site with MDCK cell lysates	32
2.6	Schematic illustration of B isoform of <i>Drosophila</i> Stardust	33
2.7	Stardust U1 region interacts with PAR6 but not with PATJ	33
2.8	Val19 and Asp20 in Stardust ECR1 are critical for its binding with PAR6	34
2.9	Schematic representation of Myc-PALS1 constructs and HA-PAR6 constructs	35
2.10	Further characterization of PALS1-PAR6 interaction	35
2.11	The interaction is primarily between the PAR6 CRIB-PDZ region and the PALS1 amino-terminus	37
2.12	Localization of PALS1 V37G mutant	38

2.13	PAR6 and PATJ compete to bind PALS1	39
3.1	Protein levels in control and PALS1 KD cell lines	54
3.2	Junction formations in control and PALS1 KD cell lines	55
3.3	Junction formations in PALS1 KD pool cells	56
3.4	The domain structure of PALS1	57
3.5	Expression of the PALS1 rescuing constructs	58
3.6	Junction formations in control, PALS1 KD, and rescue cells	59
3.7	Immunofluorescence of PATJ in PALS1 rescue cell lines	60
3.8	Immunofluorescence of cell surface E-cadherin	62
3.9	Immunostaining of cell surface E-cadherin after calcium switch	63
3.10	Surface biotinylation of E-cadherin after calcium switch	64
3.11	E-cadherin puncta in PALS1 KD pool cells	66
3.12	Costaining of E-cadherin with AJ markers	67
3.13	E-cadherin puncta in PALS1 KD cell lines	68
3.14	Exocytosis of E-cadherin is slow in PALS1 KD cells	69
3.15	E-cadherin puncta in PALS1 KD cells are different from endocytic vesicles	70
3.16	Costaining of E-cadherin and markers of intracellular compartments	72
3.17	Density distributions of cytosolic and intracellular compartmental markers	73
3.18	Density distributions of E-cadherin and Sec8	75
3.19	Immunofluorescence of Sec8	77
4.1	Schematic illustration of DLG	87

4.2	Intramolecular interaction between PALS1 SH3 domain and GUK domain	89
4.3	PALS1 carboxyl-terminus mediates the interaction with its SH3 domain	91
4.4	PALS1 carboxyl-terminus is in the closed conformation	92
5.1	Hypothetical model of the two types of PAR6 PDZ domain interactions	101
5.2	The classical adhesion-to-polarity model and the polarity-to-adhesion hypothesis	106

CHAPTER 1

INTRODUCTION

1.1 Epithelial cell polarity and apical junctional complexes

The bodies of Metazoa enclose numerous highly organized cavities and compartments that are lined by sheets of epithelial cells. To protect the integrity of these cavities and compartments, epithelial cells have developed various intercellular junctions so that they are tightly packed and strongly adherent to one another. These junctions include the tight junctions (TJs) and the zonula adherens (ZA), which together comprise the apical junctional complexes. In addition to the protective function, epithelial cells are highly polarized, and they mediate diverse activities that depend on polarization, such as absorption, secretion, transcellular transport and sensation. The polarization of epithelial cells is reflected by the asymmetric distribution of proteins and lipids into the apical and basolateral surfaces. The apical domain faces the lumen while the basolateral domain consists of the basal domain that contacts the basement membrane and the lateral domain that contacts the neighboring cells. The process of apical-basal polarization is closely coupled to the establishment of the apical junctional complexes.

The tight junction, also referred to as the zonula occludens, is the apical-most structure of the intercellular junctional complex. It carries out two important functions: first, it forms tight seals between epithelial cells and creates a selectively permeable barrier to diffusion through the intercellular space, namely the barrier function (Diamond 1977); second, it physically separates the apical and basolateral membranes

and prevents the intermixing of the components of the two membrane domains, namely the fence function (Dragsten et al 1981). Tight junctions are revealed to be the tight apposition of neighboring epithelial cells in conventional electron micrographs, while in freeze-fracture electron micrographs, they appear as a continuous network of parallel and interconnected strands that circumscribe the apex of lateral membranes (Claude 1978). Tight junctions are composed of three families of transmembrane proteins: occludin, claudins and junctional adhesion molecules (JAMs). These proteins reach across the intercellular space and connect the membranes of adjacent epithelial cells (Shin et al 2006). The functional equivalent structure in *Drosophila* epithelia is the septate junction, which lies basal to the ZA and has a different molecular composition (Knust & Bossinger 2002).

The adhesion between epithelial cells is primarily contributed by the zonula adherens, which is also called the adherens junction in vertebrates. It is an adhesive belt that encircles the cell just below the apical surface, and it is located basal to TJs in mammalian epithelial cells. Cadherins represent the primary structural component of zonula adherens and their calcium-dependent *trans*-dimerization provides the adhesion between neighboring epithelial cells. Cryo-electron microscopy of the adherens junction reveals rod-like structures extending from the extracellular surface into the intercellular space and it is suggested that they represent the extracellular domains of E-cadherin (Miyaguchi 2000). Other AJ transmembrane components include Nectins and nectin-like molecules (Ncls), and they *trans*-interact in a calcium-independent manner (Nakanishi & Takai 2004).

The apical junctional complexes are dynamic structures. They undergo dramatic rearrangement and redistribution during embryonic development. The cytoplasmic domains of the junctional structural components are associated with

various adaptor proteins as well as signaling elements, and they are linked to the cytoskeletons. These connections integrate the dynamics of cell-cell junctions with a number of cellular processes such as migration, proliferation, differentiation as well as pathological processes which include tumor cell metastasis, infiltration and microbial infections.

1.2 Apical polarity complexes

The formation of the junctional complexes is intimately linked to cell polarization. Recent studies in mammalian systems and lower organisms have revealed several evolutionarily conserved protein complexes that regulate cell polarization. The complicated interplay amongst these complexes and their orderly functioning regulate the establishment of epithelial cell polarity and the cell-cell junctions. Studies of the apical membrane domain have focused on two major complexes, the partitioning defective (PAR) complex and the Crumbs (CRB) complex (Margolis & Borg 2005). These complexes are important in recognizing the initial polarization cues, and they play a pivotal role in regulating the establishment of apical junctional complexes. Work in both the mammalian and *Drosophila* systems have demonstrated that the PAR complex and the CRB complex have a conserved function in the establishment and maintenance of apical-basal polarity.

1.2.1 Function of the PAR complex in epithelial cell polarity

The six *par* genes and *protein kinase C3* (*pkc3*) were uncovered in a screen for defects in zygotic-axis specification in *C. elegans* (Kemphues et al 1988). The *par* genes encode primarily scaffolding proteins and serine threonine kinases (Macara

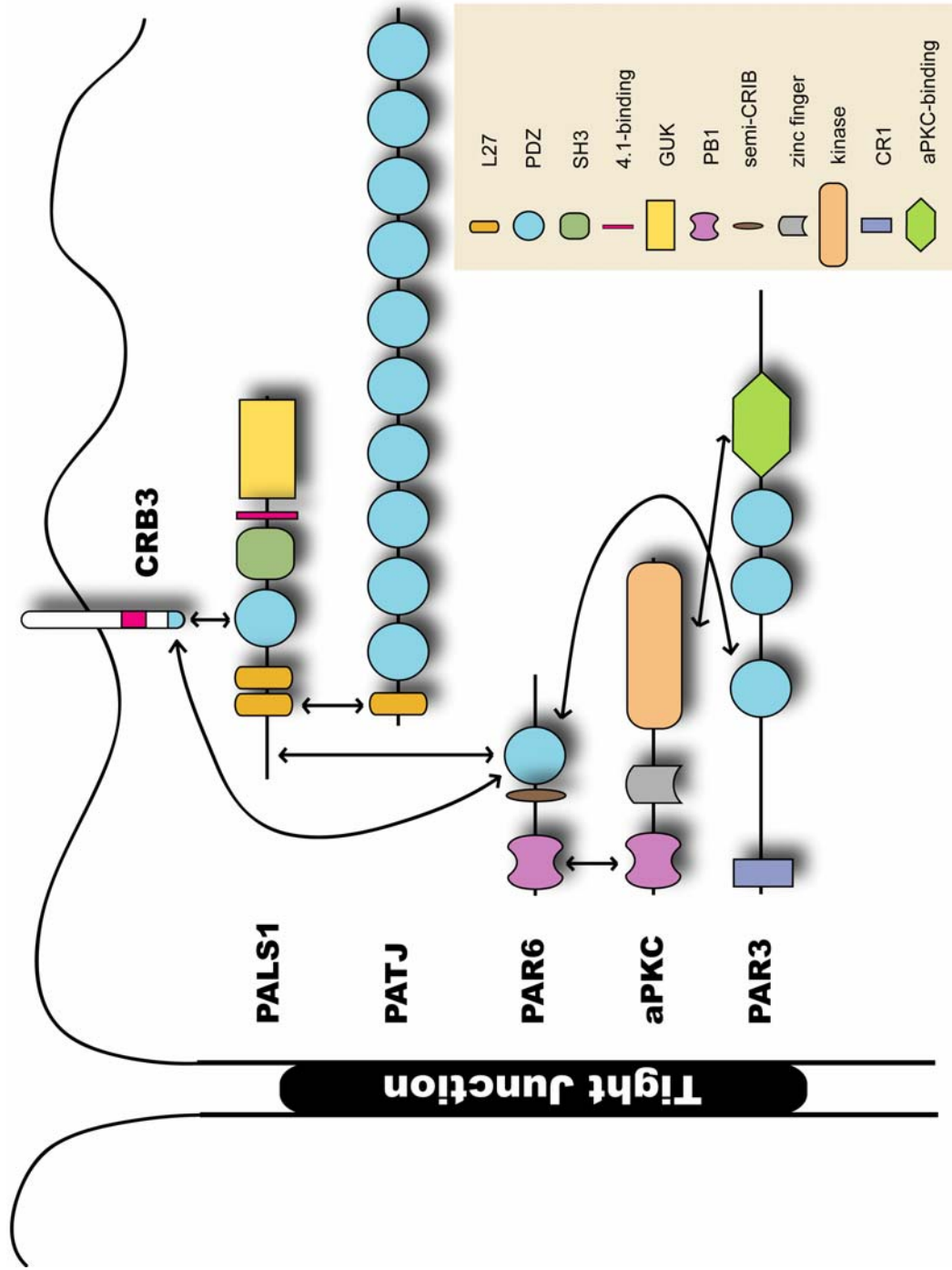
2004). PAR3 and PAR6, two scaffolding proteins as well as atypical PKC constitute the apical polarity PAR complex.

1.2.1.1 Structure of the PAR complex components and protein-protein interactions

PAR3, PAR6 and aPKC physically interact in a complex fashion (Figure 1.1). The aPKC-binding domain of PAR3 directly binds to the kinase domain of aPKC (Tabuse et al 1998), the PAR3-PAR6 interaction is between the PDZ domain of PAR6 and one of the three PDZ domains of PAR3, and the PB1 domain dimerization mediates the PAR6-aPKC interaction (Noda et al 2003, Qiu et al 2000). PAR3 can also oligomerize through its N-terminus (Benton & St Johnston 2003a, Mizuno et al 2003). In mammals, there are at least three splice variants of PAR3, four isoforms of PAR6 and two isoforms of aPKC, adding to the complexity (Gao & Macara 2004, Gao et al 2002b, Yoshii et al 2005). The *Drosophila* ortholog of PAR3 is Bazooka (Baz), which directly binds *Drosophila* aPKC and PAR6 (Rolls et al 2003, Wodarz et al 2000). The small GTPase Cdc42 has been known to be a central cell polarity regulator in many contexts, and the discovery of PAR6 as its effector largely explains this role. PAR6 binds Cdc42-GTP through its semi-Cdc42/Rac-interacting binding (CRIB) domain in concert with part of the PDZ domain (Joberty et al 2000, Johansson et al 2000, Lin et al 2000, Qiu et al 2000). The involvement of the PDZ domain was elucidated by the crystal structure of PAR6 bound to Cdc42-GTP, which showed that the semi-CRIB domain and the adjacent PDZ domain form a continuous eight-stranded sheet that binds Cdc42 (Garrard et al 2003).

In *Drosophila*, the three components of the PAR complex are dependent upon one another for correct localization in the process of epithelial morphogenesis

Figure 1.1 Domain structures of components of the PAR complex and the CRB complex. Protein domains are represented by filled shapes as denoted in the inset. Note that CRB3 is depicted larger in proportion to other proteins, and the purple and blue fills represent the FERM-binding motif and the PDZ-binding motif respectively. Protein-protein interactions are indicated by double-headed arrows.



(Petronczki & Knoblich 2001, Rolls et al 2003, Wodarz et al 2000). Yet, the three proteins do not always colocalize, and very often, PAR3 segregates from PAR6 and aPKC. This phenomenon has been observed in various cell types including *C. elegans* one-cell embryos (Tabuse et al 1998), migrating mammalian astrocytes (Etienne-Manneville & Hall 2001), *Drosophila* photoreceptors (Nam & Choi 2003) and polarized MDCK cells (Vogelmann & Nelson 2005). These findings suggest that PAR3 and PAR6-aPKC can function independently in certain situations.

1.2.1.2 Molecular actions of the PAR complex in epithelial polarity

The PAR complex is involved in a broader range of cell types than the CRB complex and it regulates more diverse polarity-related cellular events. Besides its established role in the development of *Drosophila* embryonic ectoderm (Petronczki & Knoblich 2001, Wodarz et al 2000) and the formation of TJs in mammalian epithelial cells (Gao et al 2002a, Mizuno et al 2003, Suzuki et al 2001), the PAR complex also plays a role in a variety of processes which include anterior-posterior axis specification of the *C. elegans* zygote and the *Drosophila* oocyte, the asymmetric division of *Drosophila* neuroblasts and sensory-organ precursor cells, the axon specification of mammalian hippocampal neurons, and the oriented migration and the localization of microtubule-organizing center (MTOC) in various mammalian cell types (Macara 2004, Suzuki & Ohno 2006).

A common theme is that, the PAR3-PAR6-aPKC complex resides at the side of the cell that develops into the apical/anterior domain, and the PAR1 kinase occupies the opposite side and specifies the basal/posterior domain. The molecular basis of the mutually exclusive localization of PAR3-PAR6-aPKC and PAR1 kinase is beginning to be revealed. In *Drosophila*, PAR1 phosphorylates Baz creating a

binding site for the PAR5 protein, a 14-3-3 family member. The subsequent binding of 14-3-3 to Baz inhibits the interaction between Baz and aPKC as well as the formation of the Baz-PAR6-aPKC complex, excluding the complex from the lateral membrane where PAR1 is localized (Benton & St Johnston 2003b). In mammals, an opposite mechanism has been demonstrated: aPKC phosphorylates PAR1 at the TJs, and the phosphorylation-dependent binding of 14-3-3 to PAR1 dissociates it from the apical domain (Hurov et al 2004, Suzuki et al 2004). Nonetheless, 14-3-3 also interacts with phosphorylated PAR3 in mammalian cells and the disruption of this interaction leads to polarity defects (Hurd et al 2003a), demonstrating cooperative apical and basolateral exclusion mechanisms.

The molecular actions of the PAR complex in epithelial polarity are still being elucidated but the following model can be proposed as a starting point based on data from multiple organisms (Figure 1.2). PAR3 is localized to the cell-cell contact sites early in polarizing cells through its interaction with the TJ structural component JAM-1 and the AJ components Nectin-1 and -3 (Ebnet et al 2001, Itoh et al 2001, Takekuni et al 2003). On the other hand, PAR6 and aPKC forms a precomplex with Lethal Giant Larvae (Lgl), which was originally identified as a tumor suppressor gene and later shown to be an important basolateral determinant (Ohshiro et al 2000, Peng et al 2000). Upon the binding of Cdc42-GTP, PAR6 undergoes a conformational change and this change results in stronger PAR6-aPKC interaction and higher aPKC kinase activity (Garrard et al 2003), leading to the phosphorylation of Lgl. Phosphorylated Lgl dissociates from PAR6-aPKC and frees the interaction interface of PAR6 so that PAR6-aPKC is recruited by PAR3 and forms the PAR3-PAR6-aPKC complex. This in turn prevents the colocalization of Lgl with the PAR complex and limits it to the basolateral domain (Betschinger et al 2003, Plant et al 2003, Yamanaka et al 2003).

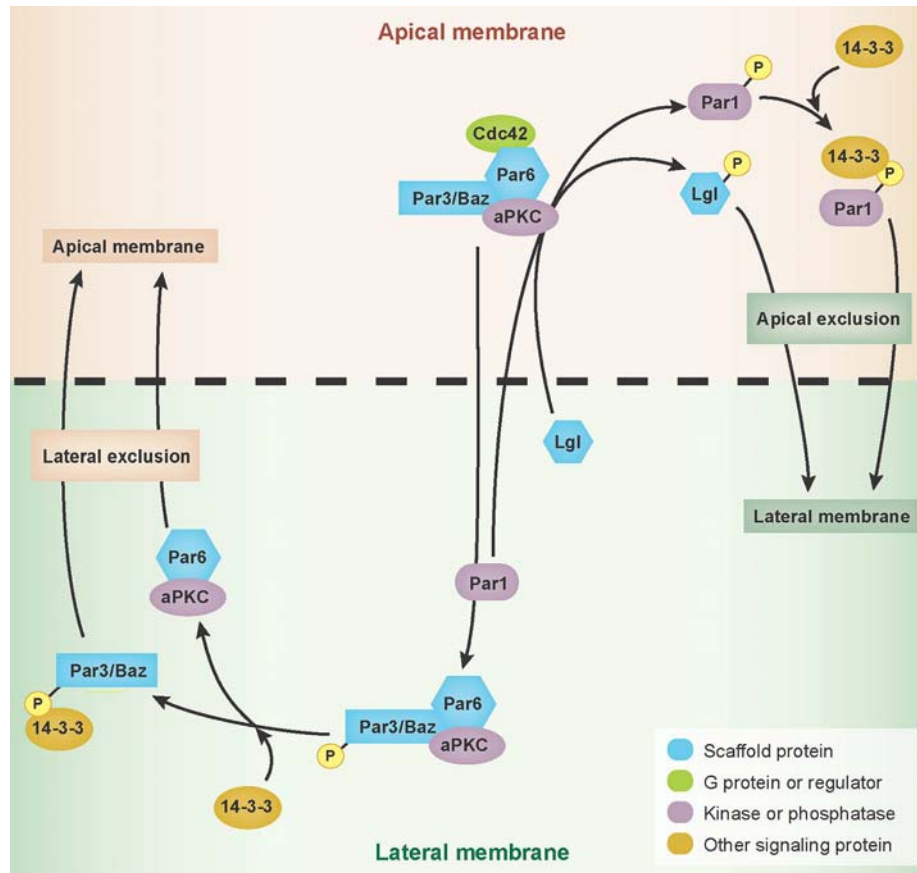


Figure 1.2 Mutual exclusion of polarity complexes in apico-basal polarity. Apical and lateral membranes are balanced by mutual exclusion of polarity proteins. The exclusion of proteins from either the apical or lateral domains is mediated by phosphorylation. For example, when Lgl crosses to the apical domain, it is phosphorylated and sent back to the basolateral surface. Similarly the localization of PAR3 and PAR1 is controlled by phosphorylation (see text for additional details).

As a result, the balance between the apical domain and basolateral domain is determined by the activity of the PAR complex at the apical domain and that of Lgl at the lateral domain (Shin et al 2006).

1.2.2 Function of the CRB complex in epithelial cell polarity

The CRB complex is composed of three proteins: Crumbs (CRB), protein associated with Lin Seven 1 (PALS1) and PALS1-associated tight junction protein (PATJ) (see Figure 1.1).

1.2.2.1 Crumbs

In *Drosophila*, CRB is localized to the apical membrane and the subapical region. The subapical region represents a spot where the apical membrane ends and the lateral membrane begins. In mammalian cells this is the site of the tight junction, but in *Drosophila* no junction is localized at this point. In *Drosophila*, CRB is an important apical membrane determinant, as the plasma-membrane-associated expression of CRB is necessary and sufficient to confer apical character on a membrane domain, and overexpression of CRB results in an expansion of the apical plasma membrane with concomitant reduction of the basolateral domain (Wodarz et al 1995). *Drosophila* CRB is a transmembrane protein with 30 EGF-like and 4 laminin A G-domain-like repeats in its extracellular domain. The exact function of this large extracellular domain is not clear, since a truncated form of CRB devoid of the entire extracellular domain is sufficient to rescue the CRB mutant *Drosophila* embryo (Wodarz et al 1995). The short cytoplasmic domain of CRB contains two functionally important motifs (Klebes & Knust 2000). The 4.1/ezrin/radaxin/moesin (FERM)-domain binding motif of zebrafish CRB binds a FERM protein Moe, and it has been shown recently that Yurt, the *Drosophila* ortholog of zebrafish Moe, interacts with the *Drosophila* CRB FERM-binding motif (Jensen & Westerfield 2004, Laprise et al 2006). This interaction is conserved between the mammalian Yurt orthologs YMO1 and EHM2 and the mammalian CRB proteins and may be part of a negative feedback loop that regulates CRB activity (Laprise et al 2006). The C-

terminal postsynaptic density/discs large/zonula occludens (PDZ)-domain binding motif, on the other hand, is recognized by the PDZ domain of Stardust (Sdt), the *Drosophila* homolog of PALS1 (Bachmann et al 2001, Hong et al 2001). The CRB-Sdt interaction is important for the biogenesis of the ZA, which is a pivotal step in the establishment of epithelial integrity (Grawe et al 1996, Tepass 1996).

Three mammalian CRB proteins have been identified, all of which consist of a transmembrane domain and an intracellular domain with the conserved FERM-binding and PDZ-binding motifs. CRB1 is the human ortholog of *Drosophila* CRB, and it is expressed primarily in the eye and brain. Mutations in CRB1 cause various diseases including Leber congenital amaurosis and retinitis pigmentosa (den Hollander et al 2001, den Hollander et al 1999). CRB2 has not been extensively characterized to date. CRB3 is expressed ubiquitously in epithelial tissues, and unlike *Drosophila* CRB and the other two mammalian CRB proteins, has a very short extracellular domain. CRB3 is localized to the apical membrane of mammalian epithelial cells and concentrated to TJs, where it interacts with PALS1 with its C-terminal PDZ-binding motif (Makarova et al 2003, Roh et al 2002b). Overexpression of CRB3 in Madin Darby canine kidney (MDCK) cells leads to delayed tight junction formation and a disruption of cell polarity (Lemmers et al 2004, Roh et al 2003). Introducing CRB3 into the mammary epithelial MCF10A cells, which express little endogenous CRB3, induces the formation of TJs (Fogg et al 2005). CRB3 has also been shown to localize to the primary cilia and it is required for ciliogenesis of MDCK cells (Fan et al 2004).

1.2.2.2 PATJ

PATJ contains one L27 domain at the N-terminus and ten PDZ domains. It interacts with PALS1 through L27 domain dimerization (Lemmers et al 2002, Roh et al 2002b), and this interaction is important for the stability of PATJ in the mammalian epithelial cells (Straight et al 2004, Wang et al 2007). PATJ serves as a scaffold and its multiple PDZ domains interact with various junction structural components, peripheral proteins and signaling elements, which include claudin-1, zonula occludens (ZO-3) and angiomin (Amot) (Roh et al 2002a, Wells et al 2006). Knockdown of PATJ in MDCK cells leads to a delay in TJ formation and cell polarity defects (Shin et al 2005), and the adenovirus protein E4-ORF1 induces the disassembly of TJs by interacting with PATJ and sequestering it from the junctions (Latorre et al 2005). *Drosophila* PATJ (DmPATJ), on the other hand, is a much smaller protein with only four PDZ domains besides the L27 domain. DmPATJ stabilizes the CRB complex and is required for rhabdomere stalk membrane maintenance during photoreceptor development (Richard et al 2006). Moreover, DmPATJ has been shown to interact with Frizzled, and it recruits atypical protein kinase C (aPKC) to Frizzled, resulting in the inhibition of Frizzled activity (Djiane et al 2005). This study indicates that DmPATJ could be a linker between the apical-basal polarity pathway and the planar cell polarity pathway.

Recent work indicates that PATJ plays a role in regulating the exocytosis of CRB3. Michel et al. reported that knockdown of PATJ in Caco2 cells causes the mislocalization of CRB3. CRB3 accumulates in a sub-apical compartment, and the CRB3-positive compartment partially overlaps with early endosomes indicated by EEA1 staining (Michel et al 2005). Our group observed similar CRB3 retention in PATJ-depleted MDCK cells, and the defect can be rescued when exogenous PATJ is re-introduced (unpublished data). These results suggest that PATJ is involved in the

formation of the apical membrane by regulating CRB3 exocytosis. It was also recently reported that a *Drosophila* syntaxin mutant leads to expansion of the apical membrane similar to that of CRB overexpression, presumably because defective endocytosis leads to excessive CRB on the apical membrane (Lu & Bilder 2005). Therefore, it appears that a balance between exocytosis and endocytosis of CRB is critical for the proper maintenance of the apical membrane domain.

1.2.2.3 PALS1/Stardust

The protein component that links CRB and PATJ in the CRB polarity complex is PALS1. PALS1 is a membrane-associated guanylate kinase (MAGUK) protein. It consists of two L27 domains, a PDZ domain, an SH3 domain, a Band 4.1-binding domain and a GUK domain (Kamberov et al 2000). The two L27 domains mediate its interaction with PATJ and Lin-7 respectively (Kamberov et al 2000, Roh et al 2002b), and the PDZ domain binds CRB3 in mammalian epithelial cells (Makarova et al 2003, Roh et al 2002b). The function of the C-terminal SH3, Band 4.1-binding and GUK domains are not known. In addition to these domains, the amino-terminal U1 region of PALS1 binds PAR6 (Hurd et al 2003b). RNA interference (RNAi)-mediated inhibition of PALS1 expression in mammalian epithelial cells leads to severe defects in cell-cell junction formation and cell polarity (Straight et al 2004). Sdt, the *Drosophila* ortholog of PALS1, acts downstream of CRB to regulate the formation of ZA and epithelial morphogenesis in flies. The mutations in Sdt produce a phenotype nearly identical to that of the CRB mutant (Tepass & Knust 1993). The PALS1 ortholog in zebrafish is Nagie Oko (Nok). It is essential in the biogenesis of photoreceptor cells in the retina (Wei & Malicki 2002), and it is required for myocardial coherence and heart tube elongation in concert with Heart and Soul/PKC ϵ

(Rohr et al 2006). A recent report suggests that Na⁺, K⁺ ATPase acts in the same genetic pathway of Nok in cardiac morphogenesis (Cibrian-Uhalte et al 2007).

1.2.3 Interplay between CRB complex and PAR complex

The CRB complex and the PAR complex work coordinately to define the apical domain of epithelial cells. The two complexes are mutually dependent upon one another for proper localization in the *Drosophila* photoreceptor (Hong et al 2003), and the knockdown of PALS1 in MDCK cells leads to the mislocalization of PAR3 (Straight et al 2004). PALS1 was shown to interact with PAR6 (Hurd et al 2003b), and this interaction is carefully characterized in Chapter 2 of this thesis. In addition to the PALS1-PAR6 interaction, biochemical studies have revealed other physical interactions between the two complexes (Figure 1.1). The PDZ domain of PAR6 also interacts directly with CRB3 (Lemmers et al 2004), and a recent study found that *Drosophila* CRB binds the PDZ domain of Sdt and DmPAR6 with similar affinity (Kempkens et al 2006). DmPATJ and DmPAR6 interact in *Drosophila* photoreceptors further tying together these two complexes that are colocalized in the rhabdomere stalk (Nam & Choi 2003). Besides the above mentioned interactions that are important for the localization of the two complexes, the aPKC-CRB and aPKC-PATJ interactions in *Drosophila* are functionally significant, as CRB was shown to be an aPKC substrate. A non-phosphorylatable CRB mutant behaves in vivo in a dominant negative fashion and disrupts epithelial cell polarity. Overexpression of a kinase-dead aPKC also causes serious defects in the structure of the epithelial layer, supporting the idea that aPKC-mediated phosphorylation of CRB may be important for cell polarity (Sotillos et al 2004).

The studies in this thesis investigate the function of PALS1 in the polarization of mammalian epithelial cells. Chapter 2 characterizes the interaction between the PAR6 PDZ domain and the N-terminal U1 region of PALS1 and further demonstrates that the interaction represents an unconventional mode of PDZ domain action. Chapter 3 reveals that PALS1 is not only important for tight junction formation, it is also involved in adherens junction biogenesis and E-cadherin trafficking. The RNAi-mediated knockdown and rescue experiments also show that the PALS1 carboxyl-terminal SH3 and GUK domains are indispensable in regulating mammalian epithelial cell polarity. To elucidate the function of the PALS1 carboxyl-terminus, in Chapter 4 a preliminary study of the SH3-GUK intramolecular interaction is presented.

BIBLIOGRAPHY

- Bachmann A, Schneider M, Theilenberg E, Grawe F, Knust E. 2001. *Drosophila* Stardust is a partner of Crumbs in the control of epithelial cell polarity. *Nature* 414: 638-43
- Benton R, St Johnston D. 2003a. A conserved oligomerization domain in *Drosophila* Bazooka/PAR-3 is important for apical localization and epithelial polarity. *Curr Biol* 13: 1330-4
- Benton R, St Johnston D. 2003b. *Drosophila* PAR-1 and 14-3-3 inhibit Bazooka/PAR-3 to establish complementary cortical domains in polarized cells. *Cell* 115: 691-704
- Betschinger J, Mechtler K, Knoblich JA. 2003. The Par complex directs asymmetric cell division by phosphorylating the cytoskeletal protein Lgl. *Nature* 422: 326-30
- Cibrian-Uhalte E, Langenbacher A, Shu X, Chen JN, Abdelilah-Seyfried S. 2007. Involvement of zebrafish Na⁺,K⁺ ATPase in myocardial cell junction maintenance. *J Cell Biol* 176: 223-30
- Claude P. 1978. Morphological factors influencing transepithelial permeability: a model for the resistance of the zonula occludens. *J Membr Biol* 39: 219-32
- den Hollander AI, Heckenlively JR, van den Born LI, de Kok YJ, van der Velde-Visser SD, et al. 2001. Leber congenital amaurosis and retinitis pigmentosa with Coats-like exudative vasculopathy are associated with mutations in the crumbs homologue 1 (CRB1) gene. *Am J Hum Genet* 69: 198-203
- den Hollander AI, ten Brink JB, de Kok YJ, van Soest S, van den Born LI, et al. 1999. Mutations in a human homologue of *Drosophila* crumbs cause retinitis pigmentosa (RP12). *Nat Genet* 23: 217-21
- Diamond JM. 1977. Twenty-first Bowditch lecture. The epithelial junction: bridge, gate, and fence. *Physiologist* 20: 10-8
- Djiane A, Yogev S, Mlodzik M. 2005. The apical determinants aPKC and dPatj regulate Frizzled-dependent planar cell polarity in the *Drosophila* eye. *Cell* 121: 621-31
- Dragsten PR, Blumenthal R, Handler JS. 1981. Membrane asymmetry in epithelia: is the tight junction a barrier to diffusion in the plasma membrane? *Nature* 294: 718-22
- Ebnet K, Suzuki A, Horikoshi Y, Hirose T, Meyer Zu Brickwedde MK, et al. 2001. The cell polarity protein ASIP/PAR-3 directly associates with junctional adhesion molecule (JAM). *Embo J* 20: 3738-48

- Etienne-Manneville S, Hall A. 2001. Integrin-mediated activation of Cdc42 controls cell polarity in migrating astrocytes through PKCzeta. *Cell* 106: 489-98
- Fan S, Hurd TW, Liu CJ, Straight SW, Weimbs T, et al. 2004. Polarity proteins control ciliogenesis via kinesin motor interactions. *Curr Biol* 14: 1451-61
- Fogg VC, Liu CJ, Margolis B. 2005. Multiple regions of Crumbs3 are required for tight junction formation in MCF10A cells. *J Cell Sci* 118: 2859-69
- Gao L, Joberty G, Macara IG. 2002a. Assembly of epithelial tight junctions is negatively regulated by Par6. *Curr Biol* 12: 221-5
- Gao L, Macara IG. 2004. Isoforms of the polarity protein par6 have distinct functions. *J Biol Chem* 279: 41557-62
- Gao L, Macara IG, Joberty G. 2002b. Multiple splice variants of Par3 and of a novel related gene, Par3L, produce proteins with different binding properties. *Gene* 294: 99-107
- Garrard SM, Capaldo CT, Gao L, Rosen MK, Macara IG, Tomchick DR. 2003. Structure of Cdc42 in a complex with the GTPase-binding domain of the cell polarity protein, Par6. *Embo J* 22: 1125-33
- Grawe F, Wodarz A, Lee B, Knust E, Skaer H. 1996. The Drosophila genes crumbs and stardust are involved in the biogenesis of adherens junctions. *Development* 122: 951-9
- Hong Y, Ackerman L, Jan LY, Jan YN. 2003. Distinct roles of Bazooka and Stardust in the specification of Drosophila photoreceptor membrane architecture. *Proc Natl Acad Sci U S A* 100: 12712-7
- Hong Y, Stronach B, Perrimon N, Jan LY, Jan YN. 2001. Drosophila Stardust interacts with Crumbs to control polarity of epithelia but not neuroblasts. *Nature* 414: 634-8
- Hurd TW, Fan S, Liu CJ, Kweon HK, Hakansson K, Margolis B. 2003a. Phosphorylation-dependent binding of 14-3-3 to the polarity protein Par3 regulates cell polarity in mammalian epithelia. *Curr Biol* 13: 2082-90
- Hurd TW, Gao L, Roh MH, Macara IG, Margolis B. 2003b. Direct interaction of two polarity complexes implicated in epithelial tight junction assembly. *Nat Cell Biol* 5: 137-42
- Hurov JB, Watkins JL, Piwnicka-Worms H. 2004. Atypical PKC phosphorylates PAR-1 kinases to regulate localization and activity. *Curr Biol* 14: 736-41
- Itoh M, Sasaki H, Furuse M, Ozaki H, Kita T, Tsukita S. 2001. Junctional adhesion molecule (JAM) binds to PAR-3: a possible mechanism for the recruitment of PAR-3 to tight junctions. *J Cell Biol* 154: 491-7

- Jensen AM, Westerfield M. 2004. Zebrafish mosaic eyes is a novel FERM protein required for retinal lamination and retinal pigmented epithelial tight junction formation. *Curr Biol* 14: 711-7
- Joberty G, Petersen C, Gao L, Macara IG. 2000. The cell-polarity protein Par6 links Par3 and atypical protein kinase C to Cdc42. *Nat Cell Biol* 2: 531-9
- Johansson A, Driessens M, Aspenstrom P. 2000. The mammalian homologue of the *Caenorhabditis elegans* polarity protein PAR-6 is a binding partner for the Rho GTPases Cdc42 and Rac1. *J Cell Sci* 113 (Pt 18): 3267-75
- Kamberov E, Makarova O, Roh M, Liu A, Karnak D, et al. 2000. Molecular cloning and characterization of Pals, proteins associated with mLin-7. *J Biol Chem* 275: 11425-31
- Kemphues KJ, Priess JR, Morton DG, Cheng NS. 1988. Identification of genes required for cytoplasmic localization in early *C. elegans* embryos. *Cell* 52: 311-20
- Kempkens O, Medina E, Fernandez-Ballester G, Ozuyaman S, Le Bivic A, et al. 2006. Computer modelling in combination with in vitro studies reveals similar binding affinities of *Drosophila* Crumbs for the PDZ domains of Stardust and DmPar-6. *Eur J Cell Biol* 85: 753-67
- Klebes A, Knust E. 2000. A conserved motif in Crumbs is required for E-cadherin localisation and zonula adherens formation in *Drosophila*. *Curr Biol* 10: 76-85
- Knust E, Bossinger O. 2002. Composition and formation of intercellular junctions in epithelial cells. *Science* 298: 1955-9
- Laprise P, Beronja S, Silva-Gagliardi NF, Pellikka M, Jensen AM, et al. 2006. The FERM protein Yurt is a negative regulatory component of the Crumbs complex that controls epithelial polarity and apical membrane size. *Dev Cell* 11: 363-74
- Latorre IJ, Roh MH, Frese KK, Weiss RS, Margolis B, Javier RT. 2005. Viral oncoprotein-induced mislocalization of select PDZ proteins disrupts tight junctions and causes polarity defects in epithelial cells. *J Cell Sci* 118: 4283-93
- Lemmers C, Medina E, Delgrossi MH, Michel D, Arsanto JP, Le Bivic A. 2002. hINADI/PATJ, a homolog of discs lost, interacts with crumbs and localizes to tight junctions in human epithelial cells. *J Biol Chem* 277: 25408-15
- Lemmers C, Michel D, Lane-Guermonprez L, Delgrossi MH, Medina E, et al. 2004. CRB3 binds directly to Par6 and regulates the morphogenesis of the tight junctions in mammalian epithelial cells. *Mol Biol Cell* 15: 1324-33

- Lin D, Edwards AS, Fawcett JP, Mbamalu G, Scott JD, Pawson T. 2000. A mammalian PAR-3-PAR-6 complex implicated in Cdc42/Rac1 and aPKC signalling and cell polarity. *Nat Cell Biol* 2: 540-7
- Lu H, Bilder D. 2005. Endocytic control of epithelial polarity and proliferation in *Drosophila*. *Nat Cell Biol* 7: 1232-9
- Macara IG. 2004. Parsing the polarity code. *Nat Rev Mol Cell Biol* 5: 220-31
- Makarova O, Roh MH, Liu CJ, Laurinec S, Margolis B. 2003. Mammalian Crumbs3 is a small transmembrane protein linked to protein associated with Lin-7 (Pals1). *Gene* 302: 21-9
- Margolis B, Borg JP. 2005. Apicobasal polarity complexes. *J Cell Sci* 118: 5157-9
- Michel D, Arsanto JP, Massey-Harroche D, Beclin C, Wijnholds J, Le Bivic A. 2005. PATJ connects and stabilizes apical and lateral components of tight junctions in human intestinal cells. *J Cell Sci* 118: 4049-57
- Miyaguchi K. 2000. Ultrastructure of the zonula adherens revealed by rapid-freeze deep-etching. *J Struct Biol* 132: 169-78
- Mizuno K, Suzuki A, Hirose T, Kitamura K, Kutsuzawa K, et al. 2003. Self-association of PAR-3-mediated by the conserved N-terminal domain contributes to the development of epithelial tight junctions. *J Biol Chem* 278: 31240-50
- Nakanishi H, Takai Y. 2004. Roles of nectins in cell adhesion, migration and polarization. *Biol Chem* 385: 885-92
- Nam SC, Choi KW. 2003. Interaction of Par-6 and Crumbs complexes is essential for photoreceptor morphogenesis in *Drosophila*. *Development* 130: 4363-72
- Noda Y, Kohjima M, Izaki T, Ota K, Yoshinaga S, et al. 2003. Molecular recognition in dimerization between PB1 domains. *J Biol Chem* 278: 43516-24
- Ohshiro T, Yagami T, Zhang C, Matsuzaki F. 2000. Role of cortical tumour-suppressor proteins in asymmetric division of *Drosophila* neuroblast. *Nature* 408: 593-6
- Peng CY, Manning L, Albertson R, Doe CQ. 2000. The tumour-suppressor genes *lgl* and *dlg* regulate basal protein targeting in *Drosophila* neuroblasts. *Nature* 408: 596-600
- Petronczki M, Knoblich JA. 2001. DmPAR-6 directs epithelial polarity and asymmetric cell division of neuroblasts in *Drosophila*. *Nat Cell Biol* 3: 43-9
- Plant PJ, Fawcett JP, Lin DC, Holdorf AD, Binns K, et al. 2003. A polarity complex of mPar-6 and atypical PKC binds, phosphorylates and regulates mammalian *Lgl*. *Nat Cell Biol* 5: 301-8

- Qiu RG, Abo A, Steven Martin G. 2000. A human homolog of the *C. elegans* polarity determinant Par-6 links Rac and Cdc42 to PKC ζ signaling and cell transformation. *Curr Biol* 10: 697-707
- Richard M, Grawe F, Knust E. 2006. DPATJ plays a role in retinal morphogenesis and protects against light-dependent degeneration of photoreceptor cells in the *Drosophila* eye. *Dev Dyn* 235: 895-907
- Roh MH, Fan S, Liu CJ, Margolis B. 2003. The Crumbs3-Pals1 complex participates in the establishment of polarity in mammalian epithelial cells. *J Cell Sci* 116: 2895-906
- Roh MH, Liu CJ, Laurinec S, Margolis B. 2002a. The carboxyl terminus of zona occludens-3 binds and recruits a mammalian homologue of discs lost to tight junctions. *J Biol Chem* 277: 27501-9
- Roh MH, Makarova O, Liu CJ, Shin K, Lee S, et al. 2002b. The Maguk protein, Pals1, functions as an adapter, linking mammalian homologues of Crumbs and Discs Lost. *J Cell Biol* 157: 161-72
- Rohr S, Bit-Avragim N, Abdelilah-Seyfried S. 2006. Heart and soul/PRKCi and nagie oko/Mpp5 regulate myocardial coherence and remodeling during cardiac morphogenesis. *Development* 133: 107-15
- Rolls MM, Albertson R, Shih HP, Lee CY, Doe CQ. 2003. *Drosophila* aPKC regulates cell polarity and cell proliferation in neuroblasts and epithelia. *J Cell Biol* 163: 1089-98
- Shin K, Fogg VC, Margolis B. 2006. Tight junctions and cell polarity. *Annu Rev Cell Dev Biol* 22: 207-35
- Shin K, Straight S, Margolis B. 2005. PATJ regulates tight junction formation and polarity in mammalian epithelial cells. *J Cell Biol* 168: 705-11
- Sotillos S, Diaz-Meco MT, Caminero E, Moscat J, Campuzano S. 2004. DaPKC-dependent phosphorylation of Crumbs is required for epithelial cell polarity in *Drosophila*. *J Cell Biol* 166: 549-57
- Straight SW, Shin K, Fogg VC, Fan S, Liu CJ, et al. 2004. Loss of PALS1 expression leads to tight junction and polarity defects. *Mol Biol Cell* 15: 1981-90
- Suzuki A, Hirata M, Kamimura K, Maniwa R, Yamanaka T, et al. 2004. aPKC acts upstream of PAR-1b in both the establishment and maintenance of mammalian epithelial polarity. *Curr Biol* 14: 1425-35
- Suzuki A, Ohno S. 2006. The PAR-aPKC system: lessons in polarity. *J Cell Sci* 119: 979-87

- Suzuki A, Yamanaka T, Hirose T, Manabe N, Mizuno K, et al. 2001. Atypical protein kinase C is involved in the evolutionarily conserved par protein complex and plays a critical role in establishing epithelia-specific junctional structures. *J Cell Biol* 152: 1183-96
- Tabuse Y, Izumi Y, Piano F, Kempthues KJ, Miwa J, Ohno S. 1998. Atypical protein kinase C cooperates with PAR-3 to establish embryonic polarity in *Caenorhabditis elegans*. *Development* 125: 3607-14
- Takekuni K, Ikeda W, Fujito T, Morimoto K, Takeuchi M, et al. 2003. Direct binding of cell polarity protein PAR-3 to cell-cell adhesion molecule nectin at neuroepithelial cells of developing mouse. *J Biol Chem* 278: 5497-500
- Tepass U. 1996. Crumbs, a component of the apical membrane, is required for zonula adherens formation in primary epithelia of *Drosophila*. *Dev Biol* 177: 217-25
- Tepass U, Knust E. 1993. Crumbs and stardust act in a genetic pathway that controls the organization of epithelia in *Drosophila melanogaster*. *Dev Biol* 159: 311-26
- Vogelmann R, Nelson WJ. 2005. Fractionation of the epithelial apical junctional complex: reassessment of protein distributions in different substructures. *Mol Biol Cell* 16: 701-16
- Wang Q, Chen XW, Margolis B. 2007. PALS1 Regulates E-Cadherin Trafficking in Mammalian Epithelial Cells. *Mol Biol Cell* 18: 874-85
- Wei X, Malicki J. 2002. *nagie oko*, encoding a MAGUK-family protein, is essential for cellular patterning of the retina. *Nat Genet* 31: 150-7
- Wells CD, Fawcett JP, Traweger A, Yamanaka Y, Goudreau M, et al. 2006. A Rich1/Amot complex regulates the Cdc42 GTPase and apical-polarity proteins in epithelial cells. *Cell* 125: 535-48
- Wodarz A, Hinz U, Engelbert M, Knust E. 1995. Expression of crumbs confers apical character on plasma membrane domains of ectodermal epithelia of *Drosophila*. *Cell* 82: 67-76
- Wodarz A, Ramrath A, Grimm A, Knust E. 2000. *Drosophila* atypical protein kinase C associates with Bazooka and controls polarity of epithelia and neuroblasts. *J Cell Biol* 150: 1361-74
- Yamanaka T, Horikoshi Y, Sugiyama Y, Ishiyama C, Suzuki A, et al. 2003. Mammalian Lgl forms a protein complex with PAR-6 and aPKC independently of PAR-3 to regulate epithelial cell polarity. *Curr Biol* 13: 734-43
- Yoshii T, Mizuno K, Hirose T, Nakajima A, Sekihara H, Ohno S. 2005. sPAR-3, a splicing variant of PAR-3, shows cellular localization and an expression

pattern different from that of PAR-3 during enterocyte polarization. *Am J Physiol Gastrointest Liver Physiol* 288: G564-70

CHAPTER 2

TIGHT JUNCTION PROTEIN PAR6 INTERACTS WITH AN EVOLUTIONARILY CONSERVED REGION IN THE AMINO TERMINUS OF PALS1/STARDUST

2.1 Introduction

Epithelial cells possess asymmetry with respect to the apicobasal axis reflected by the differential distribution of proteins and lipids in the apical and basolateral surfaces (Roh & Margolis 2003). Polarized mammalian epithelial cells have a tight junctional seal, which serves as a physical barrier that separates apical and basolateral membranes. It has been shown that proteins containing the PDZ domain play an important role during cell polarization (Sheng & Sala 2001), and multiple PDZ protein complexes are involved in the assembly and maintenance of tight junctions.

One of the major groups of PDZ proteins is the membrane-associated guanylate kinase protein, which has one or more PDZ domains as well as a SH3 domain and a noncatalytic GUK domain. Genetic and biochemical studies in *Drosophila melanogaster* have shown that membrane-associated guanylate kinase protein Stardust (Sdt) interacts with the transmembrane protein Crumbs (CRB) through its PDZ domain, and mutations in either CRB or Sdt cause polarity defects in *Drosophila* epithelia (Tepass & Knust 1993). The mammalian homologue of Sdt is PALS1 (Roh et al 2002). Like Sdt, the PDZ domain of PALS1 binds the C-terminal tail of mammalian CRB isoforms, and PALS1 also interacts with a multi-PDZ domain protein, PATJ, through L27 domain dimerization (Doerks et al 2000, Roh et al 2002). The CRB-PALS1-PATJ complex localizes to the tight junctions of mammalian

epithelial cells, and the disruption of the complex leads to defects in cell polarity (Straight et al 2004). Similarly, the *Drosophila* PATJ homologue, formerly known as discs lost (Dlt) (Bhat et al 1999, Pielage et al 2003), can interact with the L27 domain of Sdt. Therefore, the analogous complex in *D. melanogaster* is Crb-Sdt-PATJ.

Another evolutionarily conserved tight junction complex is composed of PDZ proteins PAR3, PAR6, and aPKC and the GTP-loaded form of the small GTPase Cdc42 (Joberty et al 2000, Lin et al 2000, Petronczki & Knoblich 2001, Wodarz et al 2000). The PAR3-PAR6-aPKC complex is important for determining polarity in many cell types, including *D. melanogaster* neuroblasts, the *Caenorhabditis elegans* zygote, and mammalian epithelial cells (Gao et al 2002, Lin et al 2000, Wodarz 2002). aPKC- λ and - ζ interacts with PAR6 through PB1 domain dimerization in the amino terminus of both proteins (Joberty et al 2000, Lin et al 2000, Noda et al 2003, Suzuki et al 2001), and both aPKC and PAR6 can bind PAR3 (Joberty et al 2000). PAR6 also interacts with the active form of Cdc42 and Rac. Both its Cdc42/Rac-interactive binding domain (CRIB)-like motif and the adjacent PDZ domain are required for this interaction (Joberty et al 2000, Lin et al 2000, Qiu et al 2000). The *Drosophila* homologues of PAR3, PAR6, and aPKC are Bazooka, DmPAR6, and DaPKC, respectively. They also form a complex and localize at the subapical region of the *Drosophila* epithelia (Knust & Bossinger 2002).

The two tight junction complexes have been studied separately until recently, when they were connected by the interaction between PALS1 and PAR6 (Hurd et al 2003). It was shown that PALS1 and PAR6 bind directly, and the interaction is between the PALS1 amino terminus and the CRIB and PDZ domains of PAR6. PDZ domains usually recognize the extreme carboxyl terminus of binding partners, but they can also recognize an internal binding site if the site is presented in a β -finger structure

that mimics the protein carboxyl terminus (Sheng & Sala 2001). In this chapter, we further characterized the PALS1-PAR6 interaction. We found that the PAR6 binding site in the PALS1 amino terminus and the interaction mechanism are conserved in the Sdt-DmPAR6 interaction in *D. melanogaster*. We also studied the relationship between PALS1-PATJ interaction and PALS1-PAR6 interaction, and our results indicate that the binding may be competitive rather than synergistic.

2.2 Materials and methods

2.2.1 Antibodies

Mouse monoclonal anti-Myc (9E10; Santa Cruz Biotechnology, Inc., Santa Cruz, CA), and rabbit polyclonal anti-HA (Y11; Upstate Biotechnology, Inc.) antibodies were utilized for immunoprecipitation and Western blotting experiments. Mouse anti-GST antibody (Cell Signaling) was used to detect the GST fusion proteins in the GST pulldown experiments. Mouse monoclonal anti-Myc, rat monoclonal anti-ZO-1 (Chemicon), and rabbit polyclonal anti-PALS1 (Roh et al 2002) antibodies were used in the immunostaining experiments.

2.2.2 Cell culture

MDCK type II cells and HEK293 cells were grown in Dulbecco's modified Eagle's medium (Invitrogen) containing 100 units of penicillin, 100 µg/ml streptomycin sulfate, 2 mM L-glutamine, and 10% fetal bovine serum. MDCK Myc-PALS1 (wild type and V37G mutant) and HA-PAR6B cell lines were maintained in media supplemented with 600 µg/ml G418 and 300 µg/ml hygromycin B, respectively.

2.2.3 MDCK stable cell lines

Early passage MDCK cells grown to ~30% confluence on 10-cm plastic dishes were transfected with 5 µg of pRK5-Myc-PALS1 V37G or pHA₃-PAR6B DNA constructs together with 0.5 µg of pSV2neo (for G418 selection) or pTRE2hyg (for hygromycin B selection) empty vectors using Fugene6 reagent (Roche Applied Science). Transfected cells were replated in medium containing 600 µg/ml G418 or 600 µg/ml hygromycin B 48 h after transfection. Medium was changed every 2–3 days. After 12 days of selection, surviving clones were picked and screened for Myc-PALS1 V37G or HA-PAR6B expression by immunostaining and Western blot.

2.2.4 DNA constructs

HA-PAR6B, Myc-PALS1, GST-PALS1(1–181), and Myc-PATJ constructs were generated as previously described (Hurd et al 2003, Roh et al 2002). Mutagenesis of HA-PAR6, Myc-PALS1, GST-PALS1, and Myc-PATJ constructs were carried out as previously described (Makarova et al 2000). GST-tagged Stardust (residues 1–256) and HA-tagged DmPAR6 were generated by PCR from *Drosophila* embryonic cDNA (Clontech) and cloned into pG-STag and pKH3 vectors, respectively. In identification of the Stardust U1 region, a 5'-end primer against the ECR1 and a 3'-end primer against the PDZ domain were used, and PCRs were carried out at the annealing temperatures of 50, 52, 54, and 56 °C. Only one specific product of 1.2 kb was obtained, and it was cloned into the pGEM-T easy vector (Promega) for sequencing.

2.2.5 Immunoprecipitation and blotting

Plasmids (3 μg for GST pulldown and 2 μg for coimmunoprecipitation or as indicated in the experiment) were transfected with Fugene6 reagent into HEK293 cells grown to 50% confluence on 10-cm dishes. After 48 h, cells were collected in 0.5 ml of lysis buffer (50 mM Tris (pH 7.4), 150 mM NaCl, 10% glycerol, 1% Triton X-100, 1.5 mM MgCl_2 , 1 mM EGTA, 10 mM NaF, 10 mM $\text{Na}_4\text{P}_2\text{O}_7$, 1 mM Na_3VO_5 , 1 mM phenylmethylsulfonyl fluoride, 10 $\mu\text{g}/\text{ml}$ leupeptin, and 20 $\mu\text{g}/\text{ml}$ aprotinin). HA-PAR6 stable MDCK cells were grown to confluence on 10-cm dishes and collected in 0.5 ml of lysis buffer likewise. Lysates were cleared by centrifugation (12,000 $\times g$ for 15 min at 4 $^\circ\text{C}$). For GST-PALS1 pulldowns, 10 μg of GST protein was used per experiment. Immunoprecipitation and Western blotting was performed as previously described (Hurd et al 2003).

2.2.6 Immunofluorescence Microscopy and Imaging

MDCK cells were seeded at a high density into the Lab-Tek II chamber slide system (Nalge Nunc). They were fixed in 4% formaldehyde/PBS for 10 min, permeabilized in 1% SDS/PBS for 5 min, and blocked in 2% goat serum/PBS for 1 h. Chamber slides were incubated with primary antibodies in blocking solution (monoclonal anti-Myc 9E10 (1:1000), monoclonal anti-ZO-1 (1:400), monoclonal anti-E-cadherin (1:1600), and polyclonal anti-PALS1 (1:200) overnight in a humidified chamber at 30 $^\circ\text{C}$. After extensive washes with PBS, chamber slides were incubated with fluorochrome-conjugated secondary antibody (1:1500 in blocking solution) for 2 h at 30 $^\circ\text{C}$. Subsequently, chamber slides were washed three times with PBS and mounted with ProLong antifade reagent (Molecular Probes, Inc., Eugene, OR). Immunofluorescence microscopy was performed at the University of Michigan Diabetes Center with an Olympus FluoView 500 scanning laser confocal microscope.

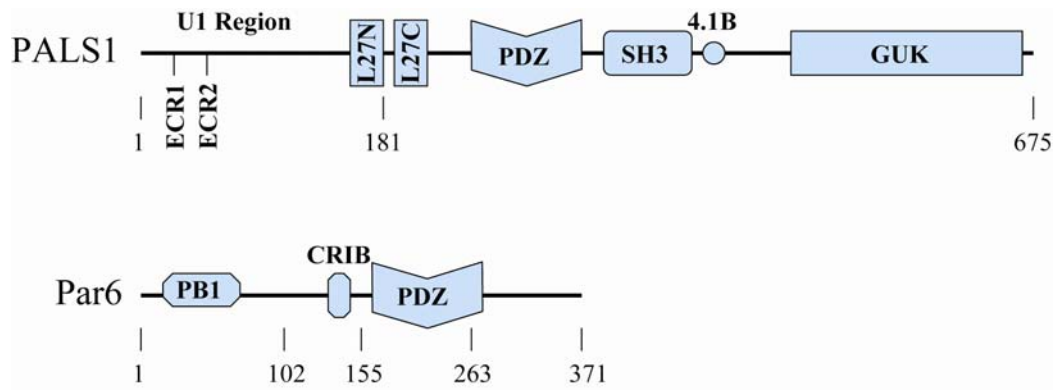


Figure 2.1 Schematic illustration of the domain structure of PALS1 and PAR6.

2.3 Results

2.3.1 PALS1 interacts with PAR6 through an evolutionarily conserved region in its amino terminus

It was previously shown that PALS1 interacts with PAR6 through its amino-terminal region aa 1–181 (Hurd et al 2003), which consists of the U1 region (aa 1–120) and the L27N domain (aa 121–181) (Figure 2.1). The L27N domain mediates the PALS1-PATJ interaction by L27 domain heterodimerization with the L27 domain of PATJ, whereas the function of the PALS1 U1 region is largely unknown. We made further deletions in the PALS1 amino terminus and performed GST pulldown experiments to precipitate HA-PAR6 expressed in HEK293 cells. We found that the first 20 amino acids of the U1 region are not required in this interaction, whereas the first 20 amino acids of the L27N domain are essential (data not shown). Thus, we determined the minimum binding region in PALS1 required for PAR6 binding to be amino acids 21–140.

	ECR1	ECR2
Dm	P HREMAVDCPD	QEQL RRRREEEER
Dr	R HREMAVDCPS	QED RRRREEEGRS
Mm	K HREMAVDCPG	QEDM RRRREEEGK
Hs	K HREMAVDCPG	QEDM RRRREEEGK

Figure 2.2 Alignment of the amino-terminal conserved regions in *Drosophila* (*Dm*), zebrafish (*Dr*), mouse (*Mm*), and human (*Hs*) PALS1. Two conserved regions were found and named ECR1 and ECR2 (for evolutionarily conserved regions 1 and 2).

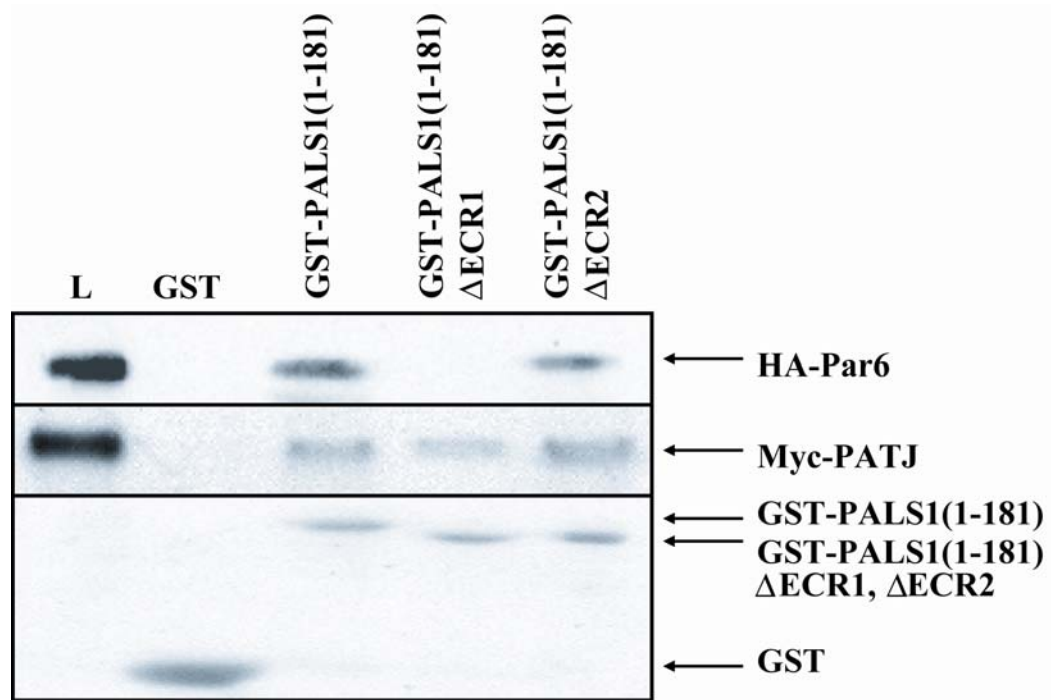


Figure 2.3 Deletion of ECR1 prevents pulldown of HA-PAR6. A recombinant GST fusion protein consisting of the U1 region and L27N domain of PALS1 (GST-PALS1(1–181)) or the same region with ECR1 or ECR2 deleted was immobilized on agarose beads and incubated with cell extract from HEK293 cells transiently transfected with HA-PAR6 or Myc-PATJ. Precipitating proteins were detected by immunoblotting for HA-PAR6 or Myc-PATJ. Cell lysates were also immunoblotted to monitor protein expression levels. GUK, guanylate kinase domain.

We performed an alignment of the PALS1 amino terminus and found two regions conserved in PALS1 from human, mouse, zebrafish, and *Drosophila* PALS1 homologue, Stardust (Figure 2.2). We named these regions evolutionarily conserved region 1 and 2 (ECR1 and ECR2, respectively). A GST-PALS1(1–181) fusion protein with the ECR1 deleted cannot bind HA-PAR6, whereas binding to Myc-PATJ is not affected (Figure 2.3). In contrast, deletion of the ECR2 region has no effect on PAR6 binding. We also expressed the ECR1 peptide alone fused to GST, but this was not able to bind PAR6. This indicates that the ECR1 region of PALS1 is necessary but not sufficient for PAR6 binding.

2.3.2 Point mutations in the PALS1 ECR1 reduce interactions with PAR6

To further characterize the PAR6 binding site, we mutated each amino acid in the PALS1 ECR1. Hydrophobic residues were mutated to glycine, whereas the other residues were mutated to alanine. GST-PALS1(1–181) containing ECR1 point mutations were bound to glutathione-agarose beads, and their ability to precipitate HA-PAR6 was tested. Two mutations, V37G and D38A, severely reduced the binding of PAR6 (Figure 2.4). In contrast, point mutations in the PALS1 L27N domain, V150G and L154G, that abolish the interaction with PATJ had no effect on PAR6 interactions. We next made more conservative mutations in Val-37 and Asp-38 by generating V37I and D38E and found near wild type binding of these two mutants to PAR6 (Figure 2.4, *bottom right panel*).

Similar experiments were also carried out in MDCK cells stably expressing HA-PAR6. The GST-PALS1(1–181) V37G and D38A bound HA-PAR6 poorly, whereas the V37I and the D38E mutants had no significant effect on binding (Figure 2.5).

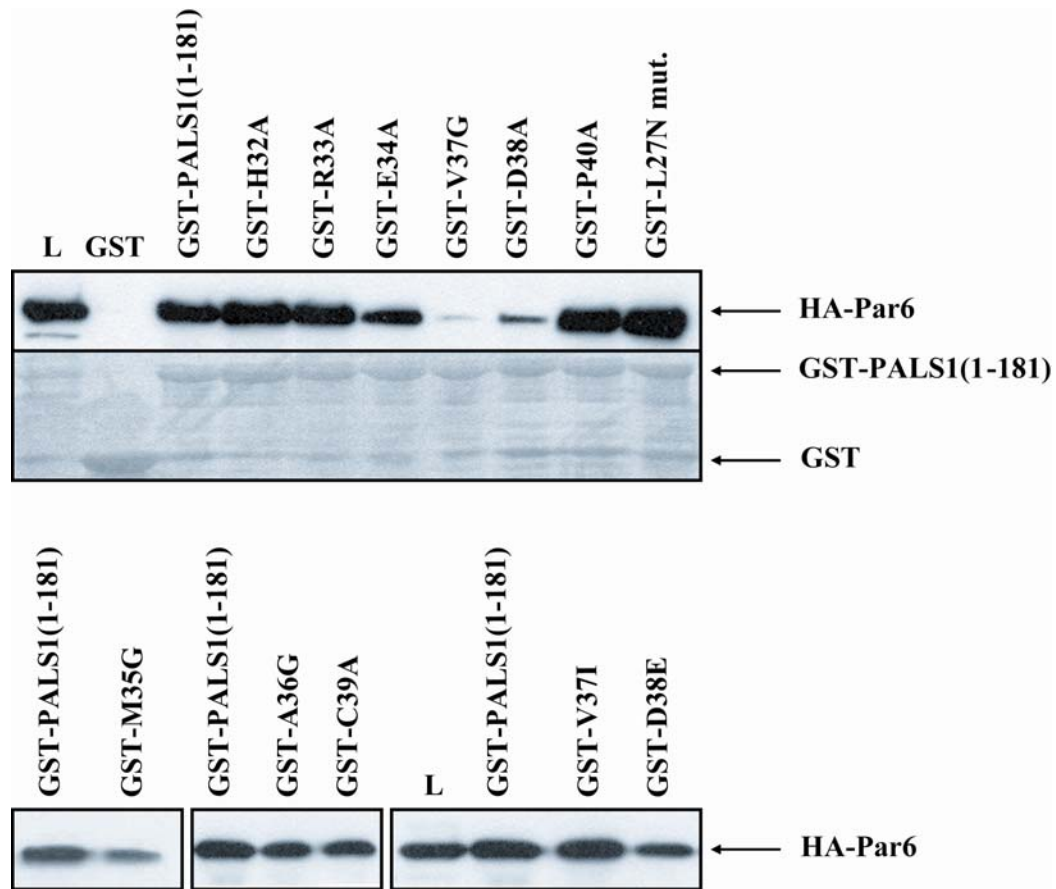


Figure 2.4 Val-37 and Asp-38 are critical for the interaction between PALS1 and Par6. Each amino acid in the ECR1 was mutated into either Ala or Gly, and the different point mutants of GST-PALS1(1-181) as well as the wild type were immobilized on agarose beads and incubated with cell lysates (*L*) from HEK293 cells transiently transfected with HA-PAR6. Both the V37G mutant and D38A mutants show a large decrease in binding. When the Val was mutated into Ile or the Asp was mutated into Glu, the pull-down of HA-Par6 was restored, suggesting a Φ -D/E binding site. The L27N mutant harbors V150G and L154G mutations, which disrupts the interaction between PALS1 and PATJ.

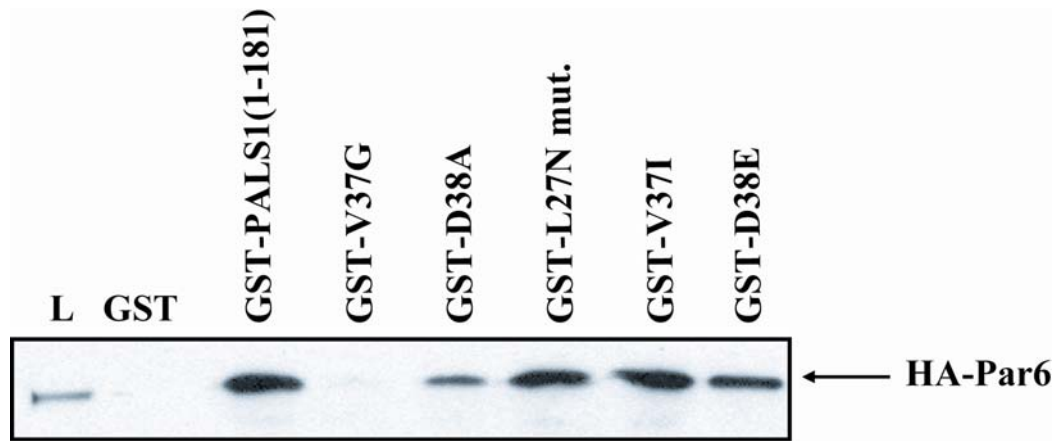


Figure 2.5 The binding site is confirmed with MDCK cell lysates. Cell lysates from a MDCK cell line stably expressing HA-PAR6 were incubated with GST, GST-PALS1(1–181), or the GST-PALS1 mutants bound to glutathione-agarose beads. The same precipitation pattern was observed when using HA-Par6 expressed in HEK293 cells.

Point mutations in the PALS1 L27N domain did not affect the interaction between PALS1 and PAR6.

2.3.3 PAR6 binding site in *Drosophila stardust*

We then examined whether this PAR6 binding site was functional in the PALS1 *Drosophila* homologue, Stardust. According to the published sequence (Hong et al 2001), Stardust has two splice variants: the 1292 aa SdtA and the 860 aa SdtB, which lacks the 432 amino acids in the U1 region encoded by alternatively spliced exon 3. We designed a 5'-primer against the ECR1 and a 3'-primer against a conserved region in the PDZ domain and performed a PCR from *Drosophila* embryonic cDNA (0.5–12-h pool). A PCR product of 1.2-kb was obtained and the sequencing of this product reveals a U1 region of 256 aa which corresponds to that of SdtB. Using additional oligonucleotides from this region, we were unable to obtain a

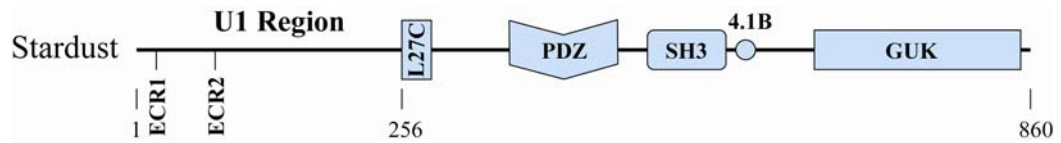


Figure 2.6 Schematic illustration of B isoform of *Drosophila* Stardust.

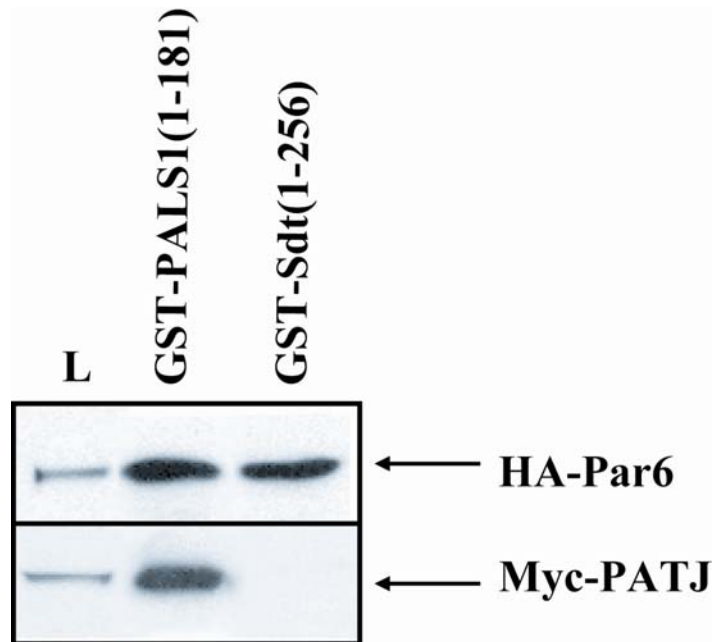


Figure 2.7 Stardust U1 region interacts with PAR6 but not with PATJ. Glutathione beads containing GST-Sdt(1–256) or GST-PALS1(1–181) were incubated with cell lysates (*L*) from HEK293 cells transiently transfected with HA-Par6 or Myc-PATJ. GST-Stardust(1–256) can pull down HA-PAR6 but not Myc-PATJ, since Stardust(1–256) lacks an L27 domain.

product containing exon 3 in any of our PCRs. Thus, we believe the predominant form of Stardust mRNA found in the embryo is SdtB as shown in Figure 2.6.

This U1 region (aa 1–256) of *Drosophila* SdtB was cloned and fused to GST. GST-Sdt(1–256) can bind HA-PAR6 in a similar fashion to GST-PALS1(1–181), but it does not interact with PATJ because it does not contain an L27 domain (Figure 2.7).

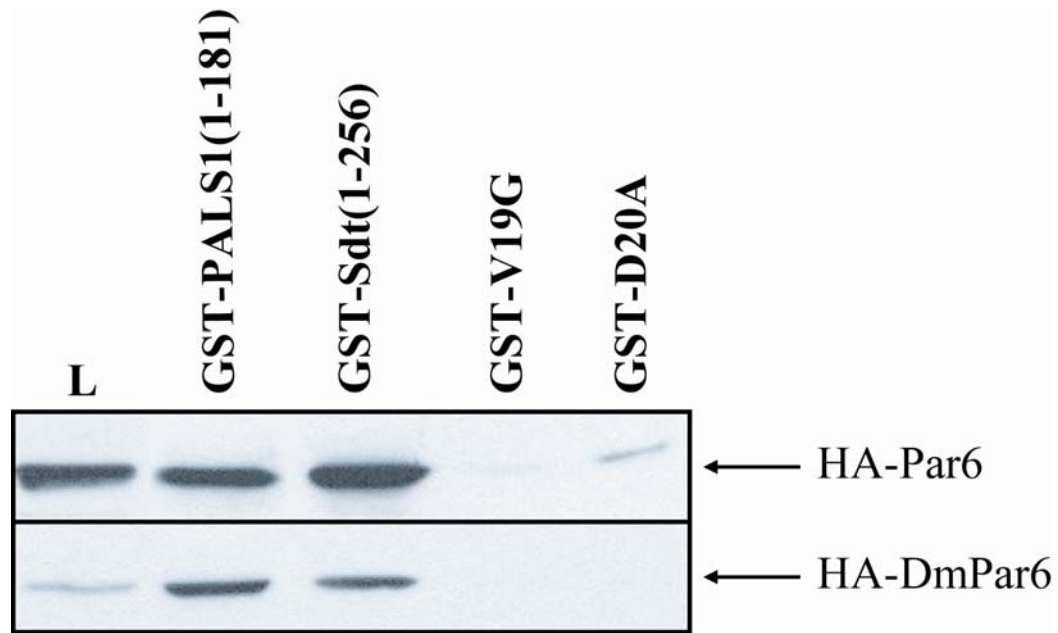


Figure 2.8 Val-19 and Asp-20 in Stardust ECR1 are also critical for its binding with PAR6. A GST pulldown experiment was carried out as above, with the GST-PALS1-(1-181), GST-Sdt-(1-256), or the GST-Sdt-(1-256) with Val-19 and Asp-20 in its ECR1 mutated to Gly and Ala, respectively, incubated with HEK293 cells transiently transfected with HA-PAR6 or HA-DmPAR6, the *Drosophila* homologue of PAR6. The V19G and the D20A mutants also show a decrease in the ability to bind both mammalian PAR6 and *Drosophila* PAR6.

Val-19 and Asp-20 in the Stardust ECR1 were analogous to the crucial binding residues Val-37 and Asp-38 in the PALS1 ECR. Mutation of these residues in GST-Sdt(1-256) to V19G and D20A impaired binding to mammalian and *Drosophila* PAR6 (DmPAR6) (Figure 2.8). These findings indicate that the same PAR6 binding site exists in Stardust ECR1, and the mechanism of interaction between PALS1/Stardust and PAR6 is likely to be conserved between *Drosophila* and the mammalian system.

2.3.4 Interaction between the PALS1 ECR1 and PAR6 CRIB-PDZ domains

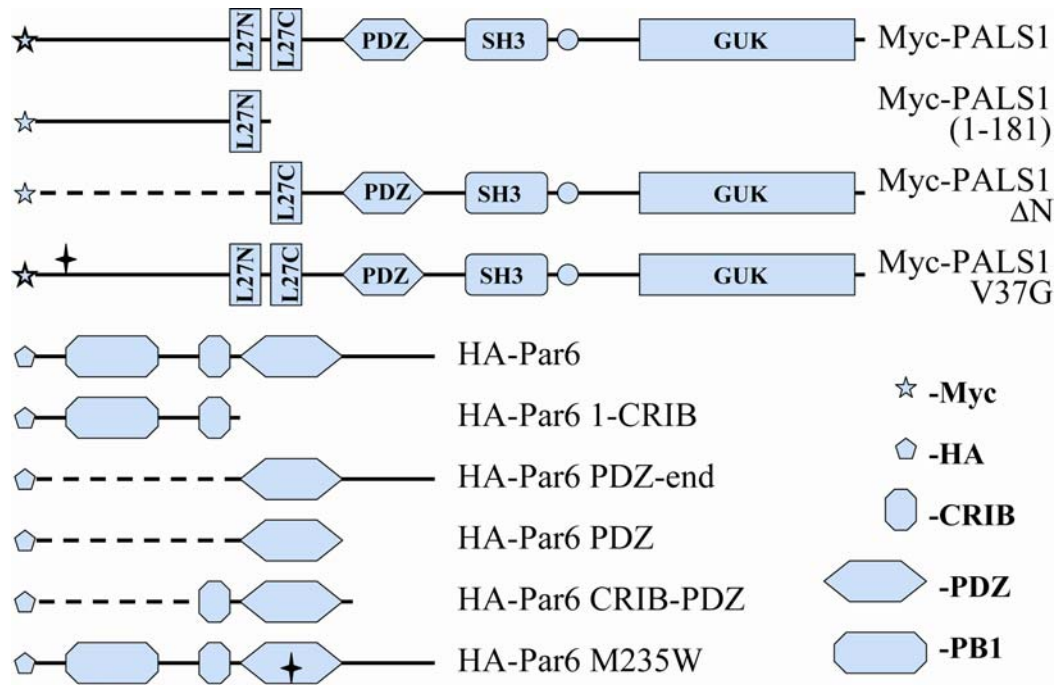


Figure 2.9 Schematic representation of Myc-PALS1 constructs and HA-PAR6 constructs. The PAR6^{M235W} mutant has a methionine mutated into tryptophan that blocks the PDZ domain binding pocket.

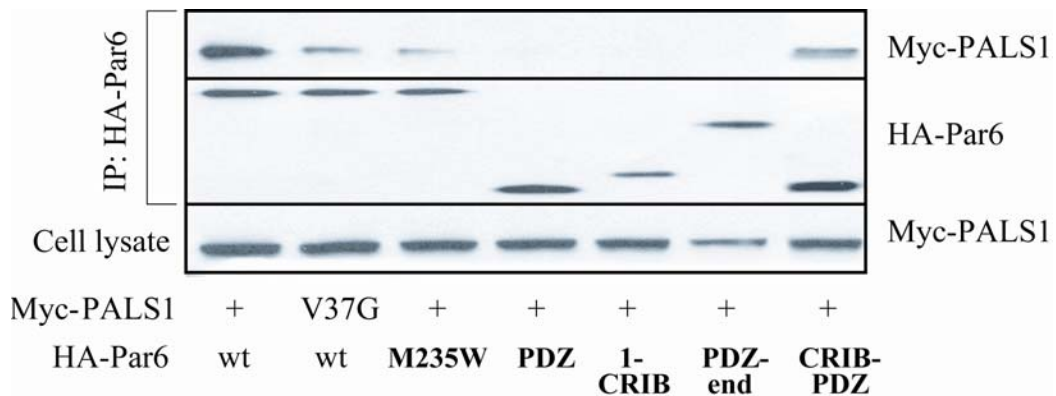


Figure 2.10 Further characterization of PALS1-PAR6 interaction. HEK293 cells were cotransfected with different Myc-PALS1 and HA-PAR6 constructs. HA-PAR6 was immunoprecipitated (IP), and the bound Myc-PALS1 was detected by immunoblotting. Point mutation in PALS1^{V37G} and PAR6^{M235W} both had decreased binding ability. The PAR6 CRIB-PDZ region is sufficient for the interaction with PALS1, although the interaction is weaker than wild type (*wt*) PAR6, whereas HA-PAR6 constructs lacking either the CRIB or PDZ domain cannot co-immunoprecipitate Myc-PALS1.

Previous results also showed that the PALS1-PAR6 interaction is mediated by a region that covers both the semi-CRIB domain and the PDZ domain in PAR6 (Hurd et al 2003). Since the PAR6 semi-CRIB domain and PDZ domain can form an integral structure and interact with Cdc42 (Garrard et al 2003), we wanted to test whether the PAR6 semi-CRIB domain and PDZ domain also work coordinately to bind PALS1 or whether either one of them is sufficient for the interaction. Different PAR6 deletion mutations were made and co-transfected into HEK293 cells with wild type Myc-PALS1 (Figure 2.9). Mutants with either the CRIB domain alone or PDZ domain alone cannot co-immunoprecipitate with Myc-PALS1, whereas the mutant with both domains present can interact with PALS1, although the interaction is not as strong as that of PAR6 wild type (Figure 2.10).

The V37A mutation was generated in full-length PALS1, and the mutant showed decreased interaction with PAR6 wild type in a coimmunoprecipitation experiment. A PAR6 point mutation, M235W, also resulted in weakened interactions with PALS1 wild type in a coimmunoprecipitation (Figure 2.10). PAR6 M235W alters a methionine residue in the PDZ binding pocket into a bulky tryptophan to block the PDZ domain-binding pocket, and this mutation abolishes the interaction between PAR6 and the two mammalian lethal giant larvae isoforms (mLgl-1 and mLgl-2) (Yamanaka et al 2003).

We noted that PALS1 V37G did not completely abolish binding with PAR6, as was seen with GST-PALS1(1–181) V37G, so it is possible that there are other PAR6 binding sites in PALS1 outside the aa 1–181 region. Also, we wanted to investigate the relationship between the PALS1 ECR1 and PAR6 PDZ domain, so we co-transfected different PALS1 truncation mutants (Figure 2.11) with either PAR6 wild type or PAR6 M235W mutant and performed coimmunoprecipitation

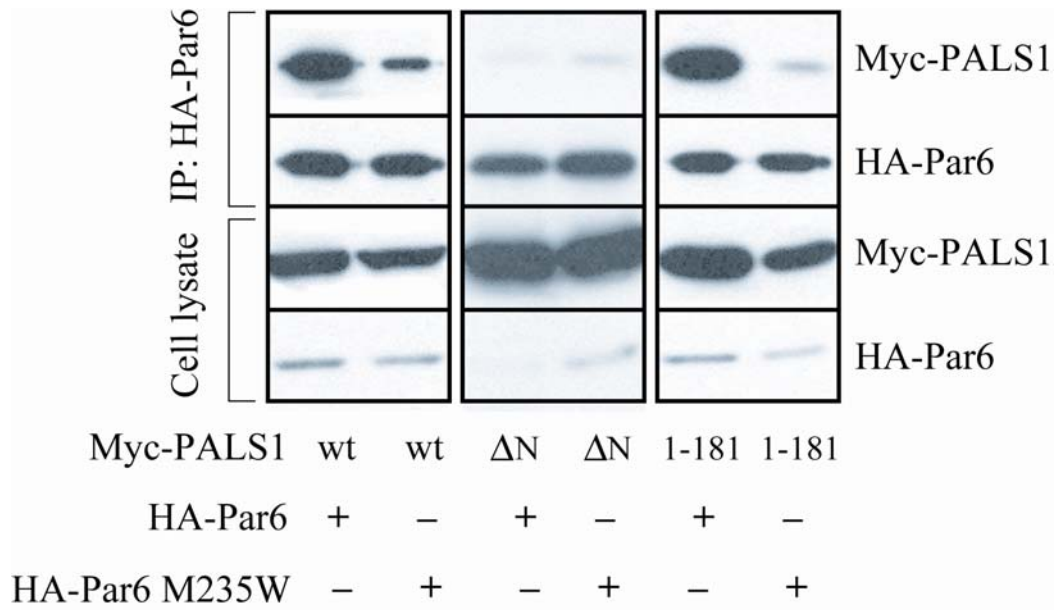


Figure 2.11 The interaction is primarily between the PAR6 CRIB-PDZ region and the PALS1 NH₂ terminus. HEK293 cells were cotransfected with Myc-PALS1, Myc-PALS1(ΔN) or Myc-PALS1-(1-181), and either HA-PAR6 or HA-PAR6^{M235W}. Co-immunoprecipitation was carried out as in *B*.

experiments. PALS1(1-181) shows a dramatic decrease in binding to PAR6 M235W like full-length PALS1, whereas the PALS1 ΔN only has residual interaction with both PAR6 wild type and PAR6 M235W. These coimmunoprecipitation results, together with the GST pulldown results in Figure 2.4 and 2.5, suggest that the PALS1-PAR6 interaction is through PALS1(1-181) and PAR6 CRIB-PDZ domains, and the interaction between PALS1 ECR1 (the valine residue) and PAR6 PDZ binding pocket is a major contributor to the binding between PALS1 and PAR6.

2.3.5 PALS1 V37G mutant is localized to the tight junction

To determine the subcellular localization of the PALS1 V37G mutant, a MDCK cell line that stably expresses Myc-PALS1 V37G was generated. As shown in Figure 2.12, Myc-PALS1 V37G mutant is localized at the tight junction as detected by

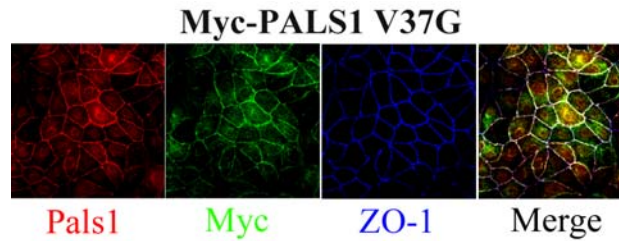


Figure 2.12 Localization of PALS1 V37G mutant. MDCK cells stably expressing Myc-PALS1 V37G were grown in chamber slides and then fixed, permeabilized, and stained for PALS1 (*red*), Myc (*green*), and the tight junction marker ZO-1 (*blue*) as described under "materials and methods".

Myc and PALS1 staining. It was co-localized with the tight junction marker ZO-1 and is above the adherens junction marker E-cadherin in the Z-section image (data not shown) just as the endogenous PALS1 did in the wild type MDCK cell line (Roh et al 2002). It was previously shown that the L27N domain of PALS1 is responsible for tight junction targeting, and deletion of just the U1 region did not disrupt the localization of PALS1 (Roh et al 2002). The V37G mutation in PALS1 U1 region does not affect the PALS1-PATJ interaction, and this probably explains the normal localization of this mutant in epithelial cells.

2.3.6 PAR6 interferes with PATJ in binding PALS1

A region of the PALS1 L27N domain is required for binding PAR6, but the reason for this requirement is not clear. However, as shown in Figure 2.4, mutations in PALS1 L27N domain that abolish PALS1-PATJ binding do not affect the PALS1-PAR6 binding; thus, we wanted to determine whether PALS1 and PATJ work synergistically to bind PAR6 as seems to be suggested by studies in *Drosophila* (Nam & Choi 2003). A constant amount of Myc-PATJ plasmid and increasing amounts of HA-PAR6 plasmid were co-transfected into HEK293 cells, and the cell lysates were

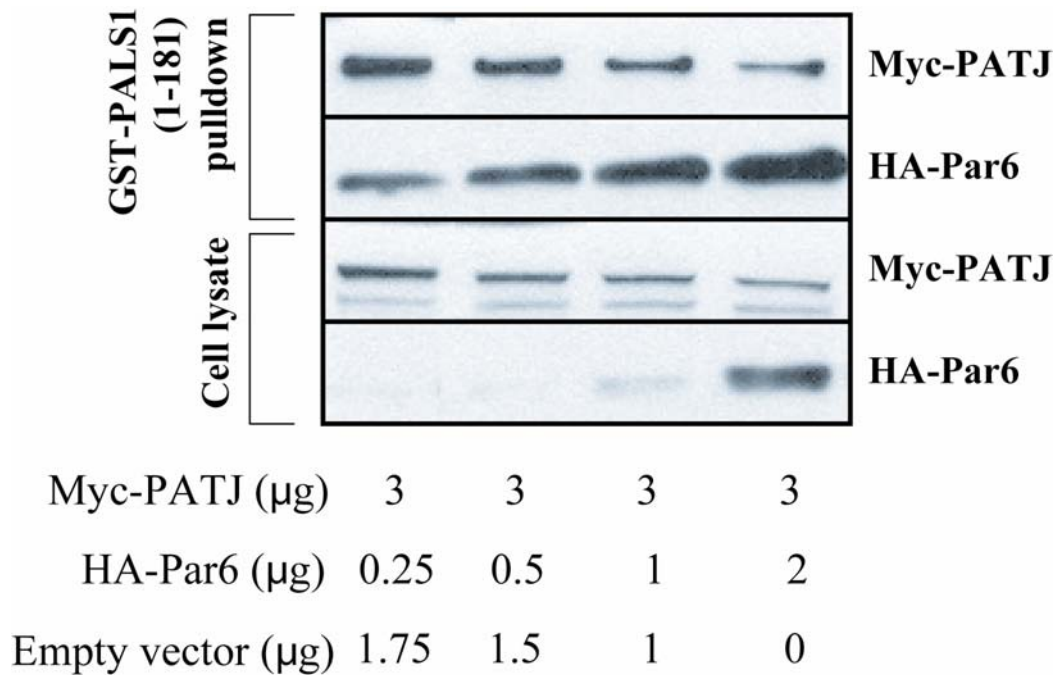


Figure 2.13 PAR6 and PATJ compete to bind PALS1. HEK293 cells were co-transfected with a fixed amount of Myc-PATJ and increasing amounts of HA-PAR6. The cell lysates were incubated with GST-PALS1-(1–181) beads, and the Myc-PATJ and HA-PAR6 precipitated were detected by anti-Myc and anti-HA immunoblot. A decreasing amount of RK5 empty vector was also transfected to make the total amount of transfected DNA equal.

incubated with GST-PALS1(1–181)-agarose beads. With the increase of PAR6 expression, there is an increase in PAR6 binding to GST-PALS1(1–181) and a decrease in PATJ binding (Figure 2.13). This result suggests that PAR6-PALS1 binding can interfere with PATJ-PALS1 binding, and these two interactions do not work synergistically.

2.4 Discussion

In this chapter, we identified the PAR6 binding site in the PALS1 amino-terminal region and showed that the same binding site also exists in Stardust, the *Drosophila* PALS1 homologue. The PALS1-PAR6 binding is mainly mediated by the

interaction between the binding site in the PALS1 ECR1 and the PAR6 PDZ domain binding pocket. PDZ domains are intracellular modules that usually bind the extreme carboxyl terminus of a protein and also can recognize internal sites when that site is presented in a β -finger structure that mimics the protein carboxyl terminus (Sheng & Sala 2001). The β -finger structure is usually stabilized by disulfide bonds or salt bridges. In the case of neuronal nitric-oxide synthase (nNOS)-syntrophin interaction, an Arg residue 9 aa downstream of the 0-position of the internal binding site in neuronal nitric-oxide synthase forms a salt bridge with the Asp residue and stabilizes the β -finger structure (Hillier et al 1999). We also found an Arg residue 9 aa downstream of Val-37 in PALS1 that is conserved among species, but the mutation of this Arg to Asp did not interfere with its binding to PAR6 in GST pulldown experiments (data not shown).

A recent report has shown that *Drosophila* PAR6 and PATJ bind to each other directly and that the interaction is between the amino terminus of DmPAR6 and the third PDZ domain of Dm-PATJ (Nam & Choi 2003). We cotransfected HEK293 cells with mammalian PAR6 and PATJ, and we did not see the coimmunoprecipitation of the two proteins. However, we do not exclude the possibility of PAR6-PATJ interaction in the process of polarization of MDCK cells, and this interaction may bring new complexity to the dynamic cooperation of the two tight junction complexes.

The newly identified mLgl-PAR6 interaction shows similarities to the PALS1-PAR6 interaction. It is mediated by binding of the amino-terminal region of mLgl, which contains several WD40 repeats, to the PAR6 PDZ domain (Betschinger et al 2003, Plant et al 2003, Yamanaka et al 2003), and the PAR6 M235W mutant cannot bind mLgl-1 or mLgl-2 (Yamanaka et al 2003). There is no detectable sequence homology between the mLgl amino terminus and PALS1 amino terminus, and there is

no sequence similar to the PALS1 ECR1 found in mLgl. However, the similarities of the two interactions suggest that further study of the mLgl-PAR6 interaction will probably help to elucidate the mechanism of the PALS1-PAR6 interaction and *vice versa*.

There was a requirement for the PALS1 L27N domain in the interaction between PAR6 and PALS1, yet its role is still not clear, since the *Drosophila* Stardust amino terminus lacking the L27 domain could still bind PAR6 (Figure 2.7). We made a series of deletions in the Stardust U1 region and found that Sdt(1–194) bound PAR6 as strongly as Sdt(1–256), and Sdt (1–154) still had substantial binding to PAR6. Based on these findings, we speculate that the first 20 amino acids of the PALS1 L27N domain help the PALS1 U1 region fold into a proper structure when the protein is expressed as a GST fusion protein. Similarly, we would speculate that this L27 region is not required in Stardust because of the larger amino terminus that can fill this role. Previous circular dichroism study suggested that L27 domains are largely unfolded individually, but when associated with their heterodimerization partners they show a significant increase in helicity as well as a cooperative unfolding transition with increasing temperature (Harris et al 2002). We propose that PALS1 may have two conformational states in its amino terminus. In state 1, when PALS1 interacts with PATJ, the PALS1 L27N domain is fully folded, heterodimerizing with the PATJ L27 domain. In state 2, the PALS1 L27N domain is largely unfolded, and the first 20 amino acids of the L27N domain fold with the adjacent U1 region to form a structure to present the PAR6 binding site in ECR1 to the PAR6 PDZ domain. However, it is possible that the PAR6 binding site is also properly presented when the PALS1 L27N domain is fully folded, but in this case PATJ binding and PAR6 binding may interfere with each other due to steric hindrance.

The fact that Stardust lacks the L27N domain but still can bind PAR6 also suggests that PATJ does not promote the PALS1-PAR6 interaction by forming a protein complex with the two, and since the PALS1 L27N domain is shared between the two interactions, it is reasonable to think that PALS1 does not interact with PAR6 and PATJ at the same time. However, these studies were performed in HEK293 cells, and it is possible that such cooperative interactions may occur during polarization in MDCK cells. The true nature of these interactions will require additional studies, in particular structural analysis. Recently, Prehoda and co-workers (Peterson et al 2004) studied the structure of the PDZ domain of *Drosophila* PAR6 bound to a carboxyl-terminal peptide ligand in the absence of Cdc42. A mutagenesis study of this carboxyl-terminal ligand suggested that the P₀ residue and the P₋₁ residue are essential for the recognition of PAR6 PDZ domain, whereas the P₋₂ residue was not important. This is in contrast to classic PDZ domain peptide interactions, where the P₀ residue and the P₋₂ residue are essential. This could help explain why we found two adjacent residues in the PALS1 ECR1 that are important for PAR6 interaction. Some of their data also supported the idea that the PALS1-PAR6 interaction is mediated by the PDZ binding pocket of PAR6. Overall, our studies indicate that the ECR1 region in PALS1 is essential for the interaction between the PAR6 CRIB-PDZ region and PALS1. Our data also show an important role for the remainder of the U1 region, suggesting that the U1 region possibly folds into a specific tertiary structure to present the ECR1 motif to PAR6. Structural studies will be necessary to confirm this speculation.

BIBLIOGRAPHY

- Bachmann A, Schneider M, Theilenberg E, Grawe F, Knust E. 2001. *Drosophila* Stardust is a partner of Crumbs in the control of epithelial cell polarity. *Nature* 414: 638-43
- Betschinger J, Mechtler K, Knoblich JA. 2003. The Par complex directs asymmetric cell division by phosphorylating the cytoskeletal protein Lgl. *Nature* 422: 326-30
- Bhat MA, Izaddoost S, Lu Y, Cho KO, Choi KW, Bellen HJ. 1999. Discs Lost, a novel multi-PDZ domain protein, establishes and maintains epithelial polarity. *Cell* 96: 833-45
- Doerks T, Bork P, Kamberov E, Makarova O, Muecke S, Margolis B. 2000. L27, a novel heterodimerization domain in receptor targeting proteins Lin-2 and Lin-7. *Trends Biochem Sci* 25: 317-8
- Gao L, Joberty G, Macara IG. 2002. Assembly of epithelial tight junctions is negatively regulated by Par6. *Curr Biol* 12: 221-5
- Garrard SM, Capaldo CT, Gao L, Rosen MK, Macara IG, Tomchick DR. 2003. Structure of Cdc42 in a complex with the GTPase-binding domain of the cell polarity protein, Par6. *Embo J* 22: 1125-33
- Harris BZ, Venkatasubrahmanyam S, Lim WA. 2002. Coordinated folding and association of the LIN-2, -7 (L27) domain. An obligate heterodimerization involved in assembly of signaling and cell polarity complexes. *J Biol Chem* 277: 34902-8
- Hillier BJ, Christopherson KS, Prehoda KE, Brecht DS, Lim WA. 1999. Unexpected modes of PDZ domain scaffolding revealed by structure of nNOS-syntrophin complex. *Science* 284: 812-5
- Hong Y, Stronach B, Perrimon N, Jan LY, Jan YN. 2001. *Drosophila* Stardust interacts with Crumbs to control polarity of epithelia but not neuroblasts. *Nature* 414: 634-8
- Hurd TW, Gao L, Roh MH, Macara IG, Margolis B. 2003. Direct interaction of two polarity complexes implicated in epithelial tight junction assembly. *Nat Cell Biol* 5: 137-42
- Joberty G, Petersen C, Gao L, Macara IG. 2000. The cell-polarity protein Par6 links Par3 and atypical protein kinase C to Cdc42. *Nat Cell Biol* 2: 531-9
- Knust E, Bossinger O. 2002. Composition and formation of intercellular junctions in epithelial cells. *Science* 298: 1955-9

- Lin D, Edwards AS, Fawcett JP, Mbamalu G, Scott JD, Pawson T. 2000. A mammalian PAR-3-PAR-6 complex implicated in Cdc42/Rac1 and aPKC signalling and cell polarity. *Nat Cell Biol* 2: 540-7
- Makarova O, Kamberov E, Margolis B. 2000. Generation of deletion and point mutations with one primer in a single cloning step. *Biotechniques* 29: 970-2
- Nam SC, Choi KW. 2003. Interaction of Par-6 and Crumbs complexes is essential for photoreceptor morphogenesis in *Drosophila*. *Development* 130: 4363-72
- Noda Y, Kohjima M, Izaki T, Ota K, Yoshinaga S, et al. 2003. Molecular recognition in dimerization between PB1 domains. *J Biol Chem* 278: 43516-24
- Peterson FC, Penkert RR, Volkman BF, Prehoda KE. 2004. Cdc42 regulates the Par-6 PDZ domain through an allosteric CRIB-PDZ transition. *Mol Cell* 13: 665-76
- Petronczki M, Knoblich JA. 2001. DmPAR-6 directs epithelial polarity and asymmetric cell division of neuroblasts in *Drosophila*. *Nat Cell Biol* 3: 43-9
- Pielage J, Stork T, Bunse I, Klambt C. 2003. The *Drosophila* cell survival gene discs lost encodes a cytoplasmic Codanin-1-like protein, not a homolog of tight junction PDZ protein Patj. *Dev Cell* 5: 841-51
- Plant PJ, Fawcett JP, Lin DC, Holdorf AD, Binns K, et al. 2003. A polarity complex of mPar-6 and atypical PKC binds, phosphorylates and regulates mammalian Lgl. *Nat Cell Biol* 5: 301-8
- Qiu RG, Abo A, Steven Martin G. 2000. A human homolog of the *C. elegans* polarity determinant Par-6 links Rac and Cdc42 to PKCzeta signaling and cell transformation. *Curr Biol* 10: 697-707
- Roh MH, Makarova O, Liu CJ, Shin K, Lee S, et al. 2002. The Maguk protein, Pals1, functions as an adapter, linking mammalian homologues of Crumbs and Discs Lost. *J Cell Biol* 157: 161-72
- Roh MH, Margolis B. 2003. Composition and function of PDZ protein complexes during cell polarization. *Am J Physiol Renal Physiol* 285: F377-87
- Sheng M, Sala C. 2001. PDZ domains and the organization of supramolecular complexes. *Annu Rev Neurosci* 24: 1-29
- Straight SW, Shin K, Fogg VC, Fan S, Liu CJ, et al. 2004. Loss of PALS1 expression leads to tight junction and polarity defects. *Mol Biol Cell* 15: 1981-90
- Suzuki A, Yamanaka T, Hirose T, Manabe N, Mizuno K, et al. 2001. Atypical protein kinase C is involved in the evolutionarily conserved par protein complex and plays a critical role in establishing epithelia-specific junctional structures. *J Cell Biol* 152: 1183-96

- Tepass U, Knust E. 1993. Crumbs and stardust act in a genetic pathway that controls the organization of epithelia in *Drosophila melanogaster*. *Dev Biol* 159: 311-26
- Wodarz A. 2002. Establishing cell polarity in development. *Nat Cell Biol* 4: E39-44
- Wodarz A, Ramrath A, Grimm A, Knust E. 2000. *Drosophila* atypical protein kinase C associates with Bazooka and controls polarity of epithelia and neuroblasts. *J Cell Biol* 150: 1361-74
- Yamanaka T, Horikoshi Y, Sugiyama Y, Ishiyama C, Suzuki A, et al. 2003. Mammalian Lgl forms a protein complex with PAR-6 and aPKC independently of PAR-3 to regulate epithelial cell polarity. *Curr Biol* 13: 734-43

CHAPTER 3

PALS1 REGULATES E-CADHERIN TRAFFICKING IN MAMMALIAN EPITHELIAL CELLS

3.1 Introduction

Polarity is an intrinsic feature of epithelial cells, and it is reflected by the differential distribution of proteins and lipids in the apical and basolateral surfaces (Roh & Margolis 2003). The apical and basolateral membranes are separated by the tight junction seal at the superior aspect of the lateral surface, which functions as a physical barrier between these membrane domains (Matter & Balda 2003, Tsukita et al 2001). The adherens junctions lay basal to the tight junctions in mammalian epithelial cells and they mediate the adhesion between neighboring cells. Studies in *Drosophila* and mammalian cells have identified a large number of proteins as the polarity determinants, and they form several evolutionarily conserved macromolecular complexes. The complicated interplay among these complexes and their orderly functioning regulates the establishment of cell polarity and the cell-cell junctions.

Included in these polarity proteins are mammalian PALS1 and its ortholog *Drosophila* Stardust (Sdt) (Knust & Bossinger 2002). Genetic and biochemical studies in *Drosophila* have shown that Sdt interacts with the transmembrane protein Crumbs (CRB) through its PDZ domain (Bachmann et al 2001, Hong et al 2001), and mutations in either CRB or Sdt cause polarity defects in *Drosophila* epithelia (Tepass & Knust 1993). Like Sdt, the PDZ domain of PALS1 binds the Carboxyl-terminal tail

of mammalian CRB isoforms, and PALS1 also interacts with a multi-PDZ domain protein, PATJ, through the binding by the N-terminal L27 (L27N) domain of PALS1 (Roh et al 2002). The PALS1-PATJ-CRB complex localizes to the tight junction of mammalian epithelial cells, and the disruption of the complex leads to defects in cell polarity (Straight et al 2004). The carboxyl-terminal L27 (L27C) domain of PALS1 interacts with an L27 domain within Lin-7 (Kamberov et al 2000), and prior work in our laboratory has shown that an evolutionarily conserved region in the N-terminus of PALS1 mediates its interaction with PAR6. This interaction links the polarity complexes PALS1-PATJ-CRB and PAR3-PAR6-aPKC together (Hurd et al 2003, Wang et al 2004). The function of the Carboxyl-terminal SH3 domain and GUK domain of PALS1 is unknown.

The cells of all epithelia analyzed so far have an adhesive belt that encircles the cell just below the apical surface, which is called the zonula adherens (Knust & Bossinger 2002). The zonula adherens, which is also called adherens junction in vertebrates, is mainly E-cadherin based, and the calcium-dependent engagement of E-cadherin mediates the adhesion of adjacent cells. In *Drosophila*, the Sdt-dPATJ-CRB complex is localized to a specialized zone apical to the zonula adherens called the subapical region or marginal zone. The subapical region like the tight junction is located apically to the zonula adherens (Knust & Bossinger 2002). However the subapical region is not the site of the intercellular seal in *Drosophila* cells which instead resides below the zonula adherens in the septate junction. In *Drosophila*, the Sdt-dPATJ-CRB complex regulates the formation of the zonula adherens and E-cadherin localization (Grawe et al 1996, Klebes & Knust 2000, Tepass 1996) although how the protein complex interacts with components of the zonula adherens remains unclear (Knust & Bossinger 2002).

Prior work in our laboratory has showed that the knockdown of PALS1 in the MDCK cells lead to tight junction and polarity defects (Straight et al 2004). In this chapter, we created new PALS1 stable knockdown cell lines with more profound reduction of PALS1 expression. Besides a more severe defect in tight junction formation, we also observed abnormal adherens junction and E-cadherin localization. We think the depletion of PALS1 disrupted the trafficking of E-cadherin to the cell periphery. This is the first report that PALS1 is involved in the regulation of adherens junction biogenesis in mammalian epithelial cells, and it may represent a conserved mechanism from *Drosophila*.

3.2 Materials and methods

3.2.1 DNA constructs

The following sequences of nucleotides with a 19-base target site (in bold) and a 9-base loop (underline) were used to generate small hairpin RNA (SiRNA) expressing plasmid against canine PALS1 mRNA: PALS1 KD#1 primer (5'-GATCC**GGAGATGAGGTTCTGGAAATTCAAGAGATTTCCAGAACCTCATCTCCTTTTTTGGAAA**-3') and PALS1 KD#2 primer (5'-GATCC**GGGATATACTTCATATCATTTCAAGAGATGATATGAAGTATATCCCCTTTTTTGGAAA**-3'). After annealing the complimentary oligonucleotides, the dimers were ligated into the precut p*Silencer* 2.1-U6 hygromycin plasmid (Ambion, Austin, TX), as directed by the manufacturer, followed by amplification of the resulting plasmids. All plasmids were verified by automated sequencing at the University of Michigan DNA Sequencing Core. The PALS1 full length and various PALS1 mutant

cDNA sequences were subcloned into a modified pKH3 vector with a tandem Flag and Myc tag fused to the N-terminus of the insert.

3.2.2 Cell culture and calcium switch experiment

MDCKII cells were cultured in DMEM plus 10% fetal bovine serum supplemented with penicillin, streptomycin, and L-glutamine. All cell culture media and supplements were purchased from Invitrogen. To create the cell lines stably expressing SiRNA constructs, MDCKII cells were transfected with 5 μg of the p*Silencer* 2.1 plasmid DNA using FuGENE 6 reagent (Roche, Indianapolis, IN). After selection with 500 $\mu\text{g}/\text{mL}$ Hygromycin (Invitrogen) for 14 days, surviving clones were isolated for the generation of cell lines. The PALS1 KD#1 cell line was co-transfected with 5 μg of the Flag-myc-PALS1 plasmid and 0.5 μg pSV2NEO and selected with 500 $\mu\text{g}/\text{mL}$ G418 (Invitrogen) for 14 days to generate the rescue cell lines. All established stable cell lines were cultured in medium containing half of the drug concentration for selection.

For the calcium switch experiments, MDCKII cell lines were grown to confluence on 12-mm Transwell filters and were then washed extensively with PBS and grown in low-calcium medium (5 μM Ca^{2+}) overnight to dissociate cell-cell contacts. The low-calcium medium was replaced the next day with normal growth medium (1.8 mM Ca^{2+}), and the cells were prepared for immunostaining at various time points afterwards (0, 3, 6, or 29 h).

3.2.3 Antibodies

PALS1, PATJ, Lin-7 and Nectin-like 2-specific antisera were generated in rabbits and affinity-purified as previously described (Borg *et al.*, 1998; Roh *et al.*,

2002). Rabbit anti-Actin antibody was purchased from Sigma (St. Louis, MO). Mouse anti-Myc (9E10) antibody was obtained from Santa Cruz (Santa Cruz, CA). Mouse anti-ZO-1, mouse anti-TfR and rat anti-E-cadherin (for immunofluorescence) antibodies were purchased from Zymed (San Francisco, CA). Mouse anti-EEA1, mouse anti- β -Catenin, mouse anti-Rab11, mouse anti-GM130, mouse anti-RalA, and mouse anti-E-cad (for western blot) antibodies were purchased from BD Biosciences Transduction Laboratories (San Jose, CA). Mouse anti- γ -Adaptin was purchased from Sigma-Aldrich; rabbit anti-Akt was purchased from Cell Signaling Technology (Danvers, MA); mouse anti-Sec8 was purchased from Stressgen Bioreagents (Ann Arbor, MI). The hybridoma generating mouse monoclonal anti-E-cadherin antibody (rr1) was purchased from the Developmental Studies Hybridoma Bank at University of Iowa (Gumbiner and Simons, 1986) (Iowa City, IA).

3.2.4 Immunoblotting

Cells cultured on one 10-cm dish were collected in 0.5 ml of lysis buffer (50 mM Tris (pH 7.4), 150 mM NaCl, 10% glycerol, 1% Triton X-100, 1.5 mM MgCl₂, 1 mM EGTA, 10 mM NaF, 10 mM Na₄P₂O₇, 1 mM Na₃VO₅, 1 mM phenylmethylsulfonyl fluoride, 10 μ g/ml leupeptin, and 20 μ g/ml aprotinin). Lysates were cleared by centrifugation (12,000 x g for 15 min at 4 °C). Western blotting was performed as previously described (Straight *et al.*, 2004).

3.2.5 Immunostaining and microscopy

Cells grown on Transwell filters were cut from the support with a scalpel, washed with PBS, fixed with 4% paraformaldehyde/PBS for 15 min, permeabilized with either 0.1% Triton X-100/PBS or 1% SDS/PBS for 5 min (or without

permeabilization as indicated); alternatively, cells were fixed and permeabilized at room temperature with 1:1 acetone/methanol for 15min. Then the cells were blocked with 2% goat serum/PBS (GS/PBS) for 1 h. The filters were then incubated with primary antibodies in GS/PBS for overnight at 30°C in a humidified chamber. After washing extensively with GS/PBS, fluorochrome-conjugated secondary antibodies in GS/PBS were added overnight at 4°C. Finally, filters were washed with PBS and mounted onto glass slides using ProLong antifade reagent (Molecular Probes). All confocal images were obtained using an Olympus Fluoview 500 inverted confocal microscope at the University of Michigan Diabetes Center. Epifluorescent images were taken using a Nikon Eclipse TE2000-U microscope.

3.2.6 Cell surface biotinylation

Cells were grown on filters and incubated with 1.5 mg/ml sulfosuccinimidyl 2-(biotinamido) ethyldithiopropionate (sulfo-NHS-SS-biotin; Pierce, Rockford, IL) at different time points after calcium switch. Biotin was applied to the basal side of the Transwell filter. After the rocking at 4°C for 30 min, the filters were washed with PBS containing 100mM glycine to quench free sulfo-NHS-SS-biotin followed by several further washes in PBS. The cells were then scraped off the filters and suspended in a radioimmune precipitation assay buffer (20 mM Tris-HCl, pH 7.4, 150 mM NaCl, 0.1% SDS, 1% Triton X-100, 1% deoxycholate, 5 mM EDTA, 10 µg/ml leupeptin, 100 µg/ml phenylmethylsulfonyl fluoride, 10 µg/ml aprotinin). The cell lysates were centrifuged, and the supernatants were incubated with streptavidin beads (Pierce, Rockford, IL) to collect bound biotinylated proteins. The samples were then subjected to SDS-PAGE followed by Western blotting with the anti-E-cadherin mAb. The

western blotting result was scanned by the Typhoon scanner and quantified with ImageQuant 5.8.

3.2.7 Metabolic labeling and pulse-chase

Cell cultures were preincubated with methionine/cysteine free medium for 1 hr. Then 300 μ Ci of [³⁵S]methionine (NEG EXPRE³⁵S³⁵S; PerkinElmer, Wellesley, MA) was added to both sides of the Transwell filter. The cells were pulse-labeled for 2 hr, rinsed 2X in PBS, and chased in regular medium for indicated length of time. Then a surface biotinylation experiment was performed. Immobilized rat anti-E-cadherin antibody was added to the collected cell lysates. After rocking overnight at 4 °C, the beads were washed and eluted with 400 μ L acid elution buffer (0.2M glycine, 1% Triton, pH2.6) at room temperature for 1 hr. Biotinylated proteins in the supernatant were precipitated by adding 5 μ L 1N NaOH, 25 μ L 1M Tris [pH7.4], 40 μ L 10% BSA and 60 μ L strepavidin beads. The beads were washed and resuspended in 30 μ L 1X SDS sample buffer, and after gel running and electro-transfer, the nitrocellulose membrane was exposed to a phosphoimage screen overnight and scanned and quantified.

3.2.8 E-cadherin endocytosis assay

MDCK or the PALS1 KD cells were seeded into the Lab-Tek II chamber slide system (Nalge Nunc). After culturing cells in serum free medium for 1 h, mouse rr1 ascites was added to make the final concentration 10%. Cells were fixed and stained as indicated after being incubated at 37°C for 3 h. For the combined endocytosis assay, cells were incubated in the low calcium medium overnight and then switched to

serum free medium containing 1/10 rr1 ascites for another 3 h of incubation at 37°C. The serum free medium contains normal amount of calcium.

3.2.9 10-15-20-30% Opti-prep gradient

The Opti-prep gradient was carried out following a published procedure (Yeaman 2003) with minor modifications. Briefly, MDCK cells grown on tissue culture plates were washed with PBS twice before being scraped off in HES buffer (20mM Hepes pH 7.4, 255mM Sucrose, 1mM EDTA, supplemented with complete protease inhibitors). The cell suspension was passed five times through 21 gauge syringe, and homogenated 20X with a 10ml Wheaton homogenator. Cell homogenates were then spun at 3,000 g for 5 min, and supernatants were collected as post-nuclear supernatant (PNS). PNS was mixed with 60% iodixanol (opti-prep) to generate a 30% solution, which was overlaid with 20%, 15% and 10% iodixanol, respectively. The gradients were spun in a NVT90 rotor at 350,000 g for 4 h at 4°C. Once completed, 13 fractions were collected from each gradient for subsequent western blot analysis.

3.3 Results

3.3.1 Depletion of PALS1 disrupts both tight junctions and adherens junctions in MDCK cells

Prior work in our laboratory showed that when the expression of the tight junction-associated protein PALS1 is markedly reduced in MDCKII cells by SiRNA

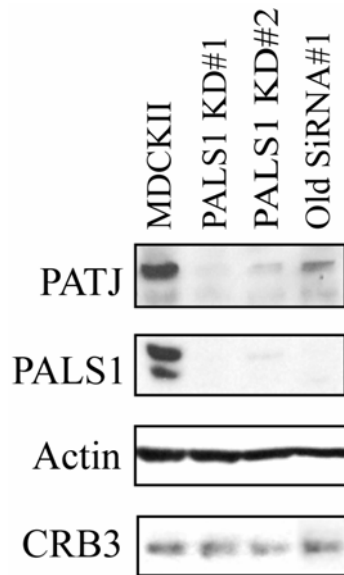


Figure 3.1 Protein levels in control and PALS1 KD cell lines. Lysates of the MDCKII wild-type cells, two independent SiRNA-expressing cell lines (PALS1 KD#1 and PALS1 KD#2), and the PALS1 KD cell line published previously (Old SiRNA#1) were blotted with the antibodies directed against the proteins indicated to the left. Actin level was used as a loading control.

expression, the expression level of PATJ is lowered accordingly, and the formation of tight junctions are significantly delayed (Straight et al 2004). To further investigate the role of PALS1 in junction formation, we designed two canine-specific SiRNA sequences and created PALS1 knockdown (KD) cell lines by stably expressing the SiRNA-encoding plasmid in the MDCKII cells. The depletion of PALS1 was shown by western blot, and as previously reported, PATJ expression was also markedly reduced (Figure 3.1). The protein level of Crumbs3 did not change significantly. Compared to the best PALS1 KD cell line reported in the previous work (Old SiRNA#1, in Straight *et al.*, 2004), the two new PALS1 KD cell lines (PALS1 KD#1 and PALS1 KD#2) have lower expression of PATJ (Figure 3.1), and we have found that the level of PATJ reflects the residual expression of PALS1. The difference in the level of PALS1 remaining is more clearly shown by immunofluorescence, where

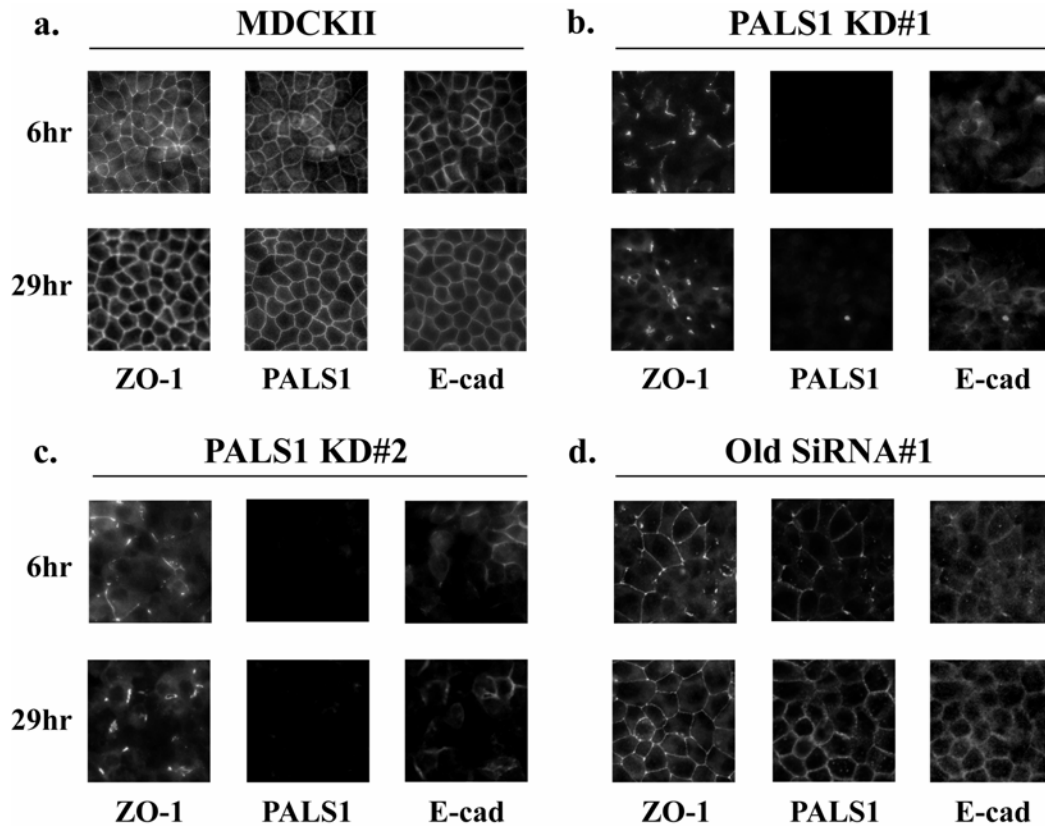


Figure 3.2 Junction formations in control and PALS1 KD cell lines. Cells grown to confluence on polyester filters were transferred to low calcium medium overnight to dissociate cell–cell contacts and then returned to normal calcium medium. At 6 and 29 h after calcium readdition, cells were fixed, permeabilized with 1% SDS, and immunostained with the antibodies indicated.

residual amount of PALS1 can be detected in the Old SiRNA#1 cell line while it was almost completely depleted from the two new PALS1 KD cell lines (Figure 3.2).

To examine the effect that the loss of PALS1 has on the formation of cell-cell contacts, calcium switch experiments were performed. Cells grown to confluence on polyester filters were transferred to low calcium medium overnight to dissociate cell-cell contacts and then switched to normal calcium medium. MDCKII cells reformed tight junction and adherens junction by 6 h after the switch, revealed by the junctional

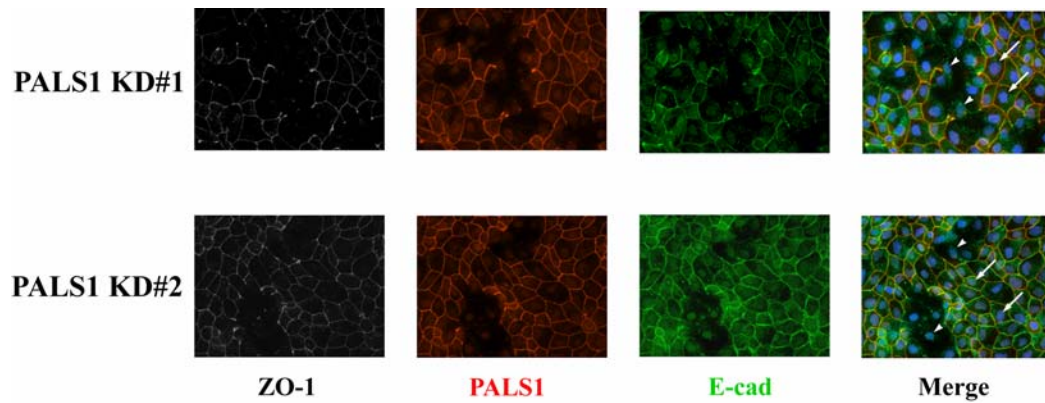


Figure 3.3 Junction formations in PALS1 KD pool cells. The pSilencer 2.1 plasmid encoding the two SiRNA sequences in PALS1 KD#1 and PALS1 KD#2 were transfected into MDCKII cells to generate pools of cells with varying degrees of PALS1 expression. Cells were immunostained 3 h after calcium switch with the antibodies indicated. Images of PALS1 staining and E-cadherin staining were merged with DAPI staining to show the loss of E-cadherin staining in PALS1 KD cells. Cells with PALS1 knocked down are indicated with arrowheads, and cells still expressing PALS1 are indicated with arrows.

staining of the tight junction marker ZO-1 and the adherens junction marker E-cadherin (Figure 3.2, a). As reported in the prior work (Straight et al 2004), the Old SiRNA#1 cells showed delayed tight junction formation (Figure 3.2, d). In contrast, the PALS1 KD#1 and PALS1 KD#2 cells did not reform tight junctions 29 h after the switch, and unexpectedly, the adherens junction structural protein E-cadherin was also missing from the cell-cell contact sites (Figure 3.2, b and c). In fact, tight junctions and adherens junctions remained partially formed in the two new KD cell lines even after 7 days of culturing on filters (data not shown). These results showed that the formation of both tight junctions and adherens junctions is disrupted in the two new PALS1 KD clonal cell lines.

We then performed the calcium switch experiment in the PALS1 KD pool cells to eliminate clonal effects of stable cell lines. The pSilencer 2.1 plasmids

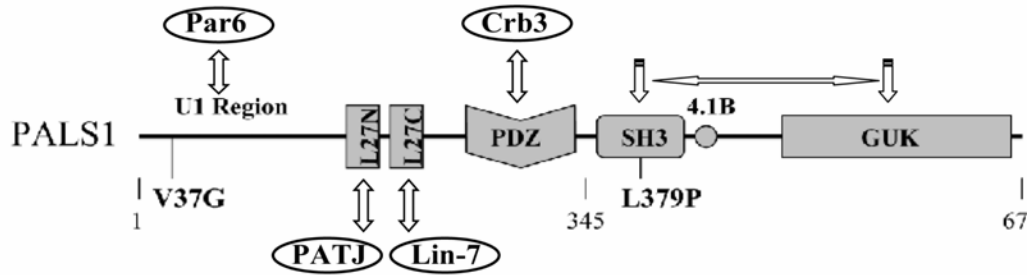


Figure 3.4 The domain structure of PALS1. The two point mutations are marked in the diagram, and various interactions and the intramolecular SH3–GUK interactions are depicted with arrows. The delC truncation mutant lacks the C-terminal residues aa 346-675.

encoding the two SiRNA sequences in PALS1 KD#1 and PALS1 KD#2 were transiently transfected into MDCKII cells. After 72 h, the KD pool cells were transferred to low calcium medium overnight, and 3 h after being switched to normal calcium medium they were fixed and immunostained. In both pools, ZO-1 and E-cadherin staining were missing from the cell-cell contact sites in cells whose PALS1 was depleted (the presence of cells were revealed by DAPI staining), and they were correctly localized in areas where PALS1 was intact (Figure 3.3). These results agreed with the clonal knockdown cells showing that the depletion of PALS1 disrupted adherens junctions.

3.3.2 Wild type PALS1 and two PALS1 mutants rescued the defects in junction formation

The PALS1 KD#1 and PALS1 KD#2 SiRNA sequences were designed against the canine-specific regions of canine PALS1, and they do not recognize murine

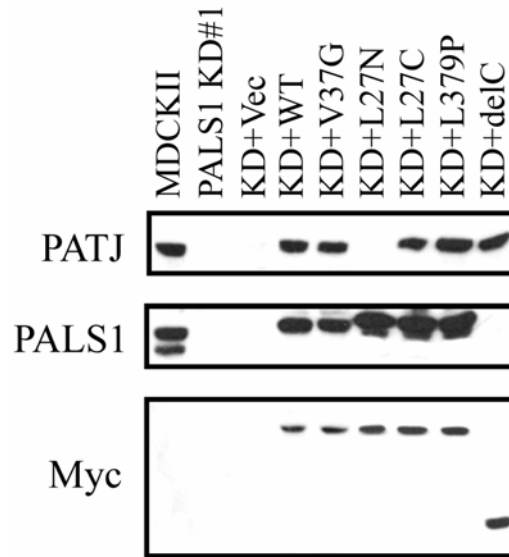


Figure 3.5 Expression of the PALS1 rescuing constructs. The MDCKII wild-type cells, the PALS1 KD#1 cells, and the PALS1 KD#1 cells expressing the empty vector and various PALS1 constructs were lysed, and the lysates were blotted with the antibodies indicated to the left.

PALS1 due to the difference of nucleotides within the 19mers. We then re-introduced murine PALS1 wild type and various PALS1 mutants to see whether they can rescue the defects in junction formation. Figure 3.4 depicts the domain structure of murine PALS1. The U1 region mutant V37G shows reduced binding with the polarity protein PAR6 (Wang et al 2004), the L27N domain mutant disrupts the interaction between PALS1 and PATJ (Roh et al 2002), and the PALS1 L27C domain mutant does not bind Lin-7 (Kamberov et al 2000). It has been shown that extensive intramolecular interactions exist between the carboxyl-terminal SH3 domain and the GUK domain of MAGUK proteins (McGee et al 2001, Tavares et al 2001). To explore the function of the carboxyl-terminus of PALS1, which has been largely unknown, we generated a point mutation L379P in the SH3 domain which disrupts the intramolecular

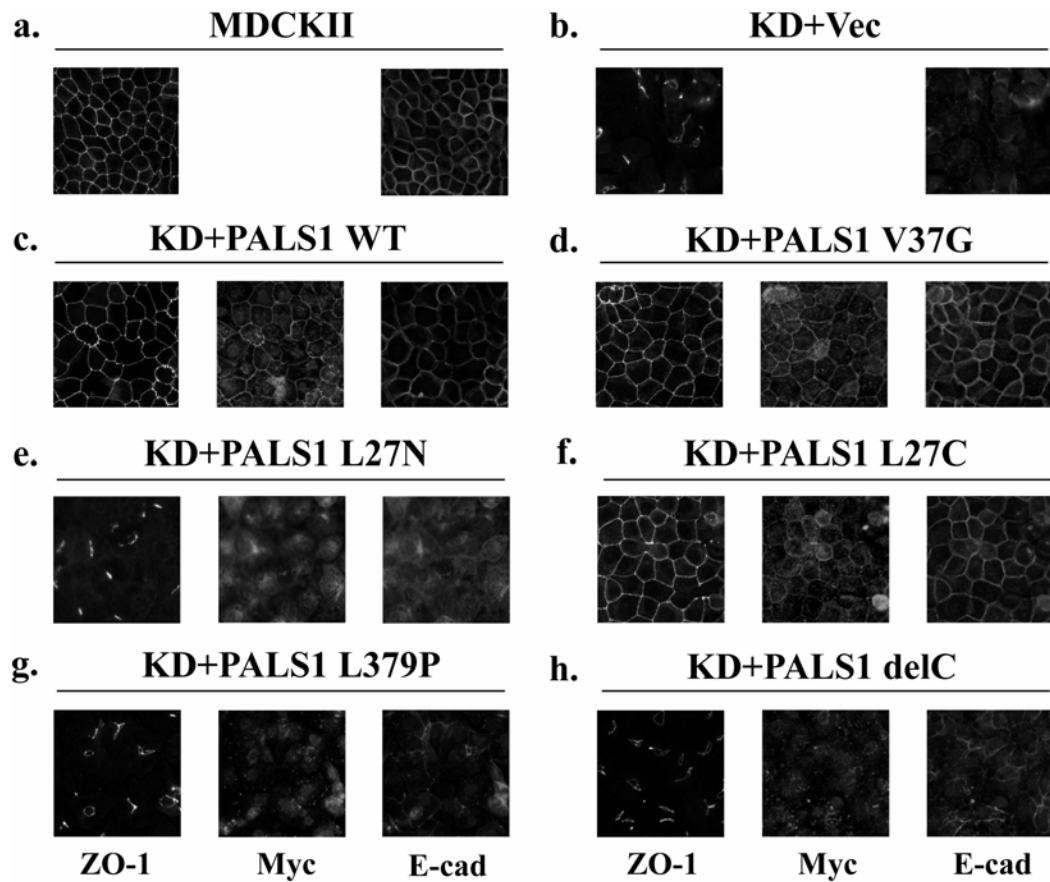


Figure 3.6 Junction formations in control, PALS1 KD, and rescue cells. Cells grown to confluence on polyester filters were incubated in low calcium medium overnight and then transferred to normal calcium medium. Six hours later, cells were fixed, permeabilized with 1% SDS, and stained with the antibodies indicated.

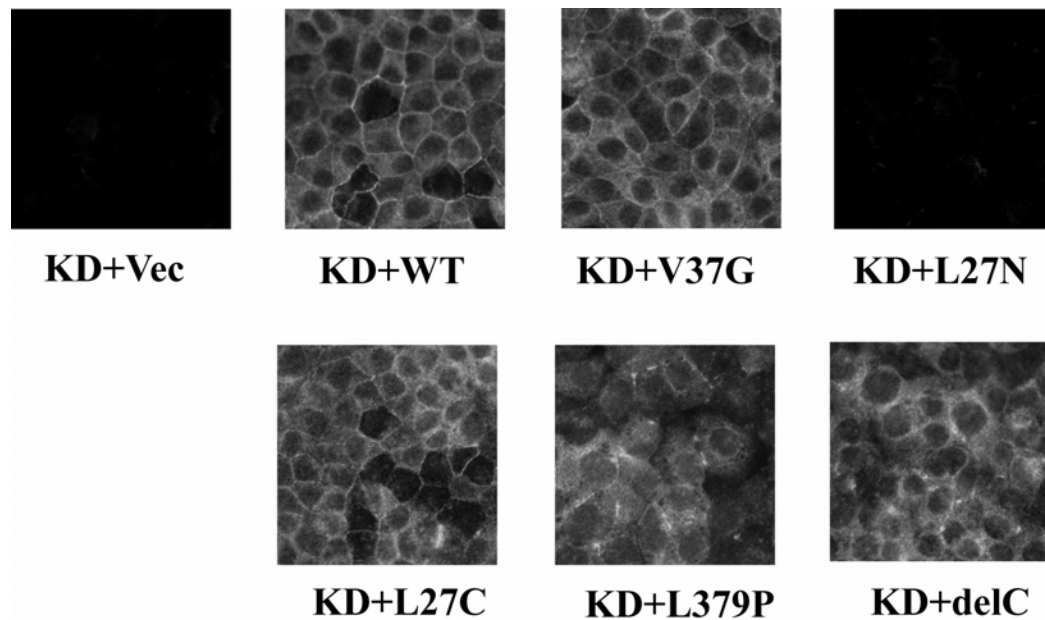


Figure 3.7 Immunofluorescence of PATJ in PALS1 rescue cell lines. PALS1 rescue cell lines were immunostained with the anti-PATJ antibody. No signal was detected in the KD+Vec cells and the KD+L27N cells.

interaction between the SH3 domain and the GUK domain (Woods et al 1996, Wu et al 2000), and a truncation mutant delC (PALS1 1-345) which lacks both domains. The wild type PALS1 and the various mutants were fused to tandem Flag and Myc tags at the N-terminus, and stably expressed in the PALS1 KD#1 cells. The expression of the exogenous PALS1 is shown in Figure 3.5 and it is comparable to endogenous PALS1. Interestingly, PATJ was rescued to close to its original level in the cells with re-expressed PALS1 except in that expressing the PALS1 L27N mutant, which is the PATJ binding-defective mutant (Figure 3.5). This result reconfirms that PATJ exists in a complex with PALS1 in the cells, and the interaction with the PALS1 L27N domain stabilizes PATJ.

We studied junction formation of the rescued cell lines at 6 h after calcium switch. The cells expressing the PALS1 wild type, as well as two mutants, PALS1

V37G and PALS1 L27C, showed full recovery of tight and adherens junctions, as shown by ZO-1 and E-cadherin staining (Figure 3.6, c, d and f), with the exogenously expressed PALS1 at the tight junctions; PATJ is also correctly localized to the junctions (Figure 3.7). In cells expressing the PALS1 L27N, L379P and delC mutant, the exogenous PALS1 is localized diffusely in the cells, and the reformation of tight and adherens junctions is similar to the PALS1 KD cells transfected with empty vector (Figure 3.6, b, e, g and h). The inability of the L27N domain deletion to rescue junction formation confirms the important role of PATJ in cell-cell contacts and cell polarity. These results also indicate the importance of the carboxyl-terminus of PALS1 in these processes.

3.3.3 There is less E-cadherin on the surface of the PALS1 KD cells

We were very interested in the possible link between PALS1 and E-cadherin, so we continued to study E-cadherin in the PALS1 KD#1 cells. We performed an RT-PCR experiment and found that the mRNA level of E-cadherin was not changed in the PALS1 KD cells (data not shown), and western blot results showed that the PALS1 KD cells had similar E-cadherin protein levels compared to wild type MDCK cells (data not shown and Figure 3.17). In Figure 3.2, 3.3 and 3.6, E-cadherin was shown to be partially missing from the cell-cell contact sites, therefore we used an antibody that recognized the E-cadherin extracellular domain to examine whether it is on the surface of the PALS1 KD cells. MDCKII cells and the PALS1 KD#1 cells were grown confluent on transwell filters for 3 days and fixed. Then the E-cadherin antibody were applied to either the upper well or the lower well without permeabilizing the cells. The MDCKII cells revealed strong E-cadherin staining signals when the antibody was added from the lower well, while the signal was very

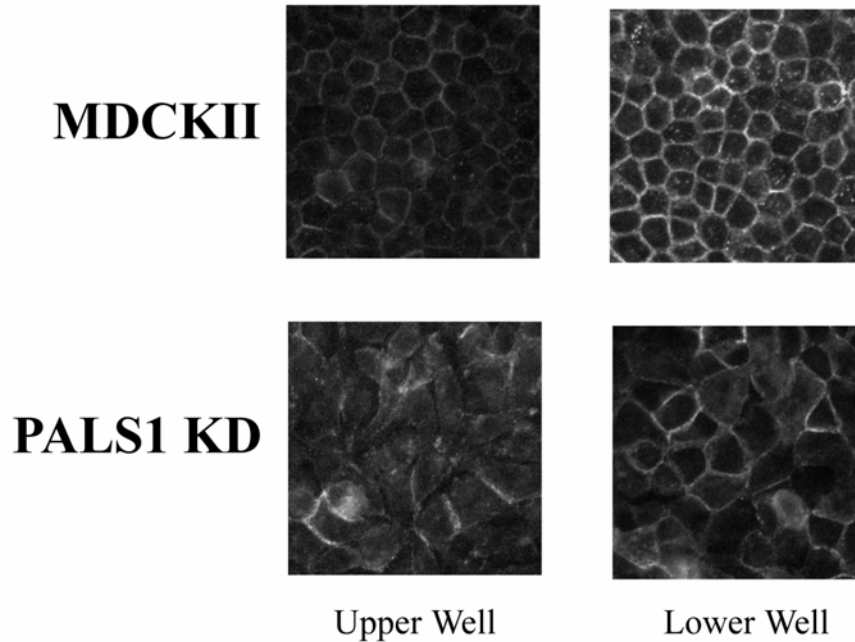


Figure 3.8 Immunofluorescence of cell surface E-cadherin. MDCKII wild-type cells and the PALS1 KD cells were grown to confluence on polyester filters and fixed. An E-cadherin antibody that recognizes the extracellular domain of E-cadherin was applied to either the top or bottom well without permeabilization.

weak when it was added from the upper well due to the intact tight junctions (Figure 3.8). In contrast, the PALS1 KD cells showed similar staining signals in the two cases because their tight junctions were defective, and compared to the MDCKII cells (Lower Well), the E-cadherin signal was much weaker (Figure 3.8). Meanwhile, E-cadherin was missing from many cell-cell contacts in the KD cells (Figure 3.8).

We then combined this assay with the calcium switch experiment. The MDCKII cells and the PALS1 KD#1 cells were fixed at 0 h, 1 h and 3 h after calcium readdition, and the E-cadherin extracellular antibody was applied to the cut filters without permeabilization. The MDCKII cells had a significant portion of E-cadherin remaining on the cell surface in the low calcium medium, and E-cadherin quickly

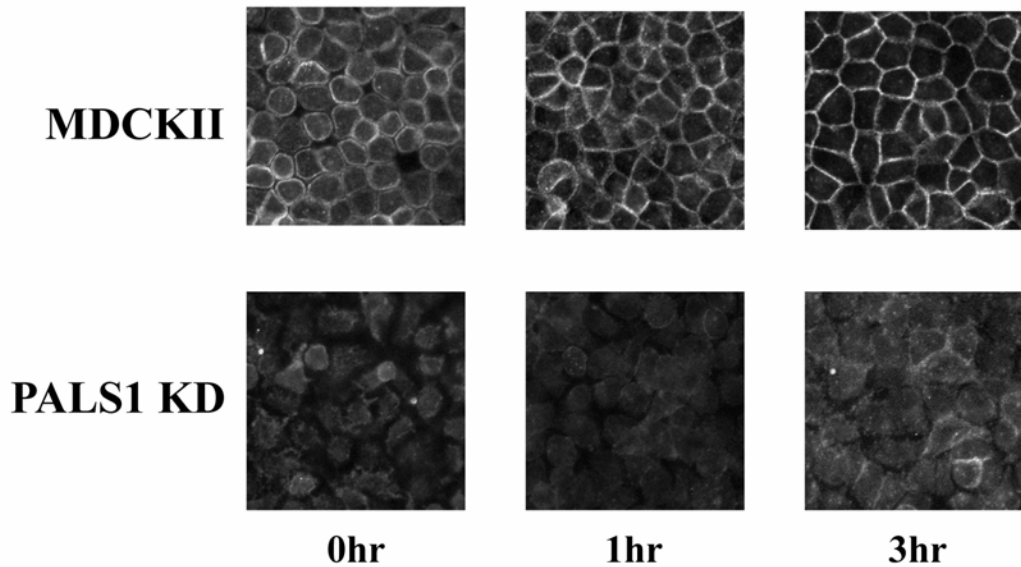
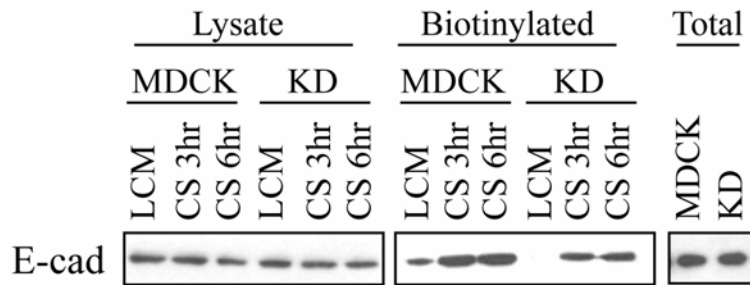


Figure 3.9 Immunostaining of cell surface E-cadherin after calcium switch. MDCKII cells and PALS1 KD cells were grown to confluence on polyester filters, and the calcium switch experiment was performed with the cells fixed at different times after the switch ($t = 0, 1, \text{ or } 3 \text{ h}$). The E-cadherin antibody that recognizes the extracellular domain of E-cadherin was applied to the cut filters without permeabilization.

translocated to the plasma membranes after the cells were transferred to the normal calcium medium (Figure 3.9). On the other hand, the PALS1 KD cells revealed very weak E-cadherin staining signals at all the three time points, which suggests that E-cadherin is not delivered to the cell surface as effectively as in the control cells (Figure 3.9).

We also did the surface biotinylation experiment to reveal the level of E-cadherin on the plasma membrane. The MDCKII cells and the PALS1 KD#1 cells were incubated with biotin at 0 h, 3 h and 6 h after being transferred from low calcium medium to normal calcium medium. Biotinylated proteins were collected by a streptavidin beads pulldown, and a subsequent E-cadherin blotting showed that there was significantly less surface E-cadherin in the KD cells at all three time points compared to the wild type cells (Figure 3.10, a). The result of E-cadherin biotinylation

a.



b.

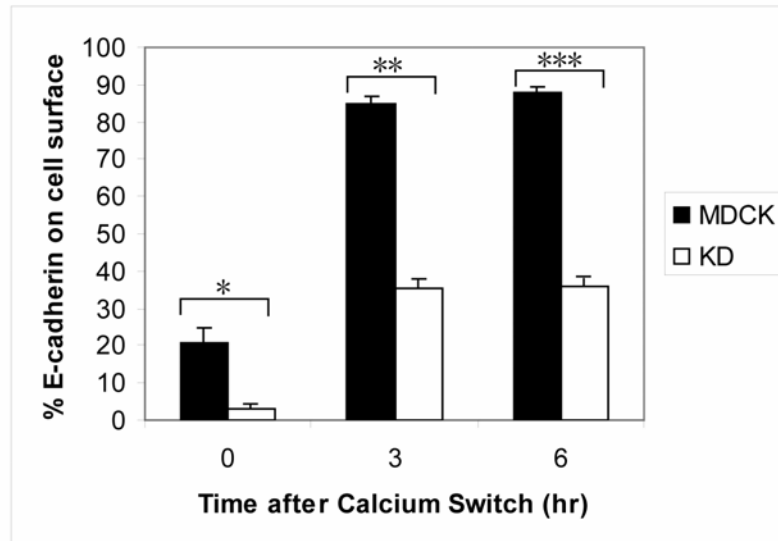


Figure 3.10 Surface biotinylation of E-cadherin after calcium switch. Cells grown to confluence on polyester filters were incubated in low calcium medium overnight and were biotinylated before or 3 or 6 h after being transferred to normal calcium medium. Cells were lysed in radioimmunoprecipitation assay buffer, and biotinylated proteins were precipitated by streptavidin beads. (a) Five percent of lysate and the biotinylated portion were blotted for E-cadherin. Two duplicated wells of cells were immunoprecipitated by the anti-E-cadherin antibody to show the total of E-cadherin. (b) Quantification of (a). Error bars represent SD/sqrt(n). *t* test: **p* < 0.05, ***p* < 0.001, ****p* < 0.001; *n* = 3 independent experiments.

in Figure 3.10 (a) as well as that of two other independent experiments was quantified in Figure 3.10 (b). The percentage of cell surface E-cadherin is evidently reduced in the PALS1 KD cells at all the three time points examined (Figure 3.10, b).

3.3.4 E-cadherin is retained in intracellular puncta in the PALS1 KD cells

Since the total protein level of E-cadherin is not changed and there is less E-cadherin on the surface of the PALS1 KD cells, we speculated that E-cadherin is accumulated intracellularly. However, initial immunofluorescence results did not reveal that (Figure 3.2). We thought it could be due to the permeabilization method we used, as the PALS1 antibody only recognizes PALS1 after the cells are permeabilized with 1% SDS and SDS could have removed some of the intracellular vesicles. Accordingly we changed the permeabilization conditions, and also increased the concentration of the E-cadherin antibody. In panel a of Figure 3.11, we grew the PALS1 KD pool cells on filters, and fixed and permeabilized the cells with 1:1 acetone/methanol 3 h after calcium switch. The cells expressing the PALS1 KD SiRNA plasmid were identified by a lack of PALS1 staining, and in these cells, E-cadherin was seen to be accumulated in puncta-like structures. In panel b, the same cells were fixed with 4% paraformaldehyde and permeabilized with 0.1% Triton, and similar result was seen with the co-staining of E-cadherin and PATJ. All the following immunofluorescence experiments were performed as in panel b of Figure 3.11.

Next we checked the E-cadherin localization in the PALS1 KD#1 cells. MDCKII cells and the PALS1 KD#1 cells were fixed 3 h after calcium switch and co-stained for E-cadherin and other adherens junction proteins including Actin, Lin-7 and Nectin-like 2 (Ncl2) (Figure 3.12, panel a-c). Compared to the junctional localization in wild type cells, the adherens junction proteins were diffuse in the PALS1 KD cells,

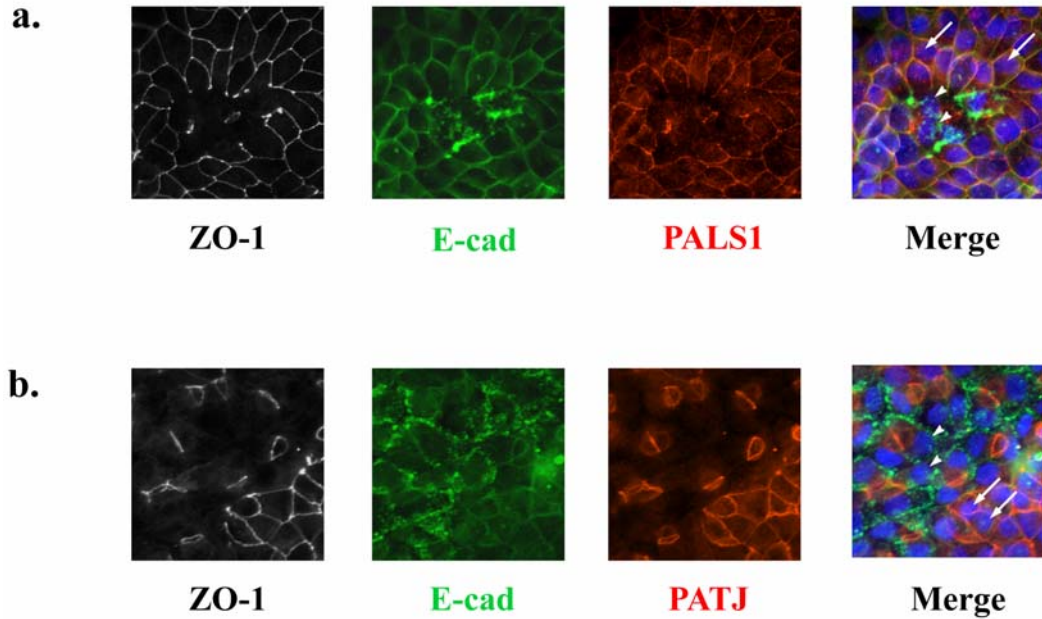


Figure 3.11 E-cadherin puncta in PALS1 KD pool cells. MDCKII cells transfected with the PALS1 SiRNA plasmid were fixed 3 h after calcium switch with acetone-methanol (a) or paraformaldehyde and permeabilized with 0.1% Triton (b). They were immunostained with the antibodies indicated subsequently. The E-cadherin staining image and the PALS1 staining image (a) or PATJ staining image (b) were merged with the DAPI staining image to show the E-cadherin-positive puncta in the PALS1 KD cells. Cells with PALS1 knocked down are indicated with arrowheads, and cells still expressing PALS1 are indicated with arrows.

and the Actin staining showed clearly that the cells were not making cell-cell contacts; E-cadherin was in puncta rather than at the junctions as well (Figure 3.12).

We were interested in the formation of these E-cadherin positive puncta during cell polarization, so we stained for E-cadherin in the MDCKII cells and the PALS1 KD#1 cells at different time points after calcium switch using the alternate staining conditions. The staining revealed an intracellular pool of E-cadherin that quickly translocated to the cell-cell contact sites in the wild type cells upon the transition to normal calcium medium (Figure 3.13, a). On the contrary, the intracellular E-cadherin puncta were seen at the 0 h time point in the PALS1 KD cells, and no obvious translocation was seen after 3 h (Figure 3.13, a). The confocal image

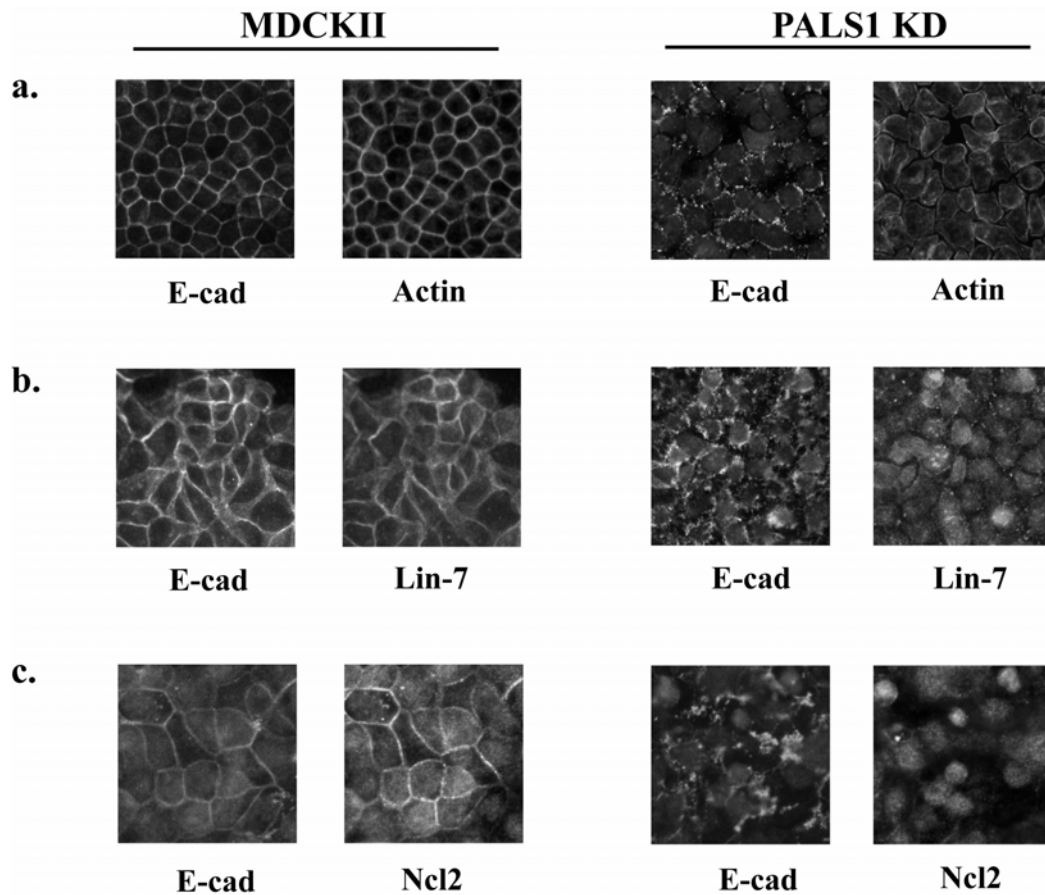


Figure 3.12 Costaining of E-cadherin with AJ markers. MDCKII cells and PALS1 KD cells were fixed 3 h after calcium switch and stained for E-cadherin and several adherens junction-localized proteins, including actin (a), Lin-7 (b), and Ncl2 (c).

in Fig. 3.13, panel b provides a magnified view of the E-cadherin localization. It is worth noting that the E-cadherin puncta in the PALS1 KD cells are localized in the cell periphery, where cell-cell contacts and junctions are waiting to form.

3.3.5 E-cadherin is not effectively exocytosed to the cell surface

E-cadherin is a transmembrane protein and it is exocytosed to the cell surface in vesicles. After delivering to the plasma membranes, E-cadherin is trafficked to and

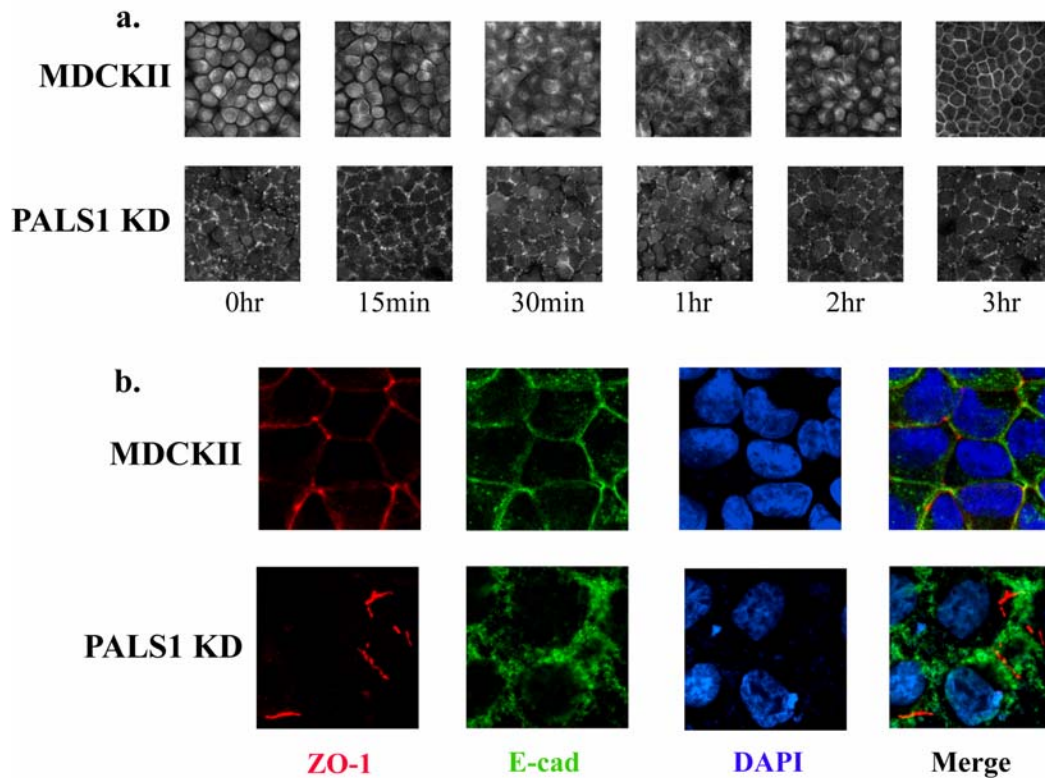
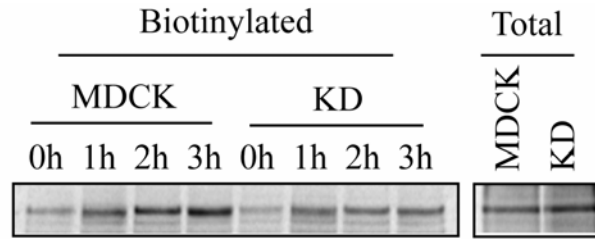


Figure 3.13 E-cadherin puncta in PALS1 KD cell lines. Localization of E-cadherin at the times after calcium switch ($t = 0$ h, 15 min, 30 min, 1 h, 2 h, or 3 h) was revealed by immunostaining (a). Magnified view of the 3-h time point by using confocal microscopy (b).

from the cell surface by exocytic and multiple endocytic pathways (Bryant & Stow 2004). It was important to determine whether the E-cadherin positive vesicles are the result of disrupted exocytosis or disrupted recycling, and to this end, we combined the pulse-chase experiment with the biotinylation assay. The MDCKII cells and the PALS1 KD#1 cells were pulse-labeled with [35 S]methionine for 2 h and after being chased for 0 h, 1 h, 2 h or 3 h the cells were incubated with biotin. The cells were then lysed and sequentially precipitated with immobilized anti-E-cadherin antibody and streptavidin beads. The bands in the autoradiation image in Figure 3.14 reflect the amount of E-cadherin that reached cell surface in the indicated length of time, and it



Quantification: 1 2.9 4.1 6.0 0.5 1.4 2.1 2.5

Figure 3.14 Exocytosis of E-cadherin is slow in PALS1 KD cells. MDCKII wild-type cells and the PALS1 KD cells were pulse labeled with [³⁵S]methionine for 2 h and chased for 0, 1, 2, or 3 h. Cells were biotinylated, and the E-cadherin reaching the surface in the period of the chase was revealed by autoradiation after sequential precipitation by the anti-E-cadherin antibody and the streptavidin beads. One duplicate of each cell line was lysed right after the pulse label and immunoprecipitated by the anti-E-cadherin antibody to show the total level; that panel (right) was from a shorter exposure to avoid saturated images. The results are representative of two experiments. Quantification of the intensity of bands is shown below.

can be seen that there was less E-cadherin exocytosed to the plasma membrane in the PALS1 KD cells at any time point.

To further confirm that E-cadherin exocytosis was misregulated, we conducted an E-cadherin endocytosis assay. We added E-cadherin antibody to the medium at a final concentration of 10%, and incubated it with the MDCKII cells or the PALS1 KD#1 cells for 3 h at 37°C. The mouse antibody rr1 recognizes the extracellular domains of E-cadherin, and an anti-mouse secondary antibody was added after the cells were fixed and permeabilized to reveal the rr1 signal. At the same time, total E-cadherin was detected by staining with a rat E-cadherin antibody. As is shown in panel a of Figure 3.15, the rr1 antibody was coupled to the E-cadherin on the cell surface and a portion of it was endocytosed into the cells highlighting intracellular vesicles (Figure 3.15 panel a, arrows). No significant difference was seen in rr1 endocytosis between the MDCKII cells and the PALS1 KD cells, while there were more prominent intracellular puncta in the KD cells revealed by the total E-cadherin

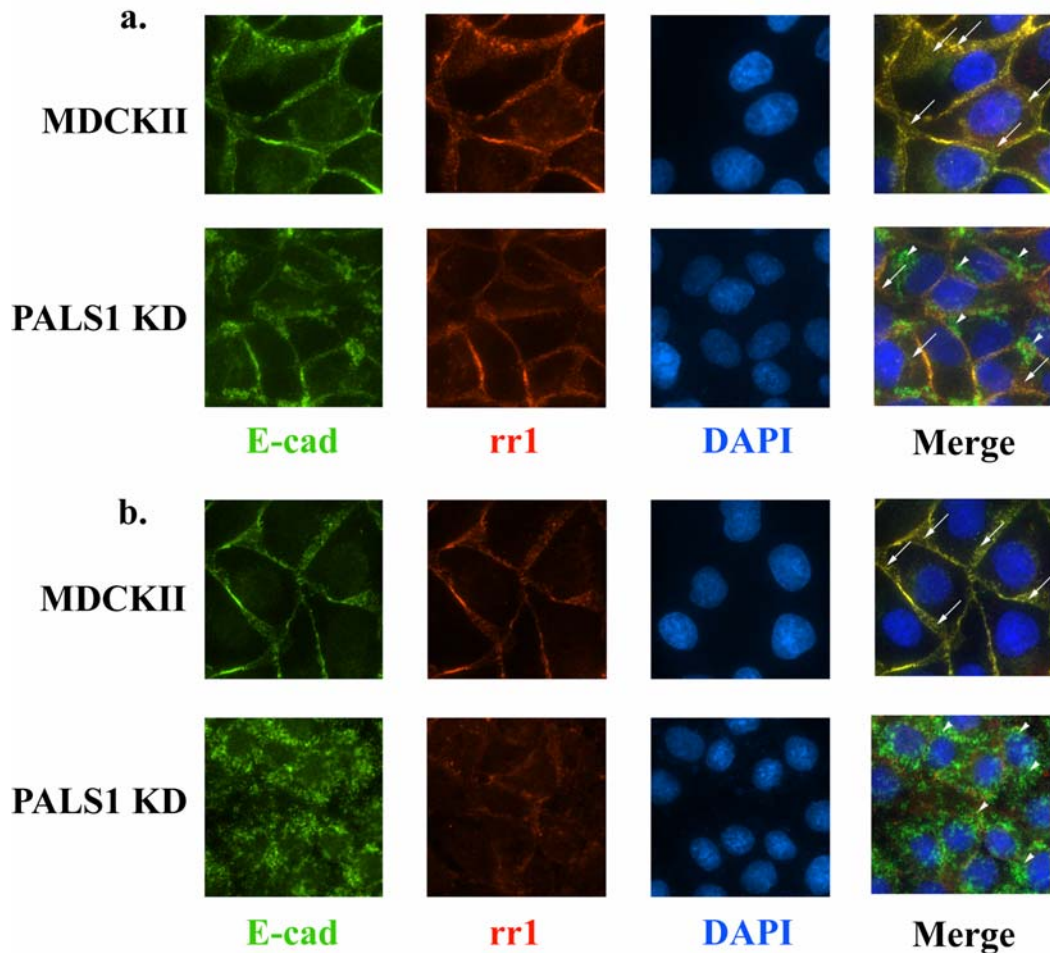


Figure 3.15 E-cadherin puncta in PALS1 KD cells are different from endocytic vesicles. Cells were incubated with normal calcium medium containing 10% rr1 anti-E-cadherin mouse ascites for 3 h directly (a) or cultured in low calcium medium overnight before the incubation (b). Total E-cadherin was shown by the immunostaining with a rat E-cadherin antibody, and the coupled rr1 mouse antibody was revealed by a fluorochrome-bound secondary antibody. Note the overlap between the total E-cadherin signal and the rr1 signal in the merge picture (arrows), and green vesicle-like structures in the PALS1 KD cells (arrowheads).

immunofluorescence and they do not totally overlap with the rr1 signals (Figure 3.15 panel a, arrowheads).

We then combined the rr1 endocytosis and calcium switch assays with the rr1 mouse antibody added at the time when the cells were transferred from low to normal calcium medium. After 3 h of incubation at 37°C, the MDCKII cells showed similar

rr1 endocytosis as in the previous experiment (Figure 3.15 panel b, arrows). On the other hand, the PALS1 KD cells had very weak rr1 signals due to the lack of E-cadherin on the cell surface, while the intracellular puncta were prominently shown by the total E-cadherin staining (Figure 3.15 panel b, arrowheads). These results support our previous conclusion that these E-cadherin positive puncta in the PALS1 KD cells cannot exocytose to the surface and bind the antibody present in the extracellular media.

To further examine the identity of the E-cadherin positive puncta in the PALS1 KD cells, we co-stained E-cadherin and several intracellular organelle markers, including the recycling endosome marker Rab11 and Transferrin Receptor (TfR), the early endosome marker EEA1, the *cis*-Golgi marker GM130 and the trans-Golgi network (TGN) marker γ -Adaptin (Figure 3.16, a-e). We did not see colocalization of E-cadherin with any of these markers.

3.3.6 Exocyst is mislocalized in the PALS1 knockdown cells

As there appeared to be a defect in E-cadherin exocytosis, we decided to study the exocyst complex as there is evidence that this complex is involved in the regulation of E-cadherin exocytosis (Langevin et al 2005, Shipitsin & Feig 2004), (Grindstaff et al 1998, Yeaman et al 2004). We used two independent assays to study the localization of the exocyst complex in the PALS1 KD cells. First, we performed an Opti-prep fractionation experiment. In Figure 3.17, the upper panel is the distribution of proteins of the MDCKII cells, while the lower panel is that of the PALS1 KD#1 cells. TfR, Rab11, RalA and Akt were blotted in both panels, and no significant difference was seen in the distribution of these proteins. When we examined E-cadherin and the exocyst component Sec8, we found a shift of peaks of

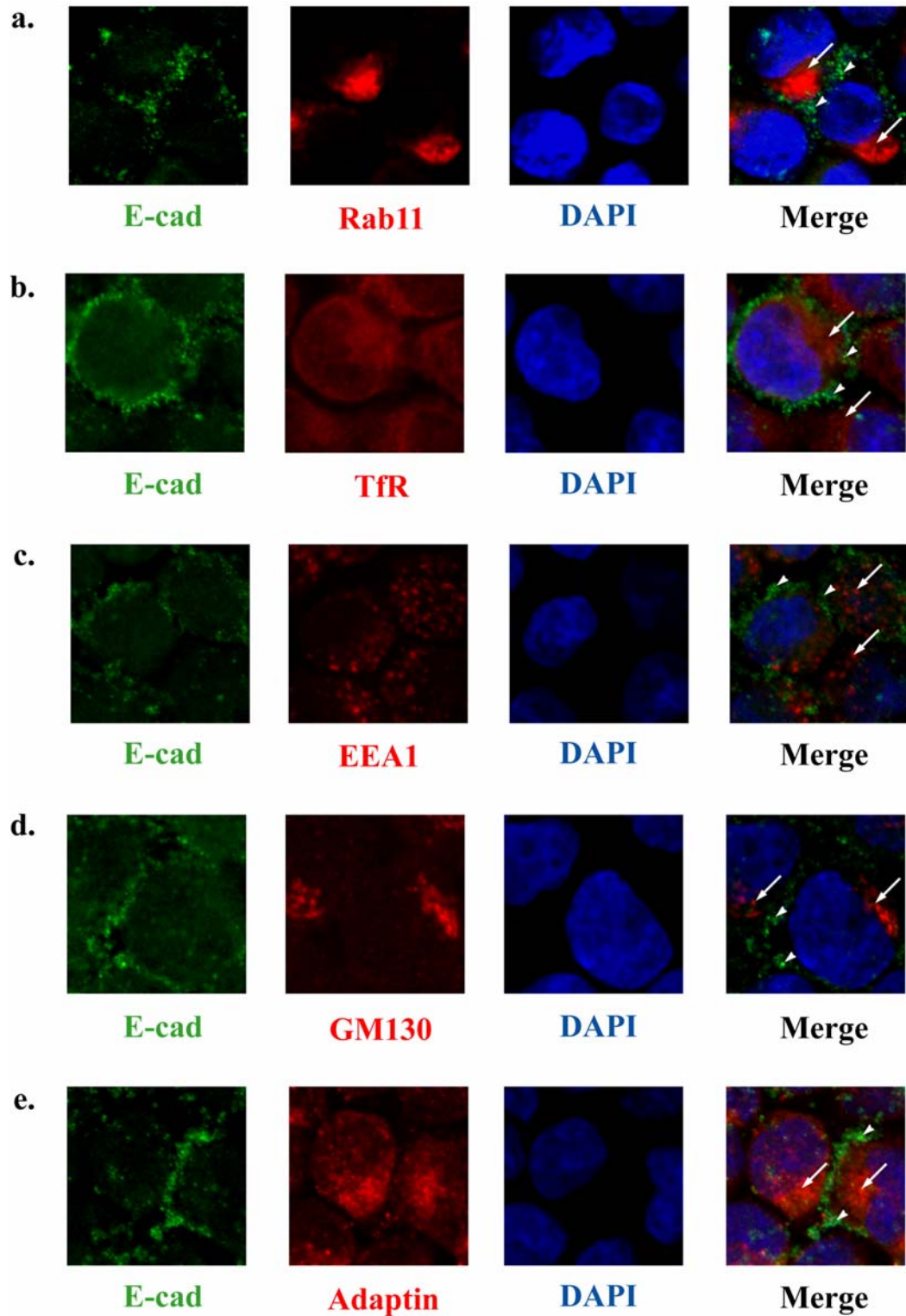


Figure 3.16 Costaining of E-cadherin and markers of intracellular compartments. The PALS1 KD cells were fixed 3 h after calcium switch and costained for E-cadherin (arrowheads) and Rab11 (a), Transferrin receptor (b), EEA1 (c), GM130 (d), and γ -adaptin (e) (arrows).

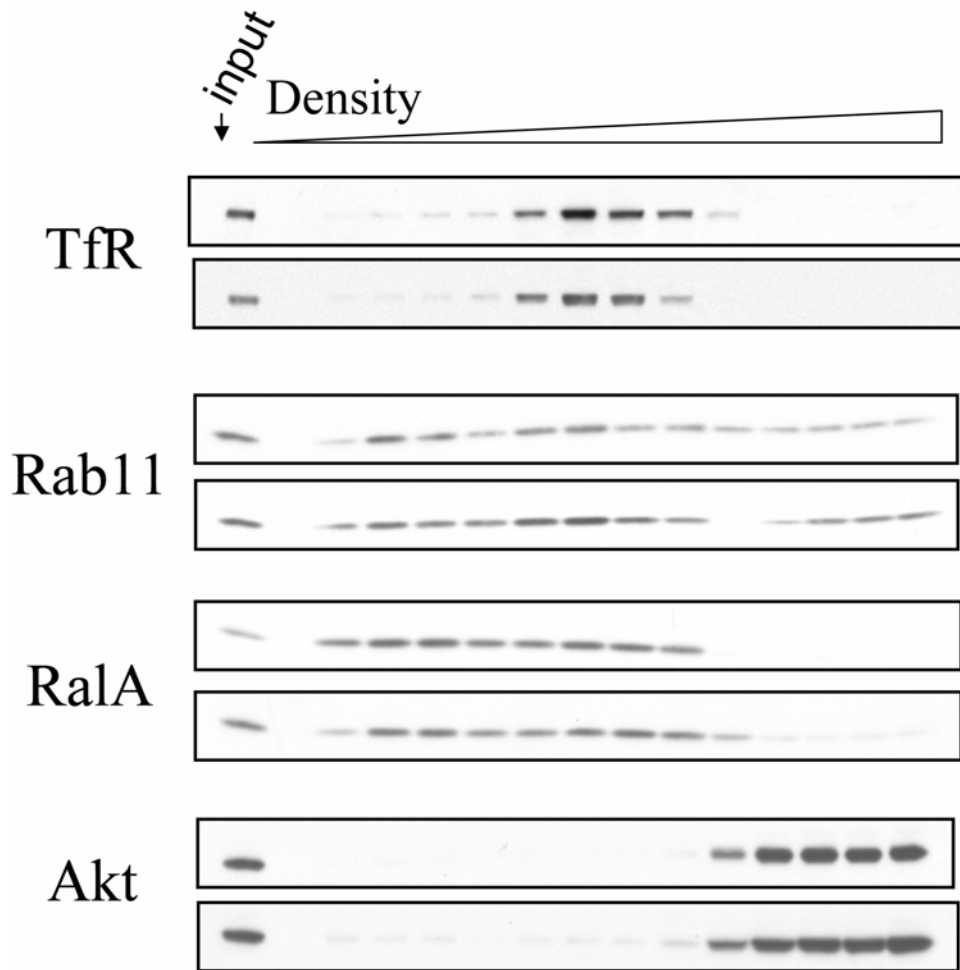
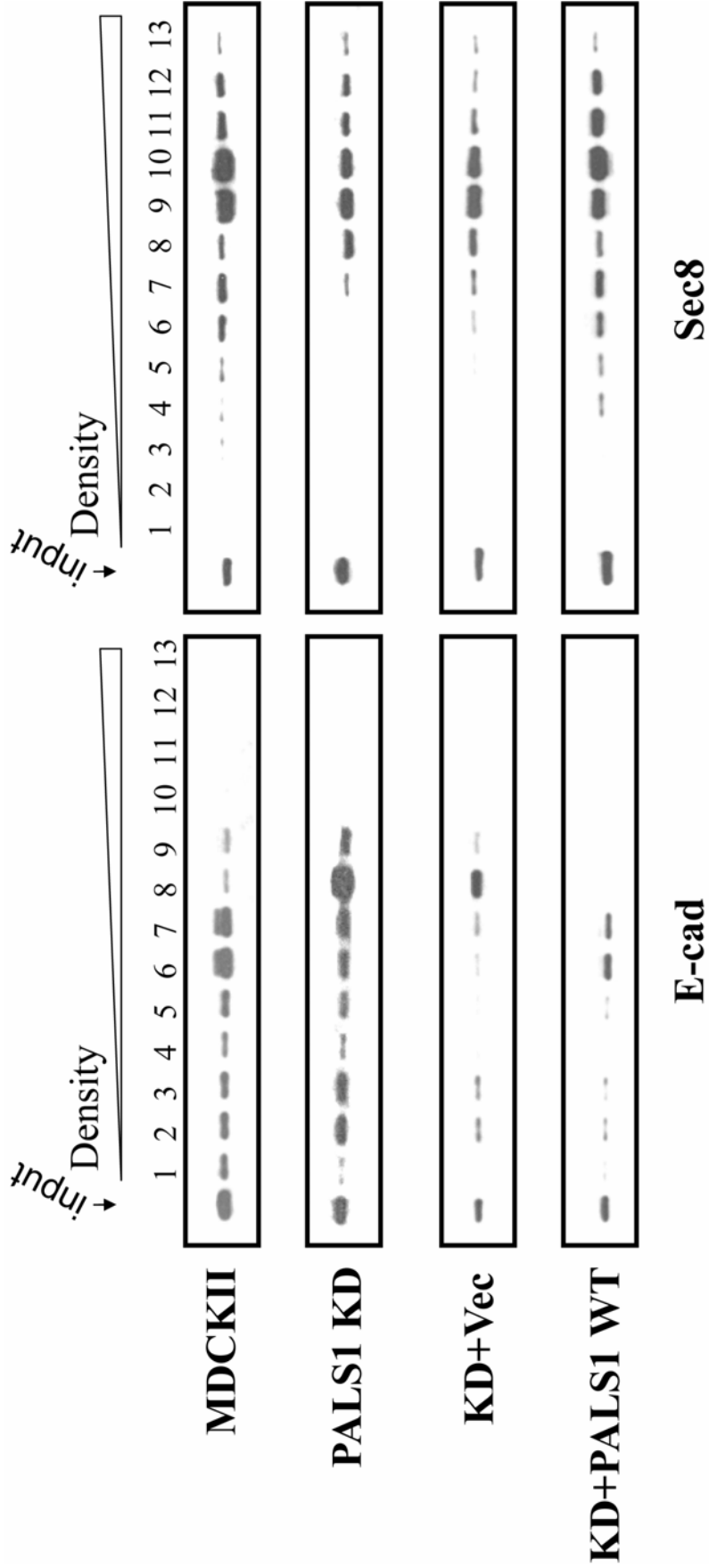


Figure 3.17 Density distributions of cytosolic and intracellular compartmental markers. MDCKII wild type and PALS1 KD cells were lysed, and the postnuclear lysates were fractionated in a 10–15–20–30% Opti-Prep. The fractions were loaded on the gel in the order of increased density and blotted for various proteins indicated to the left. Top, MDCKII cells. Bottom, PALS1 KD cells.

these two proteins in the PALS1 KD cells; moreover, E-cadherin and Sec8 co-fractionate in fraction 6 and 7 in the MDCKII cells, consistent with previous report (Yeaman 2003), while in the PALS1 KD cells, Sec8 is missing from peak 6 and 7 and the peak of E-cadherin is shifted to fraction 8 (Figure 3.18). These changes in the distribution of E-cadherin and Sec8 were rescued in the PALS1 KD cells expressing the wild type PALS1 (Figure 3.18). We also examined Sec8 localization by

Figure 3.18 Density distributions of E-cadherin and Sec8. PALS1 KD cells expressing the empty vector or mouse rescue wild-type PALS1 were fractionated and together blotted for E-cadherin and Sec8.



immunofluorescence. Sec8 is localized to the junctions in the MDCKII cells, while in the PALS1 KD cells, only fragmented spots can be seen at the cell-cell contact sites (Figure 3.19, panel a). The junctional localization is rescued in PALS1 KD cells expressing PALS1 wild type, the V37G mutant or the L27C mutant; and consistent with the result of junction rescue, Sec8 is mislocalized in PALS1 KD cells transfected with the empty vector, the PALS1 L27N mutant, the L379P mutant or the delC mutant (Figure 3.19, panel b). These results indicate that the depletion of PALS1 disrupts the localization of the exocyst complex, whereas the rescue cell lines reveal correction Sec8 localization and rescue of junction formation.

3.4 Discussion

We report here a further characterization of the tight junction associated polarity protein PALS1, utilizing a stable canine specific SiRNA that depleted PALS1 more thoroughly than our previous work (Straight et al 2004). This canine directed SiRNA lead to a more severe cellular deficit than we previously observed including a defect in adherens junction formation. We were able to rescue this adherens junction defect with wild type PALS1 and complete a structure/function analysis using mutant PALS1 constructs to rescue the defect. Consistent with the previous report, the loss of PALS1 resulted in a corresponding loss of expression of PATJ but not CRB3 (Straight et al 2004). The protein level of Lin-7, which binds the PALS1 L27C domain, was not changed in the PALS1 KD cells (data not shown). The reintroduction of exogenous PALS1 recovered the expression of PATJ, except for the PALS1 L27N mutant (Figure 3.5). We have tested the interacting ability of all the PALS1 mutants used in the rescue study, and the L27N mutant is the only one that is defective in binding PATJ. We hypothesize that when PALS1 is reduced the unbound PATJ is

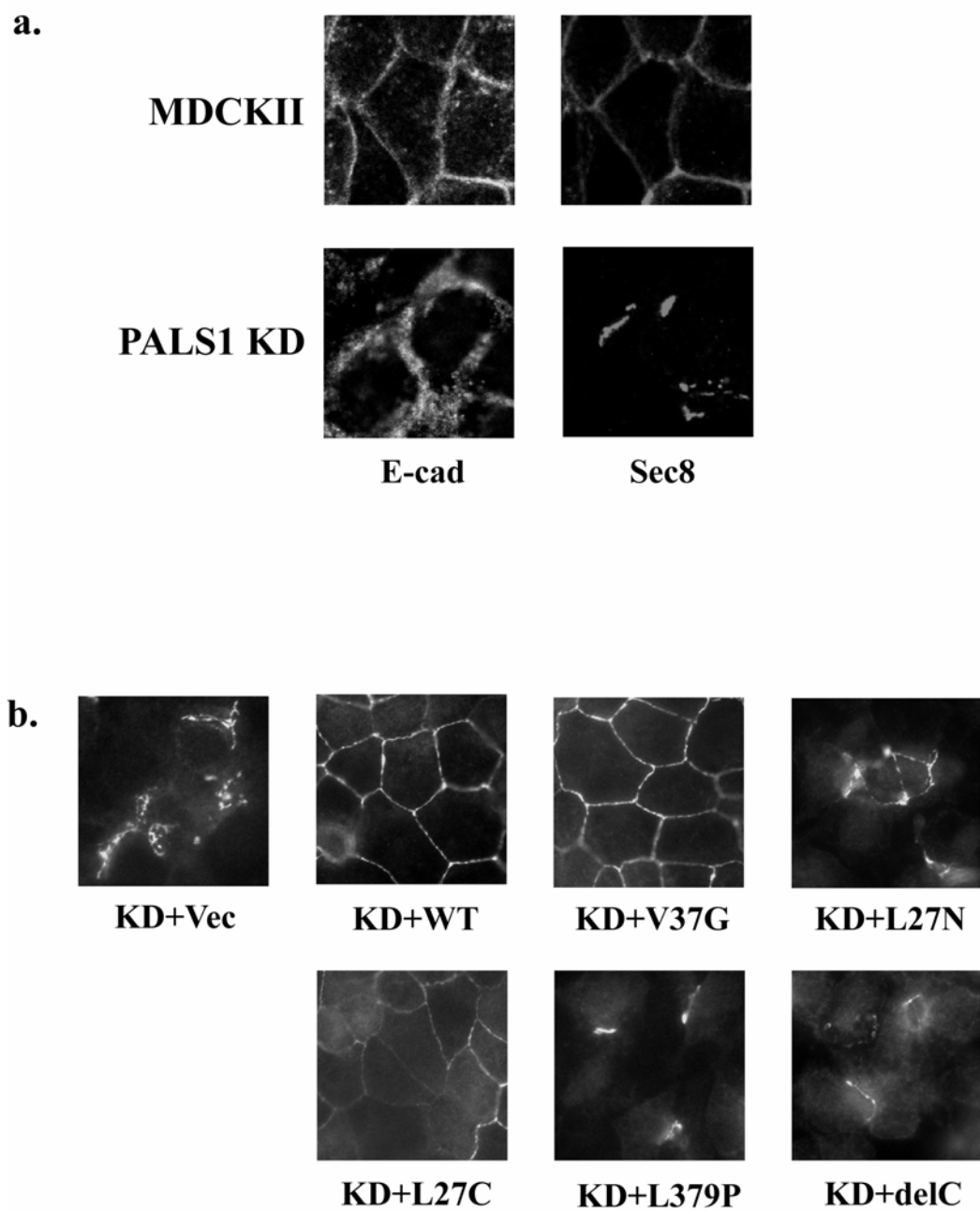


Figure 3.19 Immunofluorescence of Sec8. Sec8 is localized at the cell–cell contacts, whereas in the PALS1 KD cells Sec8 staining is disrupted (a). Sec8 was also stained in the PALS1 KD cells expressing the empty vector, the rescue wild-type mouse PALS1, and various PALS1 mutants (b).

destabilized and degraded. The results obtained from the rescue cell lines support this hypothesis, as PATJ expression was rescued in accordance with the PATJ-binding ability of the PALS1 mutants used.

New insights from these studies reveal that PALS1 is involved in the regulation of E-cadherin trafficking. With the new PALS1 KD cell lines and a modified immunostaining protocol, we were able to observe the retention of E-cadherin puncta inside the PALS1 KD cells. This defect, together with the defect in tight junction formation was corrected in some of the rescue cell lines. PALS1 wild type, V37G and L27C mutants rescued both defects 6 h after calcium switch (Figure 3.6). On the other hand, the PALS1 L27N, L379P and delC mutants failed to rescue either of the defects. These results have several implications. First, the function of the PALS1 Carboxyl-terminus has been largely unknown. Here we show for the first time that the Carboxyl-terminal SH3 and GUK domains are important for PALS1 function. It will require further study to elucidate how the PALS1 carboxyl-terminus is functioning and its interacting proteins. Second, the results of the V37G mutation was of interest to us. While this mutant does rescue the phenotype at 6 h we did note that junctional rescue was delayed with this mutant if we looked at 3 h after calcium addition (not shown). Nonetheless this mutation that reduces the binding of PAR6 to PALS1 in multiple studies (Wang et al 2004) has at best minor effects on PALS1 function. We believe that the interaction of the PALS1 complex with the Par complex is of importance but that there are redundant ways for the complexes to interact. These redundant interactions including the direct interaction of Crumbs to PAR6 (Lemmers et al 2004) can compensate for the lack of direct interactions between PALS1 and PAR6.

It is important to distinguish the role of PALS1 and PATJ in the process of junction formation. We suppose the defect in junction formation we saw is a direct effect of PALS1 depletion rather than the subsequent result of PATJ loss, since the L379P cell line and the delC cell line had PATJ expressed but did not rescue the defects (Figure 3.6). However, the recovered PATJ is mislocalized in the L379P cell line and the delC cell line (Figure 3.7). Our laboratory has done a PATJ knockdown/rescue study, and we observed that mislocalized PATJ mutants did not cause adherens junction disruption (Shin et al 2005) and unpublished data), which means, PATJ mislocalization does not cause adherens junction defects at least when endogenous PALS1 is intact (PATJ KD does not lead to PALS1 decrease). Expressing various PATJ mutants in the PALS1 KD cells would be helpful to address this question; however, PATJ cannot be stably expressed in the PALS1 KD cells due to the stability issue. A separate PATJ knockdown study in Caco2 cells reported that PATJ knockdown lead to the mislocalization of PALS1, and no adherens junction defects followed the PATJ depletion and PALS1 mislocalization (Michel et al 2005). Since PALS1 and PATJ are also localized to the apical membrane in Caco2 cells and the knockdown of PATJ does not affect tight junction formation and maintenance, it is possible that the PALS1/PATJ complex plays a slightly different role in Caco2 cells or other adherens junction regulation pathway has been upregulated to compensate.

PALS1 is localized to the tight junction in mammalian epithelial cells, and its importance in the formation of tight junctions has been established (Roh et al 2002, Straight et al 2004). E-cadherin is localized to a distinct membrane domain basal to tight junctions, and it is the major structural component of the adherens junctions. Our report is the first one to indicate that PALS1 has a role in adherens junction formation in mammalian epithelial cells but results in *Drosophila* are instructive. *Drosophila*

epithelial cells have an adhesive belt that encircles the cell just below the apical surface called the zonula adherens, where DE-cadherin and its interacting proteins Armadillo (*Drosophila* β -catenin) and $\Delta\alpha$ -catenin reside. The Sdt-dPATJ-CRB complex is localized to a distinct domain apical to the zonula adherens in the *Drosophila* epithelial cells called the subapical region. It is widely accepted that the Sdt-dPATJ-CRB complex regulates the formation of the *Drosophila* zonula adherens and E-cadherin localization (Grawe et al 1996, Klebes & Knust 2000, Tepass 1996), although how the protein complex interacts with components of the zonula adherens remains unclear (Knust & Bossinger 2002). The observations in our study suggest that this mechanism is conserved, and PALS1 regulates the formation of adherens junctions in mammalian epithelial cells in addition to its role in tight junction formation.

The intracellular trafficking of E-cadherin is regulated by a variety of exocytic and endocytic machineries that can modulate adhesion (Bryant & Stow 2004). After exiting the TGN, newly synthesized E-cadherin goes to the Rab11-positive recycling endosome (Lock & Stow 2005). It is sorted to the basolateral membranes there, and a portion of E-cadherin undergoes constant recycling between the plasma membrane and the recycling endosome (Bryant & Stow 2004). Using the E-cadherin extracellular antibody and the surface biotinylation assay we demonstrated that there is lower proportion of total E-cadherin on the surface of the PALS1 KD cells, and with the pulse-chase experiment and the rr1 endocytosis assay, we showed that the newly synthesized E-cadherin is not effectively exocytosed to the plasma membrane (Figure 3.8, 3.9, 3.14, 3.15). We were not able to identify the exact identity of the E-cadherin puncta in the PALS1 KD cells, because they do not colocalize with any of the organelle markers examined (Figure 3.16). We found that those E-cadherin puncta

are distributed in the cell periphery and at the site of cell-cell contacts, and this distribution is especially obvious when cells are confluent grown on the filters and tightly packed together (Figure 3.13). We hypothesize that in the PALS1 KD cells, the E-cadherin exocytic vesicles are correctly sorted to the cell surface from the recycling endosome, but the depletion of PALS1 either abolishes the final cue of targeting or disrupts their fusion with the plasma membrane, and that leads to the accumulation of E-cadherin puncta in the cell periphery.

We also found that the exocyst complex was mislocalized in the PALS1 KD cells using two independent methods (Figure 3.17-3.19). The exocyst is localized to the tight junctions in polarized MDCK cells (Grindstaff et al 1998, Yeaman et al 2004) and we have found that the exocyst component Sec8 colocalized with PALS1 during calcium switch experiments (data not shown). It has been reported that the exocyst complex is involved in the regulation of E-cadherin exocytosis in both mammalian cells and in *Drosophila* (Langevin et al 2005, Shipitsin & Feig 2004). On the other hand, exocyst mediates the targeting of intracellular vesicles to the specific sites of plasma membranes (Hsu et al 1999), which is consistent with our hypothesis that the docking or fusion step of E-cadherin trafficking is disrupted in the PALS1 KD cells. In polarizing MDCK cells, Sec8 and Sec6 are recruited from the cytosol to sites of cell-cell contact upon initiation of E-cadherin-dependent cell-cell adhesion, and Sec8 can be immunoprecipitated with E-cadherin (Grindstaff et al 1998, Yeaman et al 2004). Thus we hypothesize that the defects seen in the trafficking of E-cadherin in PALS1 KD cells are related to concomitant defects in exocyst function. We also believe that the relationship between E-cadherin and exocyst is non-linear and there are complicated interactions and feedback loops between the two. When PALS1 is depleted, the interactions and feedbacks are disrupted, and both E-cadherin and

exocyst are mislocalized. However further investigations will be needed to study the interplay among polarity proteins, the exocyst and E-cadherin.

BIBLIOGRAPHY

- Bachmann A, Schneider M, Theilenberg E, Grawe F, Knust E. 2001. *Drosophila* Stardust is a partner of Crumbs in the control of epithelial cell polarity. *Nature* 414: 638-43
- Bryant DM, Stow JL. 2004. The ins and outs of E-cadherin trafficking. *Trends Cell Biol* 14: 427-34
- Grawe F, Wodarz A, Lee B, Knust E, Skaer H. 1996. The *Drosophila* genes crumbs and stardust are involved in the biogenesis of adherens junctions. *Development* 122: 951-9
- Grindstaff KK, Yeaman C, Anandasabapathy N, Hsu SC, Rodriguez-Boulan E, et al. 1998. Sec6/8 complex is recruited to cell-cell contacts and specifies transport vesicle delivery to the basal-lateral membrane in epithelial cells. *Cell* 93: 731-40
- Hong Y, Stronach B, Perrimon N, Jan LY, Jan YN. 2001. *Drosophila* Stardust interacts with Crumbs to control polarity of epithelia but not neuroblasts. *Nature* 414: 634-8
- Hsu SC, Hazuka CD, Foletti DL, Scheller RH. 1999. Targeting vesicles to specific sites on the plasma membrane: the role of the sec6/8 complex. *Trends Cell Biol* 9: 150-3
- Hurd TW, Gao L, Roh MH, Macara IG, Margolis B. 2003. Direct interaction of two polarity complexes implicated in epithelial tight junction assembly. *Nat Cell Biol* 5: 137-42
- Kamberov E, Makarova O, Roh M, Liu A, Karnak D, et al. 2000. Molecular cloning and characterization of Pals, proteins associated with mLin-7. *J Biol Chem* 275: 11425-31
- Klebes A, Knust E. 2000. A conserved motif in Crumbs is required for E-cadherin localisation and zonula adherens formation in *Drosophila*. *Curr Biol* 10: 76-85
- Knust E, Bossinger O. 2002. Composition and formation of intercellular junctions in epithelial cells. *Science* 298: 1955-9
- Langevin J, Morgan MJ, Sibarita JB, Aresta S, Murthy M, et al. 2005. *Drosophila* exocyst components Sec5, Sec6, and Sec15 regulate DE-Cadherin trafficking from recycling endosomes to the plasma membrane. *Dev Cell* 9: 355-76
- Lemmers C, Michel D, Lane-Guermonprez L, Delgrossi MH, Medina E, et al. 2004. CRB3 binds directly to PAR6 and regulates the morphogenesis of the tight junctions in mammalian epithelial cells. *Mol Biol Cell* 15: 1324-33
- Lock JG, Stow JL. 2005. Rab11 in recycling endosomes regulates the sorting and basolateral transport of E-cadherin. *Mol Biol Cell* 16: 1744-55

- Matter K, Balda MS. 2003. Signalling to and from tight junctions. *Nat Rev Mol Cell Biol* 4: 225-36
- McGee AW, Dakoiji SR, Olsen O, Brecht DS, Lim WA, Prehoda KE. 2001. Structure of the SH3-guanylate kinase module from PSD-95 suggests a mechanism for regulated assembly of MAGUK scaffolding proteins. *Mol Cell* 8: 1291-301
- Michel D, Arsanto JP, Massey-Harroche D, Beclin C, Wijnholds J, Le Bivic A. 2005. PATJ connects and stabilizes apical and lateral components of tight junctions in human intestinal cells. *J Cell Sci* 118: 4049-57
- Roh MH, Makarova O, Liu CJ, Shin K, Lee S, et al. 2002. The Maguk protein, Pals1, functions as an adapter, linking mammalian homologues of Crumbs and Discs Lost. *J Cell Biol* 157: 161-72
- Roh MH, Margolis B. 2003. Composition and function of PDZ protein complexes during cell polarization. *Am J Physiol Renal Physiol* 285: F377-87
- Shin K, Straight S, Margolis B. 2005. PATJ regulates tight junction formation and polarity in mammalian epithelial cells. *J Cell Biol* 168: 705-11
- Shipitsin M, Feig LA. 2004. RalA but not RalB enhances polarized delivery of membrane proteins to the basolateral surface of epithelial cells. *Mol Cell Biol* 24: 5746-56
- Straight SW, Shin K, Fogg VC, Fan S, Liu CJ, et al. 2004. Loss of PALS1 expression leads to tight junction and polarity defects. *Mol Biol Cell* 15: 1981-90
- Tavares GA, Panepucci EH, Brunger AT. 2001. Structural characterization of the intramolecular interaction between the SH3 and guanylate kinase domains of PSD-95. *Mol Cell* 8: 1313-25
- Tepass U. 1996. Crumbs, a component of the apical membrane, is required for zonula adherens formation in primary epithelia of Drosophila. *Dev Biol* 177: 217-25
- Tepass U, Knust E. 1993. Crumbs and stardust act in a genetic pathway that controls the organization of epithelia in Drosophila melanogaster. *Dev Biol* 159: 311-26
- Tsukita S, Furuse M, Itoh M. 2001. Multifunctional strands in tight junctions. *Nat Rev Mol Cell Biol* 2: 285-93
- Wang Q, Hurd TW, Margolis B. 2004. Tight junction protein PAR6 interacts with an evolutionarily conserved region in the amino terminus of PALS1/stardust. *J Biol Chem* 279: 30715-21
- Woods DF, Hough C, Peel D, Callaini G, Bryant PJ. 1996. Dlg protein is required for junction structure, cell polarity, and proliferation control in Drosophila epithelia. *J Cell Biol* 134: 1469-82

- Wu H, Reissner C, Kuhlendahl S, Coblenz B, Reuver S, et al. 2000. Intramolecular interactions regulate SAP97 binding to GKAP. *Embo J* 19: 5740-51
- Yeaman C. 2003. Ultracentrifugation-based approaches to study regulation of Sec6/8 (exocyst) complex function during development of epithelial cell polarity. *Methods* 30: 198-206
- Yeaman C, Grindstaff KK, Nelson WJ. 2004. Mechanism of recruiting Sec6/8 (exocyst) complex to the apical junctional complex during polarization of epithelial cells. *J Cell Sci* 117: 559-70

CHAPTER 4

THE PALS1 CARBOXYL-TERMINUS UNDERGOES INTRAMOLECULAR INTERACTION

4.1 Introduction

Studies in the preceding chapter of this thesis revealed that the carboxyl-terminus of PALS1 has an indispensable function in epithelial polarity. This is shown by the inability of the PALS1 carboxyl-terminal truncation mutant and the SH3 domain mutant L379P to rescue the junction defects of the PALS1 knockdown cells. Little is known about the function of this region, which includes a SH3 domain, a Band 4.1-binding (4.1B) motif and a GUK domain. No binding partners of this region have been reported. An effort to identify interacting proteins by large-scale protein purification and mass spectrometry proved inconclusive.

Therefore, we shifted our focus onto possible intramolecular interactions of the PALS1 carboxyl-terminus, since such interactions have been reported in a structurally-related MAGUK family protein Discs Large (DLG), and the interaction is essential for DLG's function (Figure 4.1). The intramolecular interaction in DLG exposes the 4.1B motif between SH3 and GUK domains, which allows the motif to bind Protein 4.1R and to mediate the plasma membrane localization (Hanada et al 2003). The interaction is also important for the binding properties of the SH3 and GUK domains themselves. The two domains dimerize to keep the carboxyl-terminus of human DLG (hDLG) in a closed conformation to enable both domains to interact

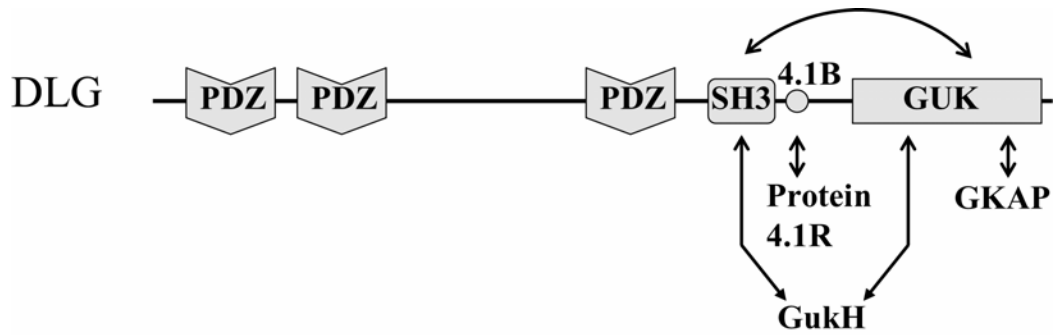


Figure 4.1 Schematic illustration of DLG, showing domains it is composed of and the interactions in its carboxyl-terminus. Note that this is the DLG-I₃ isoform which contains the 4.1B motif. The DLG-I₂ isoform does not have the 4.1B motif but maintains the other interactions depicted.

with the protein GukHolder (GukH) (Qian & Prehoda 2006). In another case, SH3 binding masks the GUK domain and inhibits its interaction with GUK-associated protein (GKAP), although the masking effect is suppressed by the hDLG amino-terminus (Wu et al 2000).

The inability of the PALS1 L379P mutant to rescue the polarity defects of the PALS1 KD cells suggests that the SH3-GUK intramolecular interaction may be present in PALS1 as well. Sequence alignment implies that L379P is the equivalent of the m30 mutation in DLG. The m30 mutation is a single amino acid substitution in the SH3 domain and was identified as responsible for promoting tumor formation in the epithelium of the imaginal disc (Woods et al 1996). The m30 mutation (L556P) of SAP97, one of the human homologues of DLG, is defective in the SH3-GUK interaction (Wu et al 2000). Therefore, the L379P point mutation may disrupt the SH3-GUK interaction in PALS1 in a similar way, thus rendering PALS1 L379P unable to rescue the polarity defects seen in PALS1 KD cells.

This chapter shows biochemical data to support the hypothesis that an intramolecular interaction indeed exists in the PALS1 carboxyl-terminus. However,

this interaction appears not to be regulated in a polarization-dependent manner.

4.2 Materials and methods

4.2.1 Cell culture

MDCK type II cells and HEK293 cells were grown in Dulbecco's modified Eagle's medium (Invitrogen) containing 100 units of penicillin, 100 µg/ml streptomycin sulfate, 2 mM L-glutamine, and 10% fetal bovine serum. Stable PALS1 KD cells rescued with Myc-PALS1, Myc-PALS1 L379P and Myc-PALS1 delC were maintained in media supplemented with 300 µg/ml G418 plus 300 µg/ml hygromycin B.

4.2.2 DNA constructs

Mouse PALS1 DNA fragments were amplified by PCR and subcloned into pGSTag and pCMVTagB (Stratagene) vectors to obtain the GST-tagged constructs and the Myc-tagged constructs, respectively. The Δ WVPS mutant was made using the single-primer mutagenesis method as previously described (Kamberov et al 2000).

4.2.3 Immunoprecipitation and blotting

Lysates from MDCKII wild type cells, the stable MDCK cell lines (Wang et al 2007) or HEK293 cells transfected with Myc-tagged PALS1 mutants were collected as previously described (Wang et al 2004). For GST-PALS1 pull-downs, 10 µg of GST protein was used per experiment.

4.3 Results

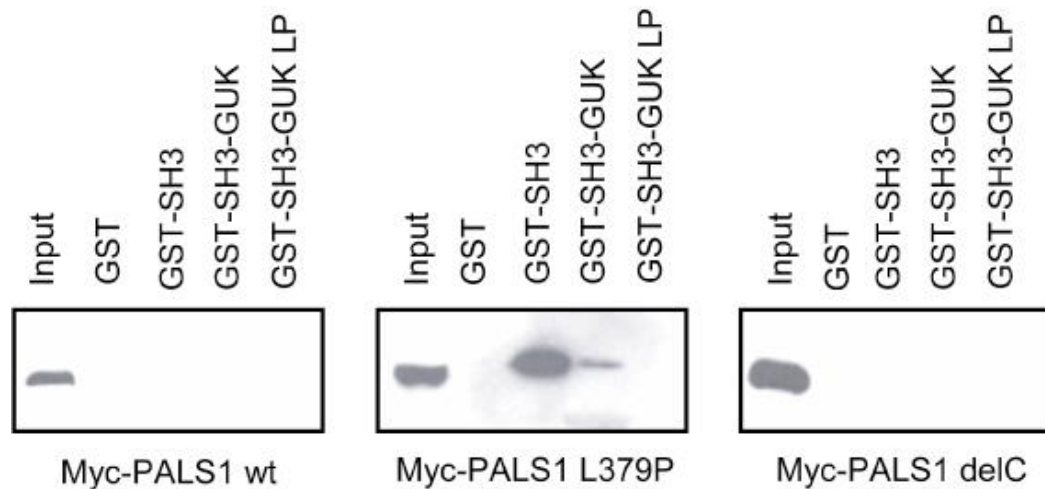


Figure 4.2 Intramolecular interaction between PALS1 SH3 domain and GUK domain. GST fusion proteins as indicated (LP refers to the L379P substitution) were incubated with lysates from MDCK cells stably expressing Myc-PALS1 wild type, Myc-PALS1 L379P or Myc-PALS1 delC. 5% input and the pull-down were blotted by the anti-Myc antibody.

To demonstrate that the SH3-GUK interaction indeed occurs in PALS1, a GST pull-down experiment was performed (Figure 4.2). Immobilized GST alone, GST-SH3, GST-SH3-GUK and GST-SH3-GUK L379P proteins were incubated with protein lysates containing myc-PALS1, myc-PALS1 L379P or myc-PALS1 delC, which were from the stable PALS1 KD/rescue cell lines constructed in Chapter 3. None of the GST fusion proteins could pull down myc-PALS1 or myc-PALS1 delC, while GST-SH3 strongly interacted with myc-PALS1 L379P; GST-SH3-GUK showed only a weak pull-down. These results indicate that an unbound native PALS1 SH3 domain (GST-SH3) can interact with an unbound native PALS1 GUK domain (myc-PALS1 L379P). The L379P mutant disrupts this interaction in the Myc-tagged PALS1 variants and releases the GUK binding site, while in the intact PALS1 carboxyl-terminus, the GUK binding site is masked by SH3 binding. A small portion of the

bacterially-expressed GST-SH3-GUK protein might have a misfolded GUK domain, which may explain the residual amount of interaction with myc-SH3-GUK L379P.

Previous studies in SAP97 showed that the SH3-GUK interaction is not a canonical SH3 domain interaction: there is no consensus SH3 binding site PXXP in the GUK domain (Li 2005); moreover, two point mutations in the SH3 domain that disrupt its recognition of the PXXP motif do not affect the SH3-GUK interaction (Wu et al 2000). A genetic screen in *Drosophila* identified a DLG mutant lacking the last 15 amino acids, and this mutant no longer displays SH3-GUK intramolecular dimerization (Newman & Prehoda, ASCB meeting 2006). Alignment of the carboxyl-terminus of PALS1 with that of DLG displayed no obvious similarity in the last 15 amino acids except for an identical WVPS motif (Figure 4.3, a). Indeed, by a pulldown experiment with GST-SH3 beads, we confirmed that deletion of the last 15 amino acid tail abolished the interaction with the Myc-4.1B-GUK mutant. Moreover, without the WVPS motif, the Myc-SH3-GUK L379P mutant could no longer be precipitated by GST-SH3 (Figure 4.3, b). These results suggest that the WVPS motif in the carboxyl-terminal tail of PALS1 is the recognition site of the SH3 domain.

It was of interest to examine whether the PALS1 SH3-GUK interaction is regulated *in vivo*, e.g. whether the PALS1 carboxyl-terminus undergoes any close-to-open conformational switch under different conditions because such switches can play an important role in the function of the protein. Examples of this are the FERM family proteins, vinculin, the Wiskott–Aldrich syndrome protein (WASP)/Scar family and formins (Alberts 2001, Bretscher et al 2002, Johnson & Craig 1995, Johnson & Craig 2000, Rohatgi et al 1999). One can imagine that the PALS1 4.1B motif interacts with an as yet unidentified FERM protein, and that interaction could be regulated by the conformational switch of PALS1 carboxyl-terminus. FERM proteins can associate

a.

Drosophila DLG: **KSMIWSQSGPTIWVPSKESL**
956 970
Mouse PALS1: **LRLINKLDTEPQWVPSTWLR**
661 675

b.

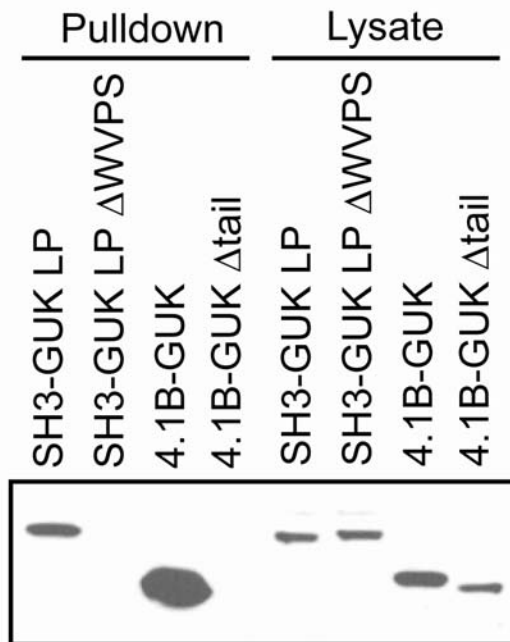


Figure 4.3 PALS1 carboxyl-terminus mediates the interaction with its SH3 domain. (a) Alignment of *Drosophila* DLG carboxyl-terminus with that of mouse PALS1. The last 15 amino acids are in blue and are referred to as tail, among which the four homologous amino acids are in red and are referred to as WVPS motif. (b) Myc-tagged PALS1 mutants were expressed in 293 cells and the cell lysates were incubated with the immobilized GST-SH3 fusion protein. Cell lysates and pull-down were blotted with the anti-Myc antibody.

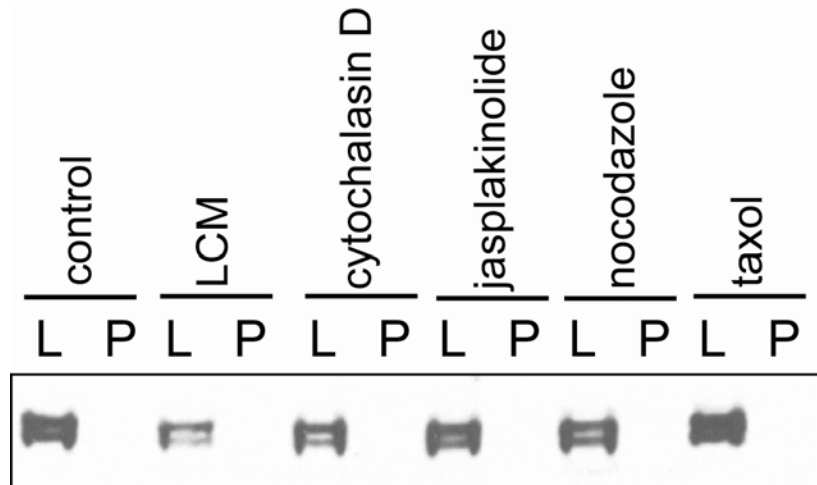


Figure 4.4 PALS1 carboxyl-terminus is in the closed conformation. MDCK cells were incubated in standard medium (control lanes), low calcium medium (LCM lanes) or treated with different drugs for 1 h as indicated. Cells were lysed and then incubated with GST-SH3 beads. Lysates (L) and pull-downs (P) were blotted by the anti-PALS1 antibody. No positive results in the pull-down lanes were detected, indicating that the SH3 domain and the GUK domain were bound to each other and they kept the PALS1 carboxyl-terminus in the closed conformation.

with both the actin cytoskeleton and microtubules and they play an important role in stabilizing the membrane skeletons (Bretscher et al 2002). Both the actin cytoskeleton and microtubules undergo dramatic rearrangements during epithelial polarization. If PALS1 indeed interacts with a FERM protein and it is anchored to the cytoskeletons through a FERM protein, it is possible that the PALS1-FERM interaction is subject to regulation when the actin skeleton or the microtubules are restructured, and one of the ways of regulation is through conformational change of PALS1 carboxyl-terminus. In this regard, we treated wild type MDCK cells with drugs that disrupt actin or microtubules (cytochalasin D and nocodazole) and those that stabilize actin or microtubules (jasplakinolide and taxol). We also incubated cells in low calcium medium overnight. As is shown in Figure 4.4, GST-SH3 could not pull down endogenous PALS1 from the lysate of the control cells, suggesting that PALS1

carboxyl-terminus is in the closed conformation under normal conditions in polarized cells. None of the treatments used induced the opening, shown by the negative result of the pulldown (Figure 4.4). We hypothesize that the SH3-GUK intramolecular interaction is stable, and the PALS1 carboxyl-terminus is in a constant closed conformation. No conformational change of DLG carboxyl-terminus has been reported either. Therefore, it is possible that the MAGUK proteins need to maintain the carboxyl-terminal intramolecular interaction to be functional.

4.4 Discussion

In this chapter, the hypothesized PALS1 carboxyl-terminal intramolecular interaction was confirmed by GST pulldown experiments and the SH3 domain recognition site was pinpointed as the WVPS motif in the carboxyl-terminal tail (Figure 4.2, 4.3). The WVPS motif is actually outside of the GUK domain. More biochemical experiments are needed to see whether there is additional SH3 binding site within the GUK domain as well as the connecting region between the SH3 domain and the GUK domain. If the WVPS motif is the exclusive binding site, this intramolecular interaction does not represent a canonical SH3-GUK interaction. However, it is not clear how the PALS1 SH3 domain recognizes unconventional motifs like WVPS. More investigations, especially structural data, are needed to further elucidate the nature of this interaction.

Recent research has shown that components of the PAR polarity complex are subject to phosphorylation-mediated regulation during epithelial polarization and PAR6-aPKC forms a pre-complex with Lgl in the early stage of polarization before PAR6-aPKC interacts with PAR3 in the late stage of polarity establishment (see Chapter 1). The dynamics of the PAR complex is critical for the establishment of the

apical-basal polarity, as the balance between the apical domain and basolateral domain is determined by the activity of the PAR complex at the apical domain and that of Lgl at the lateral domain (Shin et al 2006 and Figure 1.2). We tested the interaction between PALS1 and its binding partners in different stages of epithelial polarization; however, no changes were detected (data not shown). Results in this chapter suggest that the carboxyl-terminal intramolecular interaction might not be subject to regulations either (Figure 4.4). It is possible that regulations do not occur at the level of PALS1 itself, but rather, at the level of the proteins that interact with PALS1. Thus, PALS1 provides a stable interacting platform and acts as a core adapter protein.

BIBLIOGRAPHY

- Alberts AS. 2001. Identification of a carboxyl-terminal diaphanous-related formin homology protein autoregulatory domain. *J Biol Chem* 276: 2824-30
- Bretscher A, Edwards K, Fehon RG. 2002. ERM proteins and merlin: integrators at the cell cortex. *Nat Rev Mol Cell Biol* 3: 586-99
- Hanada T, Takeuchi A, Sondarva G, Chishti AH. 2003. Protein 4.1-mediated membrane targeting of human discs large in epithelial cells. *J Biol Chem* 278: 34445-50
- Johnson RP, Craig SW. 1995. F-actin binding site masked by the intramolecular association of vinculin head and tail domains. *Nature* 373: 261-4
- Johnson RP, Craig SW. 2000. Actin activates a cryptic dimerization potential of the vinculin tail domain. *J Biol Chem* 275: 95-105
- Kamberov E, Makarova O, Roh M, Liu A, Karnak D, et al. 2000. Molecular cloning and characterization of Pals, proteins associated with mLin-7. *J Biol Chem* 275: 11425-31
- Li SS. 2005. Specificity and versatility of SH3 and other proline-recognition domains: structural basis and implications for cellular signal transduction. *Biochem J* 390: 641-53
- Qian Y, Prehoda KE. 2006. Interdomain interactions in the tumor suppressor discs large regulate binding to the synaptic protein GukHolder. *J Biol Chem* 281: 35757-63
- Rohatgi R, Ma L, Miki H, Lopez M, Kirchhausen T, et al. 1999. The interaction between N-WASP and the Arp2/3 complex links Cdc42-dependent signals to actin assembly. *Cell* 97: 221-31
- Shin K, Fogg VC, Margolis B. 2006. Tight junctions and cell polarity. *Annu Rev Cell Dev Biol* 22: 207-35
- Wang Q, Hurd TW, Margolis B. 2004. Tight junction protein Par6 interacts with an evolutionarily conserved region in the amino terminus of PALS1/stardust. *J Biol Chem* 279: 30715-21
- Woods DF, Hough C, Peel D, Callaini G, Bryant PJ. 1996. Dlg protein is required for junction structure, cell polarity, and proliferation control in Drosophila epithelia. *J Cell Biol* 134: 1469-82
- Wu H, Reissner C, Kuhlendahl S, Coblenz B, Reuver S, et al. 2000. Intramolecular interactions regulate SAP97 binding to GKAP. *Embo J* 19: 5740-51

CHAPTER 5

CONCLUSIONS AND PERSPECTIVES

5.1 PALS1 is an important regulator of mammalian epithelial cell polarity

PALS1 is an important polarity regulator in mammalian epithelial cells. It interacts with both CRB3 and PATJ to integrate the three into one complex, and it is at the center of a complex tight-junction-associated adaptor protein network. In addition to α PKC ζ , whose depletion renders cells nonviable, loss of PALS1 expression was found to cause the most severe defects in tight junction formation and cell polarity in a systematic RNAi-based study in MDCK cells (Macara, ASCB meeting 2006).

The biochemical pathways through which PALS1 regulates epithelial polarity are not yet clear, partially because PALS1 and many of its interacting partners are adaptor proteins with no intrinsic signaling activity. The studies in this thesis further elucidate the function of PALS1, and together with other research efforts clarify the role of this protein.

In this thesis, I have shown that PALS1 interacts with the Cdc42-effector protein PAR6, linking the CRB complex and the PAR complex together. In addition, PALS1 stabilizes PATJ and regulates E-cadherin trafficking and thus adherens junction formation, hypothetically through the action of the exocyst. Meanwhile, the carboxyl-terminus of PALS1 undergoes an intramolecular interaction, which could potentially represent an essential regulatory role of this region. Taken together, the findings further demonstrate that PALS1 is an important regulator of mammalian

epithelial polarity. New aspects regarding the molecular actions of PALS1 have been revealed, and they are elaborated as follows.

5.1.1 The PALS1-PAR6 interaction represents an unconventional mode of PDZ action

The PALS1-PAR6 interaction is mediated by the amino-terminal U1 region of PALS1 and the PDZ domain of PAR6, but it is not a conventional PDZ domain interaction. The interaction mode is unusual in two aspects.

First, the PDZ binding site is internal and two adjacent amino acids are critical for recognition. PDZ domains usually bind the extreme carboxyl-terminus of proteins and in special cases can also recognize internal sites when that site is presented in a β -finger structure that mimics the protein carboxyl-terminus (Sheng & Sala 2001). The β -finger structure is usually stabilized by disulfide bonds or salt bridges, as in the case of neuronal nitric-oxide synthase (nNOS)-syntrophin interaction (Hillier et al 1999). Under both circumstances, the PDZ domain recognizes the extreme carboxyl amino acid (P_0) and the one two to the last (P_{-2}), or the two equivalent amino acids in the β -finger structure. But in the PALS1-PAR6 interaction, two adjacent amino acids are recognized by the PAR6 PDZ domain. Meanwhile, according to the crystal structure, the amino terminus of PALS1 is not folded into a β -finger (Peterson et al 2004) to fit in the PAR6 PDZ domain and no evidence of a salt bridge in PALS1 U1 region has been found (Q Wang unpublished data). In comparison to the structures of PDZ domains in complex with carboxyl-terminal ligands, PAR6 PDZ domain shows a different conformation in its carboxylate-binding loop when binding the PALS1 internal site, so that it bypasses the requirement of the carboxylate group (Penkert et al 2004).

Second, the PAR6 PDZ domain alone cannot interact with the PALS1 amino-terminus; the PDZ domain and the adjacent semi-CRIB domain are both required. The PDZ domain and the semi-CRIB domain are closely coupled together, as Cdc42-loading in the semi-CRIB domain induces conformational changes of the PDZ domain. On the other hand, the PDZ domain of PAR6 and the semi-CRIB domain function as a whole to bind Cdc42, because the semi-CRIB domain and the PDZ domain form a continuous eight-stranded sheet as the Cdc42-binding pocket (Garrard et al 2003).

These two unconventional folds are related to each other. The protein sequence of the PAR6 PDZ domain aligns well with other canonical PDZ domains. However, no similar PDZ interactions as that of PALS1-PAR6 have been reported. It could be a result of the close coupling between the PAR6 PDZ domain and the adjacent semi-CRIB domain. As is shown by the crystal structure, when Cdc42 is bound to the semi-CRIB domain, the structure of the unbound PAR6 PDZ domain overlaps with those of the canonical PDZ domains; however, when the semi-CRIB domain is free, the unbound PAR6 PDZ domain reveals an obvious structural deviation (Peterson et al 2004). It has been shown that the Cdc42-free, ligand-bound PAR6 PDZ domain (both terminal and internal) has a non-canonical conformation as that of the Cdc42-free unbound PAR6 PDZ domain (Penkert et al 2004), and Cdc42-loading can induce the conformational change in the carboxyl-terminal-ligand-bound PDZ domain similar to the unbound PDZ domain (Peterson et al 2004), yet whether the PALS1-binding PAR6 PDZ domain is restored to the canonical PDZ conformation after Cdc42 binding is unknown. On the other hand, the affinity of the PALS1-PAR6 interaction is not increased after Cdc42 binding like that of the carboxyl-terminal ligand, which suggests a correlation between affinity and

conformation of PAR6 PDZ domain. The residue at the end of the carboxylate binding loop of the PAR6 PDZ domain is proline, while most canonical PDZ domains have a glycine at this position. When the proline is mutated to glycine, Cdc42 binding no longer enhances the affinity of the carboxyl-terminal ligand to the PAR6 PDZ domain, e.g. the semi-CRIB domain and the PDZ domain are decoupled, whilst the binding to PALS1 is unaffected (Peterson et al 2004). Based on these observations, I propose that when PAR6 PDZ domain is bound to PALS1, it will not respond to Cdc42 loading in the adjacent semi-CRIB domain, and the conformation as well as the binding affinity remain unchanged (Figure 5.1, upper panel). It is possible that the overhanging PALS1 U1 region keeps the PDZ carboxylate-binding loop in the deviated conformation, and hinders the coupling between the semi-CRIB domain and the PDZ domain, with an effect similar to the proline-to-glycine mutant. In this way, by binding to the PALS1 internal ligand, PAR6 PDZ domain is locked in the Cdc42-free conformation even if Cdc42 is loaded, and the non-canonical Cdc42-free conformation in turn accounts for the unconventional mode of internal ligand recognition.

5.1.2 PALS1 and CRB3 differentially regulates PAR6

In 2004, Peterson and coworkers screened a library of GST fusions to class I (-S/T-X-V-COOH) and class II (- ϕ -X- ϕ -COOH: ϕ = hydrophobic residue) PDZ ligand sequences, and they found that the PAR6 PDZ domain binds to the class I carboxyl-terminal ligand -VKESLV-COOH. At that time, no physiological carboxyl-terminal ligand of PAR6 was known, and later it was shown that CRB3 carboxyl tail binds PAR6 PDZ domain *in vivo* (Lemmers et al 2004). The carboxyl-terminal sequence of CRB3 is -ERLI-COOH, and it partially aligns with the sequence -VKESLV-COOH

identified in the screen. Since Cdc42 binding can increase the affinity of carboxyl-terminal ligand binding, it follows that the PAR6-CRB3 interaction is up-regulated by Cdc42, presumably due to the conformational change of the PAR6 PDZ domain (Figure 5.1, lower panel).

Cdc42 is a central polarity regulator, and PAR6 is an important Cdc42 effector in the context of epithelial polarization. Cdc42 binding to the semi-CRIB domain not only induces conformational changes of PAR6 PDZ domain itself, it also leads to an overall structural change of the full length PAR6 protein (Garrard et al 2003). If PALS1 could decouple PAR6 semi-CRIB domain and PDZ domain as predicted, it is also possible that PALS1 binding would inhibit the overall structural change and the Cdc42-responsiveness of PAR6, and thus be a PAR6 negative regulator. On the contrary, CRB3 does not possess the structural basis for these features. Therefore, PALS1 and CRB3 could differentially regulate PAR6. Further work needs to be done to test the validity of this hypothesis and how PAR6 selects between PALS1 and CRB3 for interaction. Understanding of the two interactions could be important for understanding how the CRB complex and the PAR complex are coordinated during epithelial polarization.

5.1.3 The Lin-7-PALS1-PATJ stabilization hierarchy

Our lab has previously demonstrated that knockdown of PALS1 by RNAi leads to a decrease in PATJ protein levels and that is not a result of reduced transcription or translation of PATJ (Straight et al 2004). My work reconfirmed this result, and furthermore I demonstrated that PATJ expression can be rescued when

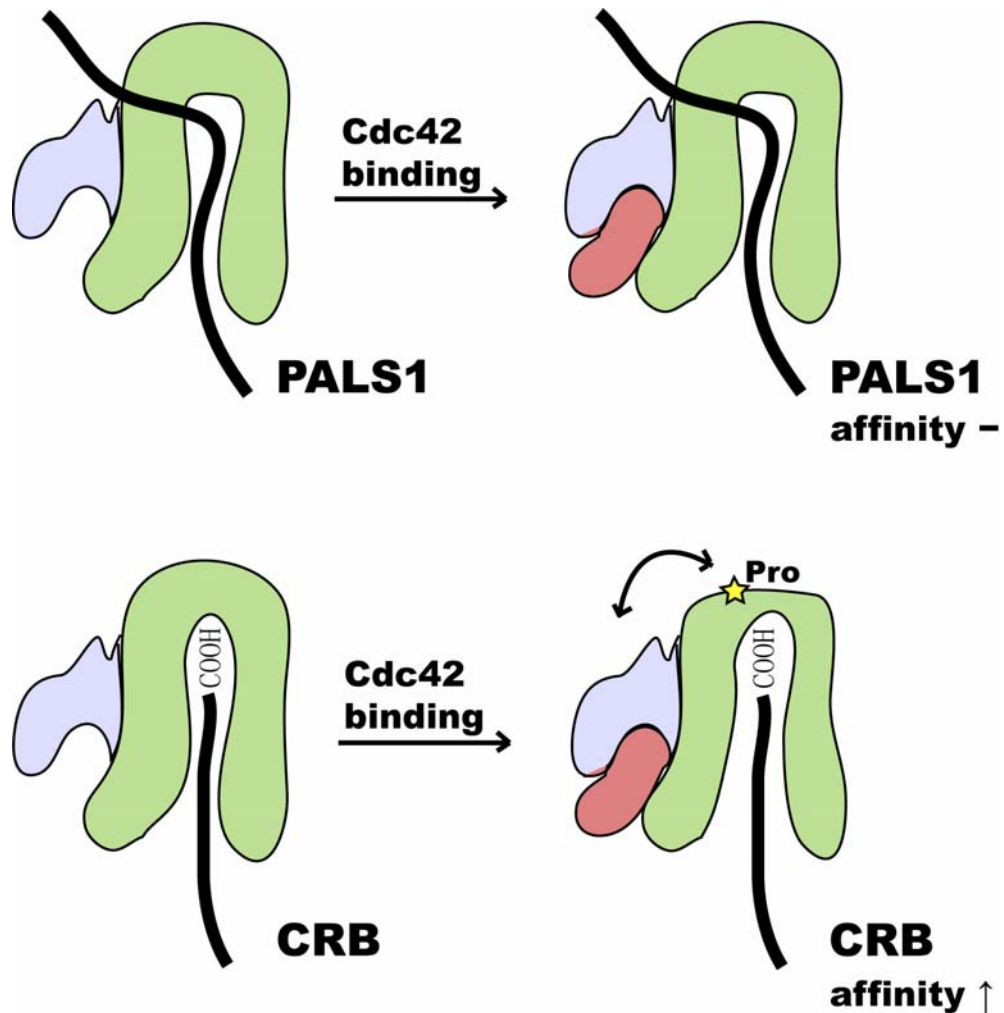


Figure 5.1 Hypothetical model of the two types of PAR6 PDZ domain interactions. The green, grey and red shapes represent the PAR6 PDZ domain, the semi-CRIB domain and Cdc42, respectively. When the PAR6 PDZ domain binds internal ligand such as PALS1, the overhanging PALS1 region hinders the coupling between the semi-CRIB motif and the PDZ domain, so that Cdc42 binding does not induce conformational change of the PDZ domain, and thus does not increase the affinity of PAR6-PALS1 interaction. When the PAR6 PDZ domain binds carboxyl-terminal ligands such as CRB, the PDZ domain and the semi-CRIB domain are free to couple (indicated by the double-headed arrow). Therefore, Cdc42 causes the PDZ domain to switch to the canonical PDZ domain conformation, and the affinity between PAR6 PDZ domain and its carboxyl-terminal ligand is enhanced. The rigid proline residue at the carboxylate binding pocket (marked by the star) is essential for this coupling.

exogenous PALS1 and PALS1 mutants are introduced, except for the PALS1 L27N PATJ binding mutant (Wang et al 2007). These results suggest that PATJ is stabilized through its interaction with PALS1, and without this interaction PATJ cannot stably exist *in vivo*. A recent study from our group added to the complexity of this stabilization story. Straight and coworkers knocked down the PALS1-binding protein Lin-7 in MDCKII cells, and the depletion of Lin-7 was concomitant with the loss of both PALS1 and PATJ. Quantitative reverse transcription PCR and pulse-chase experiments showed that PALS1 protein degradation was increased in the Lin-7 shRNA cells (Straight et al 2006), and presumably that in turn lead to the enhanced degradation of PATJ. On the other hand, knockdown of PATJ has no effect on PALS1 level (Shin et al 2005), and Lin-7 protein level is not affected in the PALS1 knockdown cells (Q Wang unpublished data).

These data give rise to the notion of a stabilization hierarchy: Lin-7 stabilizes PALS1 and PALS1 stabilizes PATJ, while the reverse is not true. It is not clear how Lin-7 stabilizes PALS1 though, since in fully polarized epithelial cells PALS1 is localized to tight junctions, while Lin-7 is at adherens junctions. It is possible that Lin-7 binds and stabilizes PALS1 in the early polarization stage, and this mechanism is not required after PALS1 reaches tight junctions.

5.1.4 The adhesion-to-polarity model versus the polarity-to-adhesion hypothesis

My study revealed that PALS1 has a role in regulating the trafficking of E-cadherin, the structural component of adherens junctions and an important mediator of cell-cell adhesion. It is widely accepted that cell-cell adhesion initiates polarization and adhesion is the primary polarity cue. My observations add a new perspective to

this classical model and suggest the possibility that polarity proteins could be mobilized before or at the same time as adhesion.

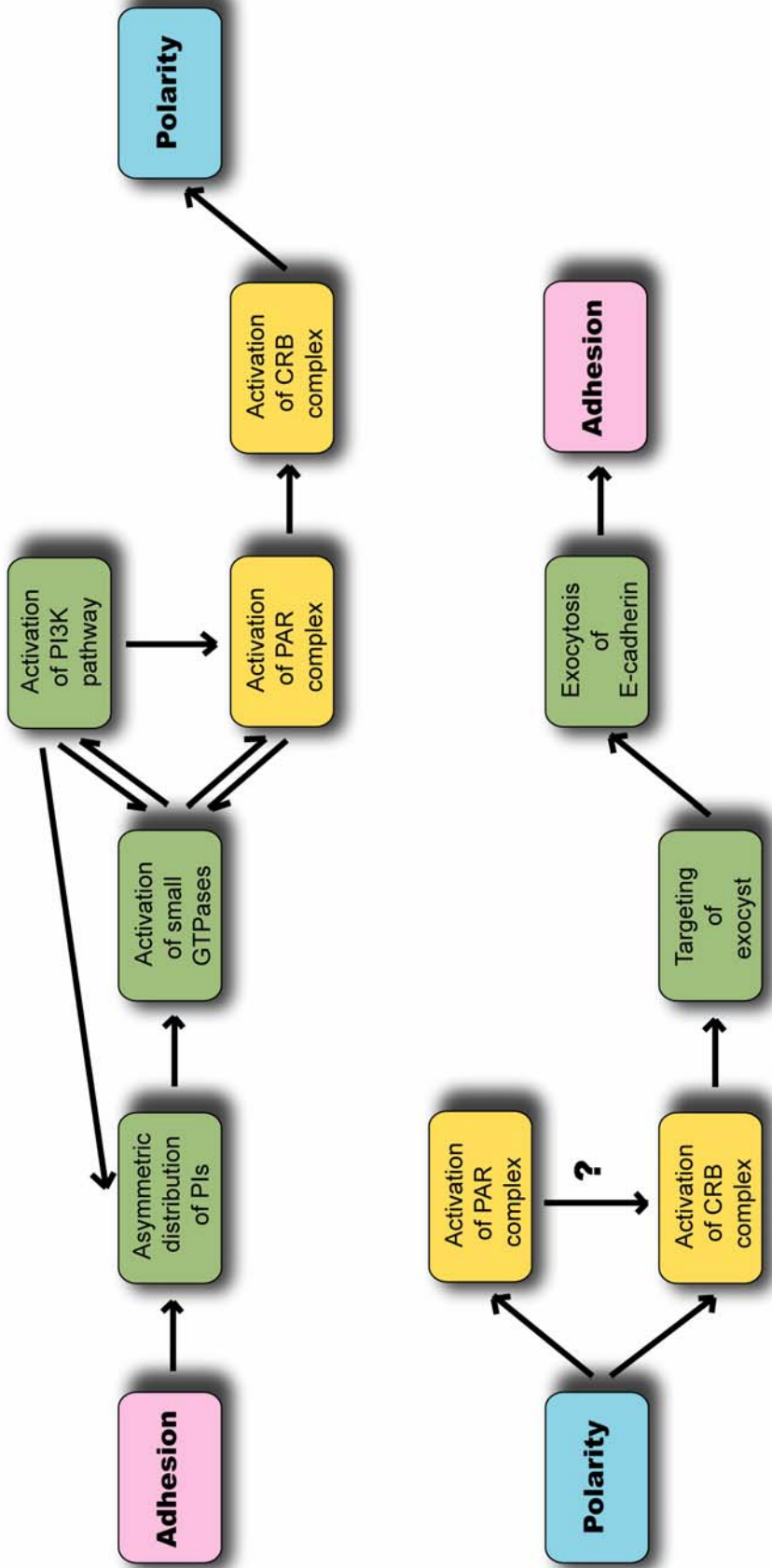
E-cadherin *trans*-dimerizes with E-cadherin on adjacent cells in a Ca^{2+} -dependent manner and this feature has been exploited to develop the calcium switch model. When cultured in low Ca^{2+} medium, cells round up and lose most contacts with their neighboring cells. At this time, the majority of E-cadherin has been endocytosed and stored in intracellular compartments, although a small fraction of E-cadherin and other cell adhesion molecules (CAMs) remain at the cell surface. Upon the re-introduction of Ca^{2+} to the growth medium, E-cadherin from adjacent cells make contact and initiate the *trans*-dimerization. Nectin and Nectin-like molecules also participate in this initial contact, although it is not clear whether their Ca^{2+} -independent adhesion temporally proceeds that of E-cadherin. This initial contact serves as a spatial cue of apical-basal polarity, and it initiates a series of signaling events and leads to the rapid exocytosis of more E-cadherin and other CAMs, including future tight junction components. They also form the nascent junctional structures— spot-like adherens junction at the cell-cell contact sites. These spot-like adherens junctions serve to anchor and nucleate cytoskeletal actin and induce an overall change in cell shape. In the next phase, the tight junction components separate from the adherens junction components and move apically to form tight junctions, and the spot-like adherens junctions fuse into mature adherens junction belts. At the same time, intracellular vesicles dock and fuse to the boundary of the apical and the basolateral membrane domains, which is where the tight junctions assemble. The addition of lipids and proteins leads to the growth of the lateral membrane and the vertical extension of the epithelial cells (Nakanishi & Takai 2004, Nelson 2003, Suzuki & Ohno 2006, Yeaman et al 1999).

Dominant as the adhesion-to-polarity model is, recent studies have indicated the possibility that initiation of polarization could be independent of adhesion. In 2004, Baas et al. discovered that activation of the mammalian PAR4 protein LKB1 is sufficient to induce the remodeling of the actin cytoskeleton in contact-naïve intestinal epithelial cells to form brush borders, and junctional proteins; ZO-1 and p120, redistribute to a dotted circle at the periphery of single cells (Baas et al 2004). Recent reports also showed that correct localization of Bazooka is independent of ZA, while the recruitment of *Drosophila* E-cadherin (DE-Cad) into apical spot junctions requires Bazooka (Harris & Peifer 2004).

My studies showed that knockdown of PALS1 in MDCKII cells not only causes serious tight junction defects, but also disrupts adherens junctions by interfering with E-cadherin trafficking. E-cadherin is retained in intracellular puncta in the cell periphery, and cells fail to make contacts to one another. The exocytosis of E-cadherin is slowed, and the ineffectiveness of E-cadherin cell surface delivery can be partially explained by the mislocalization of the exocyst complex (Wang et al 2007). These results suggest that the activity of polarity proteins is not a secondary phenomenon to cell-cell contacts, but is also involved in the initiation of cell adhesion. It asks the question whether polarity proteins regulate cell adhesion or vice versa. The most likely answer is that processes involving polarity complexes and adhesion complexes work intimately together to establish final epithelial polarity. It seems likely that early adhesion events activate polarity proteins which then feed forward to reinforce adhesion which promotes further polarization (summarized in Figure 5.2).

5.1.5 PALS1 regulates adherens junction formation

Figure 5.2 The classical adhesion-to-polarity model and the polarity-to-adhesion hypothesis. Activity of the CRB complex and the PAR complex are denoted by yellow shapes, and other steps of the polarization process are in green. It is not clear how the activation of PAR complex precedes adhesion. A speculated pathway is that it joins the CRB complex pathway by activating components of the CRB complex, and this step is represented by an arrow with a question mark.



My study shows that PALS1 not only is important for tight junction biogenesis, it is also involved in the regulation of adherens junction formation. It is the first report to indicate that tight-junction-associated PALS1 has a role in adherens junction formation in mammalian epithelial cells. However, the concept of CRB complex regulating zonula adherens biogenesis in *Drosophila* is not new, and actually Crumbs and Sdt were first identified as regulators of *Drosophila* epithelial zonula adherens and DE-cadherin localization (Tepass & Knust 1993), therefore, PALS1's involvement in zonula adherens/adherens junction biogenesis may be a mechanism conserved between species. The Sdt-dPATJ-CRB complex is localized to a distinct domain apical to the zonula adherens in the *Drosophila* epithelial cells called the subapical region. There are no tight junction equivalent structures in the subapical region though; the *Drosophila* functional equivalents to mammalian tight junctions are the septate junctions, which lay basal to ZA and have a distinct molecular composition. It is not clear though how Sdt acts on DE-cadherin from a different domain of localization (Knust & Bossinger 2002), while PALS1 regulates E-cadherin trafficking from a distinct domain too. The similar modes of the spatially-disparate interaction further suggest that PALS1 regulating adherens junction formation may be a mechanism conserved from *Drosophila*.

5.2 Perspectives

The studies in this thesis investigated the role of PALS1 in the establishment of apical-basal polarity in mammalian epithelial cells. New aspects of the protein itself as well as its interaction with other proteins involved in the process have been revealed, yet many issues remained unsolved and new questions have been raised.

In Chapter 4, a preliminary study of the intramolecular interaction in the PALS1 carboxyl-terminus is presented. PALS1 SH3 domain was shown to interact with the WVPS motif in the carboxyl-terminal tail, and no close-to-open conformational switch of the PALS1 carboxyl-terminus was detected. Following these observations, function of the 4.1B motif will be investigated. A PALS1 4.1B deletion mutant will be made, and the localization of the del4.1B mutant as well as other carboxyl-terminal truncation mutants will be examined. We speculate that the 4.1B motif binds a FERM protein, and several candidate proteins will be tested.

Besides the function of the carboxyl-terminus, there are other unsolved issues regarding how PALS1 regulates the establishment of apical-basal polarity in mammalian epithelial cells. My studies in this thesis and other studies have suggested that PALS1 plays diverse roles in the polarization of mammalian epithelial cells and in the formation of cell junctions, but how these diverse roles are coordinated temporally and spatially is not clear. Changes in the interactions between PALS1 and its binding partners have not been detected, therefore, regulation could occur on other levels, e.g. not on the adaptor protein itself, but on the proteins it adapts. It will be helpful to be able to study the *in vivo* activity and localization of PALS1 at the single molecular level, by means of real time confocal imaging and fluorescent resonance energy transfer (FRET).

Recent reports have revealed more details of how CRB complex and PAR complex function at the molecular level, especially how they are linked to other signaling pathways. For example, PAR3/Baz is involved in the differential distribution of phosphoinositides, which has an essential role in specifying the apical domain and the basolateral domain (Gassama-Diagne et al 2006, Martin-Belmonte et al 2007, Pinal et al 2006); PAR3, PAR6 and PATJ have been shown to interact with

GTP exchange factors (GEFs) or GTPase-activating proteins (GAPs) of the Rho family small GTPases, and they contribute to the local activation/inactivation of the small GTPases, which in turn modulate specific steps in epithelial polarization (Chen & Macara 2005, Liu et al 2004, Mertens et al 2005, Nishimura et al 2005, Wells et al 2006). Direct links between PALS1 and other signaling pathways are yet to be discovered. It is possible that PALS1 is at the center of a complicated adaptor protein network, and it integrates and localizes diverse signaling pathways to serve for the establishment of epithelial polarity and junction biogenesis.

BIBLIOGRAPHY

- Baas AF, Kuipers J, van der Wel NN, Batlle E, Koerten HK, et al. 2004. Complete polarization of single intestinal epithelial cells upon activation of LKB1 by STRAD. *Cell* 116: 457-66
- Chen X, Macara IG. 2005. Par-3 controls tight junction assembly through the Rac exchange factor Tiam1. *Nat Cell Biol* 7: 262-9
- Garrard SM, Capaldo CT, Gao L, Rosen MK, Macara IG, Tomchick DR. 2003. Structure of Cdc42 in a complex with the GTPase-binding domain of the cell polarity protein, Par6. *Embo J* 22: 1125-33
- Gassama-Diagne A, Yu W, ter Beest M, Martin-Belmonte F, Kierbel A, et al. 2006. Phosphatidylinositol-3,4,5-trisphosphate regulates the formation of the basolateral plasma membrane in epithelial cells. *Nat Cell Biol* 8: 963-70
- Harris TJ, Peifer M. 2004. Adherens junction-dependent and -independent steps in the establishment of epithelial cell polarity in *Drosophila*. *J Cell Biol* 167: 135-47
- Hillier BJ, Christopherson KS, Prehoda KE, Brecht DS, Lim WA. 1999. Unexpected modes of PDZ domain scaffolding revealed by structure of nNOS-syntrophin complex. *Science* 284: 812-5
- Knust E, Bossinger O. 2002. Composition and formation of intercellular junctions in epithelial cells. *Science* 298: 1955-9
- Lemmers C, Michel D, Lane-Guermonprez L, Delgrossi MH, Medina E, et al. 2004. CRB3 binds directly to Par6 and regulates the morphogenesis of the tight junctions in mammalian epithelial cells. *Mol Biol Cell* 15: 1324-33
- Liu XF, Ishida H, Raziuddin R, Miki T. 2004. Nucleotide exchange factor ECT2 interacts with the polarity protein complex Par6/Par3/protein kinase Czeta (PKCzeta) and regulates PKCzeta activity. *Mol Cell Biol* 24: 6665-75
- Martin-Belmonte F, Gassama A, Datta A, Yu W, Rescher U, et al. 2007. PTEN-mediated apical segregation of phosphoinositides controls epithelial morphogenesis through Cdc42. *Cell* 128: 383-97
- Mertens AE, Rygiel TP, Olivo C, van der Kammen R, Collard JG. 2005. The Rac activator Tiam1 controls tight junction biogenesis in keratinocytes through binding to and activation of the Par polarity complex. *J Cell Biol* 170: 1029-37
- Nakanishi H, Takai Y. 2004. Roles of nectins in cell adhesion, migration and polarization. *Biol Chem* 385: 885-92
- Nelson WJ. 2003. Adaptation of core mechanisms to generate cell polarity. *Nature* 422: 766-74

- Nishimura T, Yamaguchi T, Kato K, Yoshizawa M, Nabeshima Y, et al. 2005. PAR-6-PAR-3 mediates Cdc42-induced Rac activation through the Rac GEFs STEF/Tiam1. *Nat Cell Biol* 7: 270-7
- Penkert RR, DiVittorio HM, Prehoda KE. 2004. Internal recognition through PDZ domain plasticity in the Par-6-Pals1 complex. *Nat Struct Mol Biol* 11: 1122-7
- Peterson FC, Penkert RR, Volkman BF, Prehoda KE. 2004. Cdc42 regulates the Par-6 PDZ domain through an allosteric CRIB-PDZ transition. *Mol Cell* 13: 665-76
- Pinal N, Goberdhan DC, Collinson L, Fujita Y, Cox IM, et al. 2006. Regulated and polarized PtdIns(3,4,5)P3 accumulation is essential for apical membrane morphogenesis in photoreceptor epithelial cells. *Curr Biol* 16: 140-9
- Sheng M, Sala C. 2001. PDZ domains and the organization of supramolecular complexes. *Annu Rev Neurosci* 24: 1-29
- Shin K, Straight S, Margolis B. 2005. PATJ regulates tight junction formation and polarity in mammalian epithelial cells. *J Cell Biol* 168: 705-11
- Straight SW, Pieczynski JN, Whiteman EL, Liu CJ, Margolis B. 2006. Mammalian lin-7 stabilizes polarity protein complexes. *J Biol Chem* 281: 37738-47
- Straight SW, Shin K, Fogg VC, Fan S, Liu CJ, et al. 2004. Loss of PALS1 expression leads to tight junction and polarity defects. *Mol Biol Cell* 15: 1981-90
- Suzuki A, Ohno S. 2006. The PAR-aPKC system: lessons in polarity. *J Cell Sci* 119: 979-87
- Tepass U, Knust E. 1993. Crumbs and stardust act in a genetic pathway that controls the organization of epithelia in *Drosophila melanogaster*. *Dev Biol* 159: 311-26
- Wang Q, Chen XW, Margolis B. 2007. PALS1 Regulates E-Cadherin Trafficking in Mammalian Epithelial Cells. *Mol Biol Cell* 18: 874-85
- Wells CD, Fawcett JP, Traweger A, Yamanaka Y, Goudreault M, et al. 2006. A Rich1/Amot complex regulates the Cdc42 GTPase and apical-polarity proteins in epithelial cells. *Cell* 125: 535-48
- Yeaman C, Grindstaff KK, Nelson WJ. 1999. New perspectives on mechanisms involved in generating epithelial cell polarity. *Physiol Rev* 79: 73-98